IODP Workshop on Using Ocean Drilling to Unlock the Secrets of Slow Slip Events

Workshop Field Trip Guide

4 - 5 August 2011
Gisborne, New Zealand

Field Trip Leaders
Nicola Litchfield; Andy Nicol; Kate Clark; Robert Langridge; Agnes Reyes

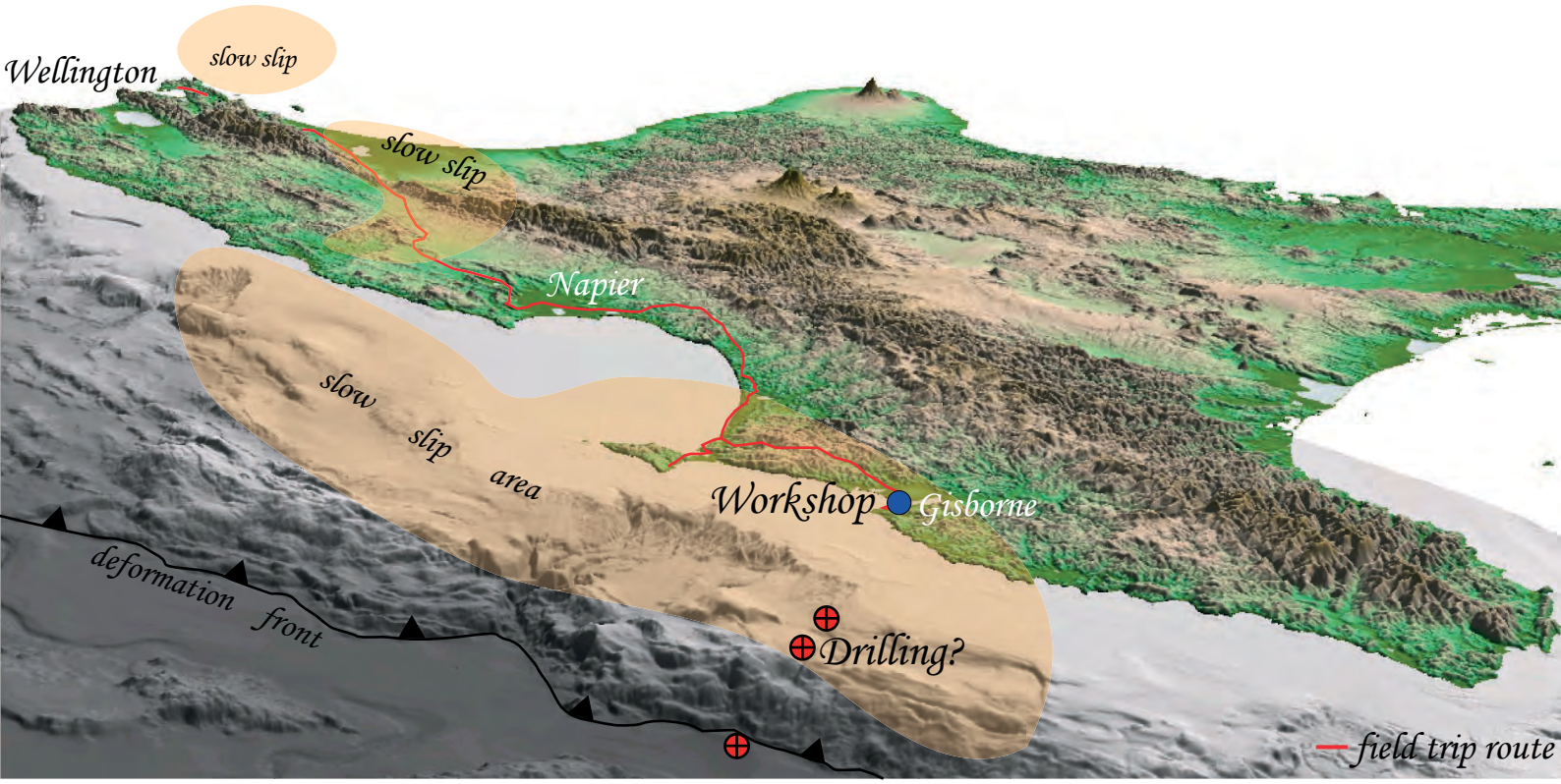

ministry of science + innovation
TE PŪNAHA HIRINGA WHAKAEA

GNS SCIENCE
TE PŪ AO

BIBLIOGRAPHIC REFERENCE

Litchfield, N.; Nicol, A.; Clark, K.; Langridge, R.; Reyes, A.; Wallace, L.M.; Mountjoy, J.J. 2011. IODP Workshop on Using Ocean Drilling to Unlock the Secrets of Slow Slip Events: Workshop Fieldtrip Guide. *GNS Science Miscellaneous Series 40*. 73p.

Nicola Litchfield, GNS Science, PO Box 30368, Lower Hutt, New Zealand
Andy Nicol, GNS Science, PO Box 30368, Lower Hutt, New Zealand
Kate Clark, GNS Science, PO Box 30368, Lower Hutt, New Zealand
Robert Langridge, GNS Science, PO Box 30368, Lower Hutt, New Zealand
Agnes Reyes, GNS Science, PO Box 30368, Lower Hutt, New Zealand
Laura Wallace, GNS Science, PO Box 30368, Lower Hutt, New Zealand
Joshu Mountjoy, NIWA, Private Bag 14901, Wellington

ISSN 1177-2441
ISBN 978-0-478-19848-5

CONTENTS

FIGURES

TABLES

HEALTH AND SAFETY ISSUES

PLEASE READ!

There are certain inherent hazards associated with the fieldtrip and participants must heed and observe the warnings and time limitations imposed at certain stops by the trip leaders. Caution must also be exercised when crossing public roads, standing on the road reserve, or farm track locations where vehicles or machinery may be in use.

Participants should carry any personal medications, including those for allergic reactions (e.g. insect stings, pollen, food allergies).

The weather in August can be variable, although we hope for warm sunny conditions! Participants need to be prepared for cold, warm, wet, and/or dry conditions. The expectation is that temperatures would be in the range from 4°C (39F) to 11°C (52F. Sturdy walking/running shoes or lightweight boots are recommended. A hat, rain and windproof coat, and warm clothing (layers) are essential. If the weather is warm, drink plenty of water to combat dehydration. Please don't underestimate the climatic variations that are possible or the potential to get sunburnt.

An average level of fitness and mobility is required for this trip; there will be some clambering over rocks. There are a number of natural inland and coastal cliffs, and these may be unstable. The party is requested therefore to stay clear of such areas that are vertical or capped by young sediments, and to not linger at cliff exposures at all. The fieldtrip leaders will point out comparatively safe outcrops to inspect: please keep to these.

In addition, due to the changing nature of the weather in August, we cannot guarantee that conditions will be exactly as we expect them. Conditions change frequently sometimes on a daily if not hourly basis. Circumstances on the day may dictate what is appropriate in terms of access and Health and Safety considerations.

When visiting roadside stops, the fieldtrip leaders will have overall responsibility for the safety of the site and of the participants. Please exit on the verge/left side of your vehicle if safe to do so and wait for a safety briefing for the site before moving away from your vehicle. If you need to go onto the road surface itself ("live lane"), for example to take photos, you must ensure you have a traffic spotter whose full attention is solely to alert you to approaching traffic.

DAY 1 FIELD TRIP SCHEDULE

Stop no.	Location	Feature	Pg
	Gisborne		
1/1	Kaiti Hill	Lookout with views of Poverty Bay and the uplifted forearc	11
1/2	Morere Hot Springs	Hot springs from the Hikurangi accretionary prism	14
1/3	Mahia Peninsula	Holocene and Pleistocene marine terraces	18
1/4	Wairoa Lagoons	Holocene coseismic subsidence	25
	Lunch in Wairoa		
1/5	Mohaka River	Late Quaternary fluvial terraces	28
1/6	Lake Tutira	Landslide-dammed lake with a Holocene earthquake and storm record	30
1/7	Bluff Hill	Lookout over Ahuriri Lagoon, uplifted in the 1931 Hawke's Bay earthquake (also referred to as the 1931 Napier earthquake)	34
1/8	Napier	Drive-through to observe art-deco buildings constructed after the 1931 earthquake	40
	Hastings		

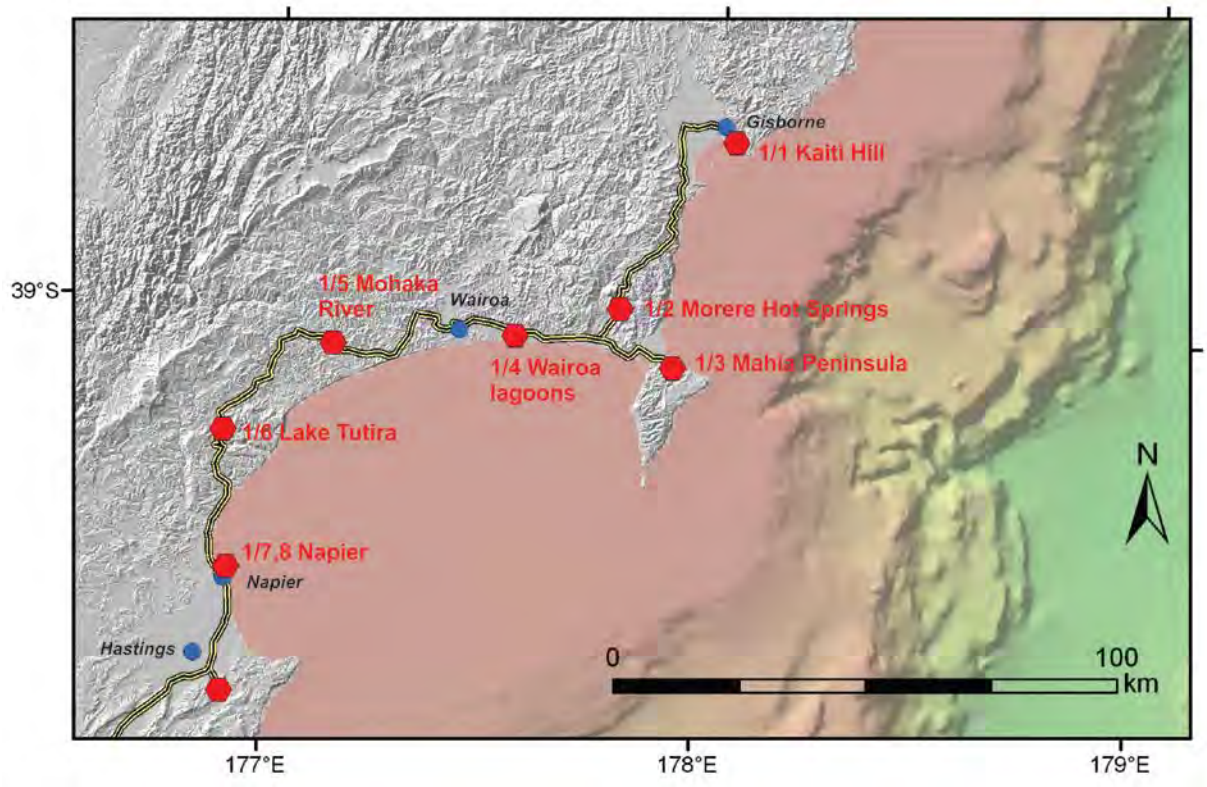

Figure 1 Map detailing Day 1 fieldtrip route.

DAY 2 FIELD TRIP SCHEDULE

Stop no.	Location	Feature	Pg
	Hastings		
2/1	Te Mata Peak	Lookout with views across the uplifted forearc and to the axial ranges	45
2/2	Poukawa Fault	Active forearc reverse fault, part of which ruptured in the 1931 Napier Earthquake	46
2/3	Mohaka Fault	Major fault of the central North Island Dextral Fault Belt	52
	Lunch in Woodville		
2/4	Saddle Road	Lookout on the axial ranges with views to the Wanganui Basin (west) and forearc (east)	56
2/5	Wanganui Basin	Overview of the south Wanganui Basin	59
2/6	Ohariu Fault	Major fault of the southern North Island Dextral Fault Belt.	61
	Wellington		

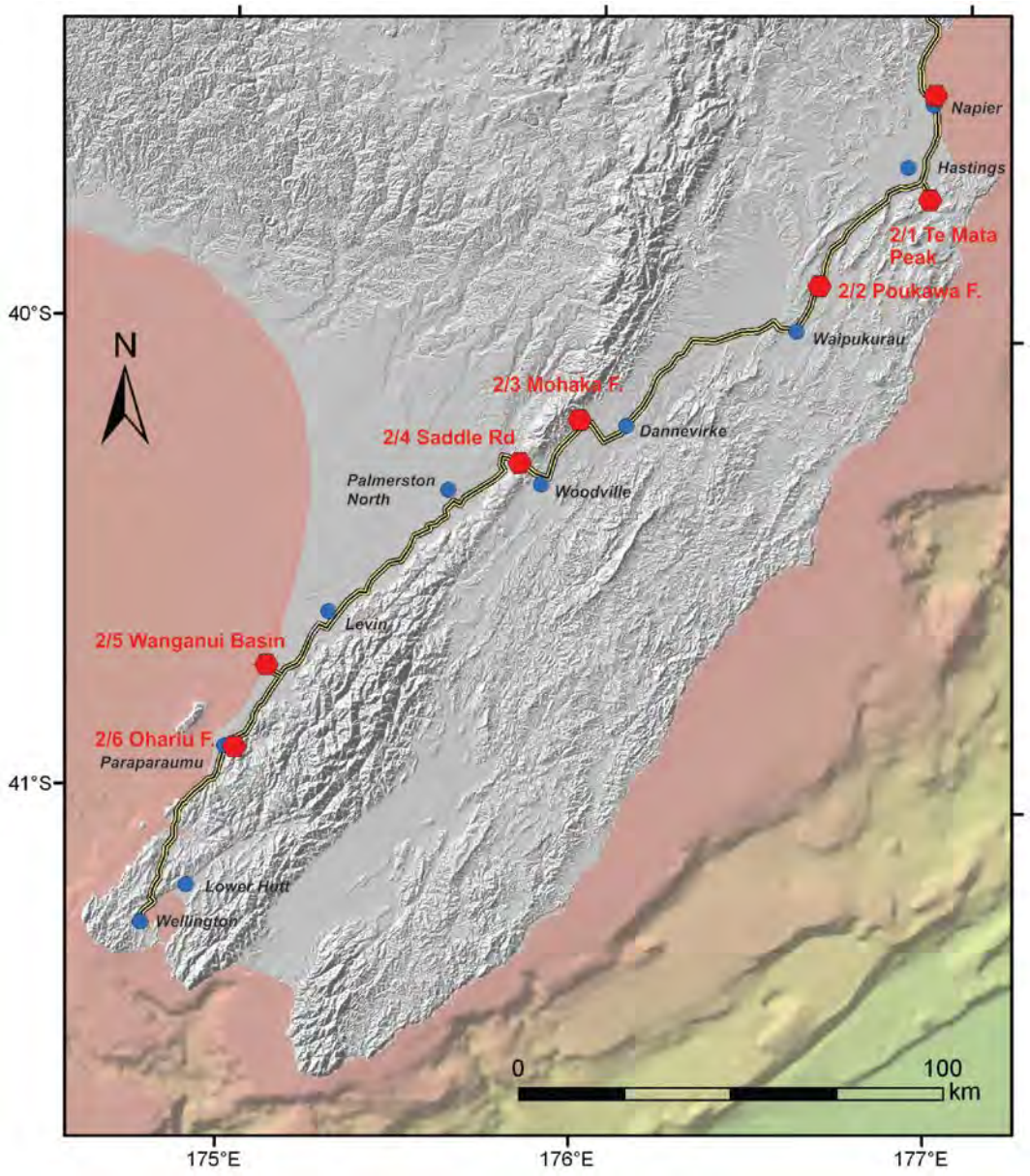

Figure 2 Map detailing Day 2 fieldtrip route.

INTRODUCTORY MATERIAL

Introduction to the Tectonic Setting of the Hikurangi Margin

The active Hikurangi subduction margin, New Zealand, occupies the transition zone from ocean-ocean subduction at the Kermadec Trench in the north, to oblique continental collision in the South Island (Figure 1). The Cretaceous Hikurangi Plateau (an oceanic plateau) subducts westward beneath the continental lithosphere of the Australian Plate along the offshore Hikurangi Trough at a rate of ~45 mm/yr. The subducting slab is well defined by recent seismicity (Figure 2), and seismic tomography studies reveal a high P-wave velocity (V_p) region extending to >300 km depth, corresponding to the relatively cold, dense subducting Pacific slab (*Reyners et al.*, 2006). Within New Zealand, active volcanism related to subduction of the Pacific Plate is largely confined to the central North Island, in the Taupo Volcanic Zone (TVZ), although active volcanism also occurs at Mt Taranaki, well back from the main arc (Figure 1a).

Deformation of the overriding Australian Plate includes shortening, extension, vertical-axis rotations and strike-slip faulting. Oblique convergence between the Pacific and Australian Plates (Figure 1) is partitioned in the North Island. On geological timescales, most (> 80%) of the convergent component of relative plate motion occurs on the subduction thrust, with the remainder accommodated on upper plate reverse faults. At latitude 40°30' S, average shortening rates in the upper plate have been ~6 mm/yr since the Oligocene. The margin-parallel component of Pacific/Australian relative plate motion is accommodated by a combination of strike-slip faulting and clockwise rotation of eastern North Island (*Beanland and Haines*, 1998; *Wallace et al.*, 2004). Strike-slip in the upper plate commenced at 1-2 Ma and mainly (>~40%) occurs on the North Island Dextral Fault Belt (Figure 1; also referred to as the North Island Fault System or North Island Shear Belt). Late Quaternary rates of strike-slip on these faults (including the Mohaka Fault which we are visiting on day 2) range up to ~15 mm/yr and decrease northwards along the margin.

The importance of upper-plate shortening increases southwards from a maximum of 42 km post Miocene extension to at least 84 km shortening since 24 Ma (*Nicol et al.*, 2007). The southward increase in upper plate shortening rates is due to rapid clockwise rotation of the eastern North Island forearc relative to the bounding Pacific and Australian Plates (Figure 3). The rapid clockwise rotation also produces (a) a rapid northward increase in convergence rates from 20 mm/yr at the southern Hikurangi Trough to 50-60 mm/yr of convergence offshore of northeastern North Island (Figure 3), and (b) back-arc rifting in central North Island. Clockwise vertical-axis rotations of the eastern Hikurangi margin (relative to stable Australian Plate) were ~3°/Myr from the present to 10 Ma , with a total rotation of about 45-50° in the last 24-30 Myr (*Nicol et al.*, 2007). Nearly pure convergence dominated the Hikurangi margin upper plate tectonics before 10 Ma, after which time the component of margin-parallel relative plate motion increased to the present. The Hikurangi margin is a good example of a plate boundary where for long periods of time (e.g., >5 Myr) vertical-axis rotations in the overriding plate account for most (50-100%) of the total margin-parallel plate motion.

Geological mapping combined with offshore seismic reflection and bathymetry studies shows a well-developed imbricated upper plate between the central Hikurangi Trough and the strike-slip faulted axial ranges of the North Island (*Davey et al.*, 1986; *Lewis and Pettinga*, 1993; *Barnes and Mercier de Lepinay*, 1997; *Nicol and Beavan*, 2003). The frontal wedge is

up to 150 km wide, and includes an inner, highly deformed pre-subduction Cretaceous and Paleogene sequence covered with deformed Miocene-Recent basins, and an outer accretionary wedge of mainly Plio-Pleistocene turbidites (*Lewis and Pettinga*, 1993; *Lewis et al.*, 1998; *Barnes et al.*, 2010) (Figure 4). In the central part of the margin, the accretionary wedge reaches about 70 km in width, and is characterised by long (~100 km) thrust ridges and slope basins (*Davey et al.*, 1986; *Barnes and Mercier de Lepinay*, 1997; Lewis et al., 1998; Figure 1a and 4b). Seismic reflection data including a variety of archived oil company sections, NIGHT (Henrys et al., 2006), R/V Sonne (*Barnes et al.*, 2010), and high-fold data recently acquired by the New Zealand Ministry for Economic Development (*Barker et al.*, 2009), highlight the presence of major thrust faults in the upper plate, many of which splay from the plate interface to the surface. Prominent examples of the latter include the structures beneath the Kidnappers and Lachlan ridges (KR and LR on Figure 1a, and Figure 4b) (*Barnes et al.*, 2002; *Barnes and Nicol*, 2004; *Henrys et al.*, 2006). From ~41.5°S, the width of the accretionary wedge narrows towards the southwest and fairly dramatically northeastward of Hawke Bay (*Collot et al.*, 1996; Figure 4). The northern portion of the Hikurangi margin (east of Raukumara Peninsula) is relatively sediment-starved (Figure 1a) (*Lewis et al.*, 1998), and exhibits frontal subduction erosion associated with subducting seamounts (e.g., *Collot et al.*, 1996; *Collot et al.*, 2001; *Barker et al.*, 2009; *Bell et al.*, 2010; Figure 4c), and a mix of normal and reverse faulting in the remnant prism.

An important aspect of subduction at the Hikurangi-Kermadec margin is the along-strike variation in the character of the subducting plate. At the Hikurangi Trough, a thick, oceanic plateau (the Hikurangi Plateau) is being subducted; the Pacific Plate changes northward to normal oceanic crust (Cretaceous) that subducts at the Kermadec Trench (Figure 1). The Hikurangi Plateau thickens southward from 10 km in the north, to 15 km adjacent to the Chatham Rise (*Davy and Wood*, 1994). It is studded with seamounts, which are more numerous in the north. The plateau is Cretaceous in age (*Mortimer and Parkinson*, 1996) and covered by a Cretaceous and Cenozoic sedimentary sequence (*Davy et al.*, 2008). In the Hikurangi Trough, this cover has been inferred to comprise a subducting sequence including >500 m of low velocity (~2.5-3.5 km/s) Cretaceous volcaniclastics and/or limestone/chert (>100 Ma), ~600 m of Cretaceous clastic sedimentary rocks (100-70 Ma), and ~200 m of Cretaceous-Oligocene pelagic sedimentary rocks (70-32 Ma), and an accreting, upper sequence of mainly Plio-Pleistocene turbidites (*Barnes et al.*, 2010). The turbidite sequence thickens southward from ~ 1 km off northeastern North Island to ~6 km off northeastern South Island (*Lewis et al.*, 1998) (Figure 1a). The southward increase in thickness of the subducting Pacific Plate and its cover sequence accompanies a southward decrease in convergence rate at the trench. Subduction terminates where the Chatham Rise (a continental fragment, 27 km thick; *Reyners and Cowan*, 1993) intersects the margin.

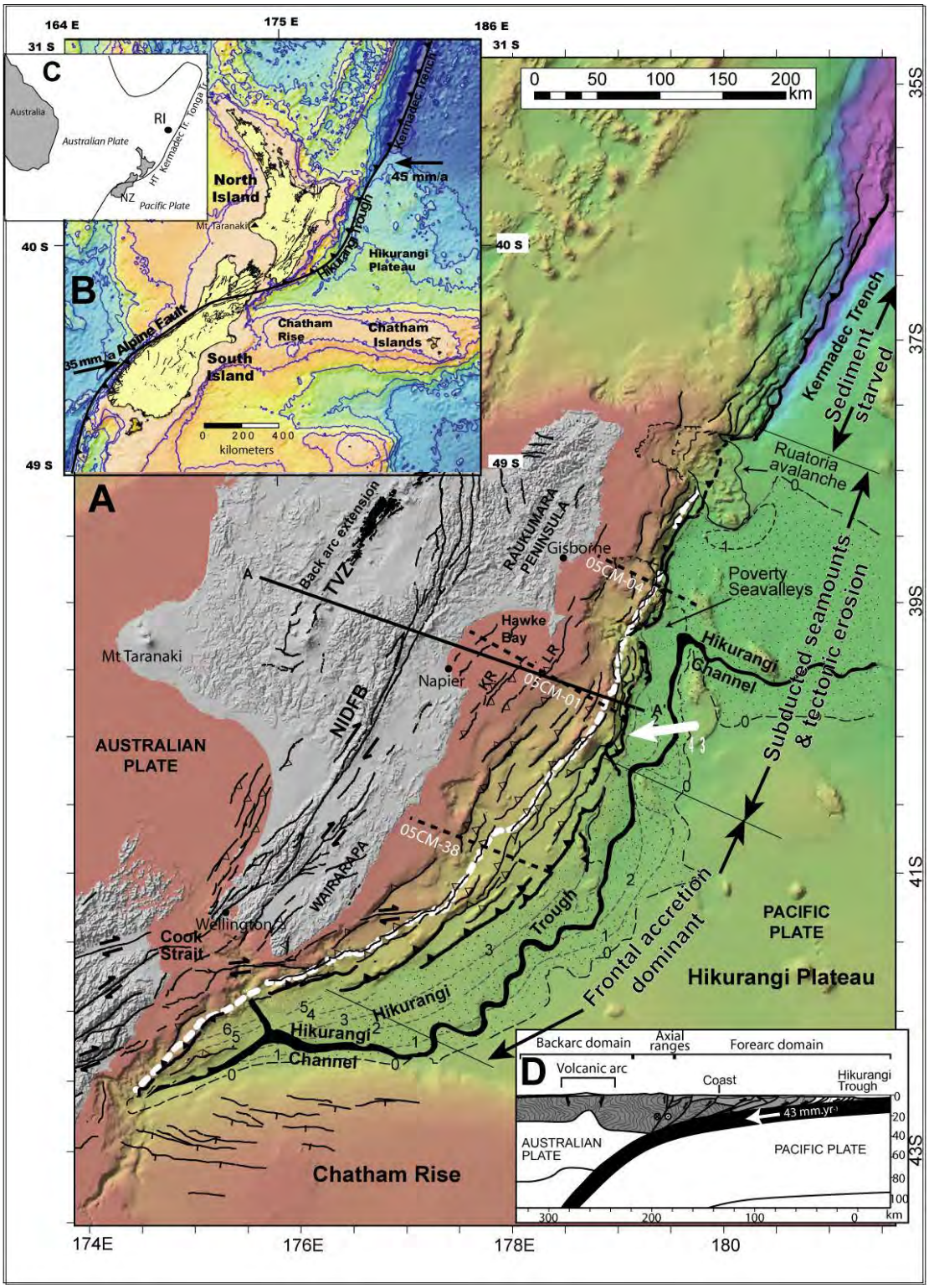

Figure 3 Tectonic setting of the Hikurangi margin; figure modified from Barnes et al. (2010). and Wallace et al. (2010). (A) detailed bathymetry (NIWA), topography and active faulting (black lines) of the onshore and offshore subduction margin. Dashed contours indicate sediment thickness on lower plate from Lewis et al. (1998). Bold white dashed line shows the back of the accretionary wedge and the front of a deforming buttress of Cretaceous and Paleogene rocks covered by Miocene to Recent slope basins (from Lewis et al., 1997; Barnes et al., 1998b; Barnes et al., 2009). A-A' line denotes cross-section location in (D). Dashed black lines show locations of seismic reflection lines from Figure 4, labelled by line number. White arrow shows Pacific/Australia relative plate motion in the region from Beavan et al. (2002). Onshore active faults from GNS Science active faults database (http://maps.gns.cri.nz/website/af/). TVZ = Taupo Volcanic Zone; NIDFB = North Island Dextral Fault Belt; LR = approximate location of Lachlan Ridge; KR = approximate location of Kidnappers Ridge; (B) broader-scale New Zealand tectonic setting; (C) inset, regional tectonic framework; RI = Raoul Island; NZ = New Zealand, HT = Hikurangi Trough. (D) Interpretive cross-section across the strike of the subduction margin. Cross-section location denoted by A-A' line on (A).

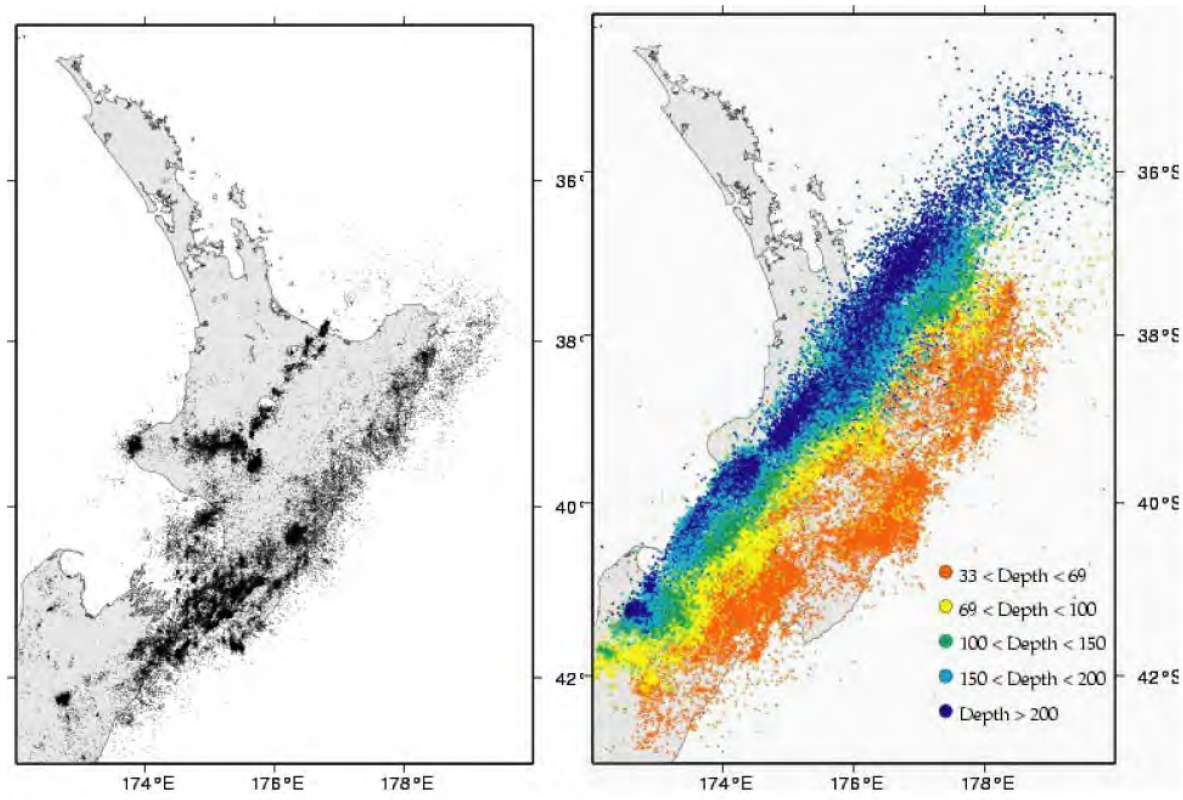

Figure 4 Selected seismicity between January 1990 and December 2007 (inclusive), from the GeoNet database (http://geonet.org.nz). Events shown are only those that were recorded by 6 or more stations, with nine or more observed phases, with unrestricted location depths, and RMS of arrival time residuals less than 1.0 s. Magnitude range of events shown is 0.29-6.99. **Left:** Events shallower than 33 km; **Right:** Events greater than 33 km depth.

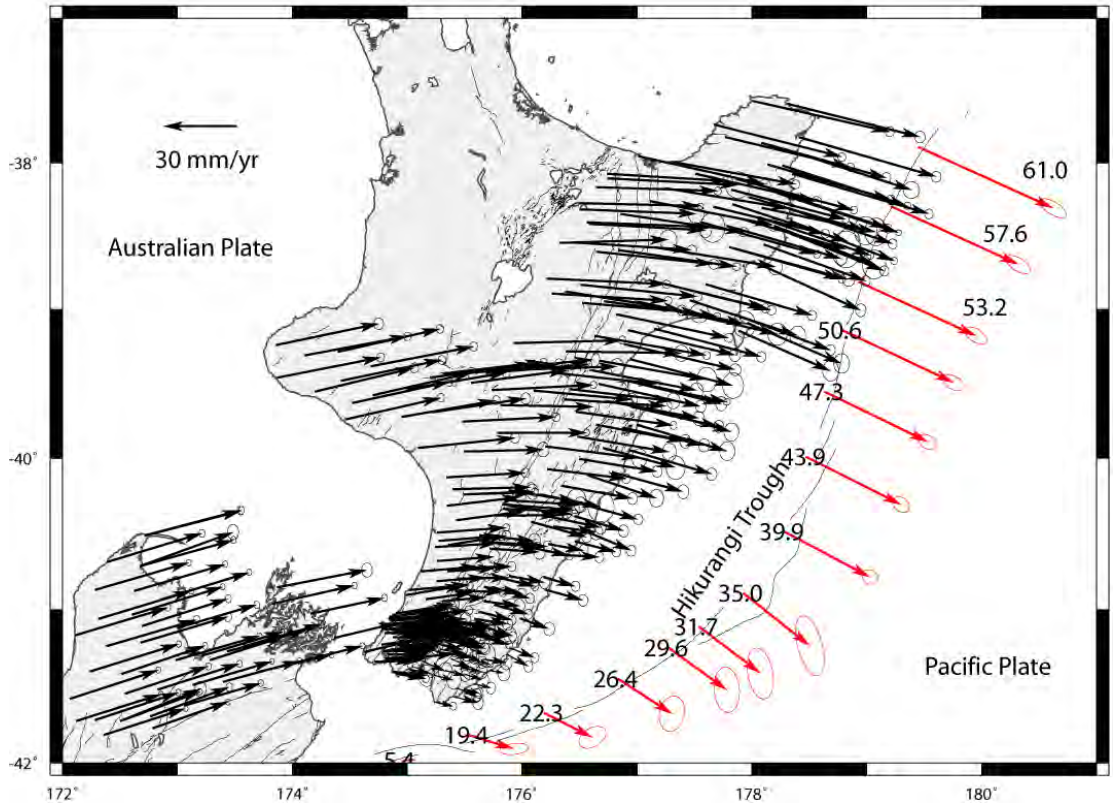

Figure 5 GPS velocities (black) relative to the Pacific Plate; red vectors show estimated long-term convergence rate at trench labelled in mm/yr (Wallace et al., 2004).

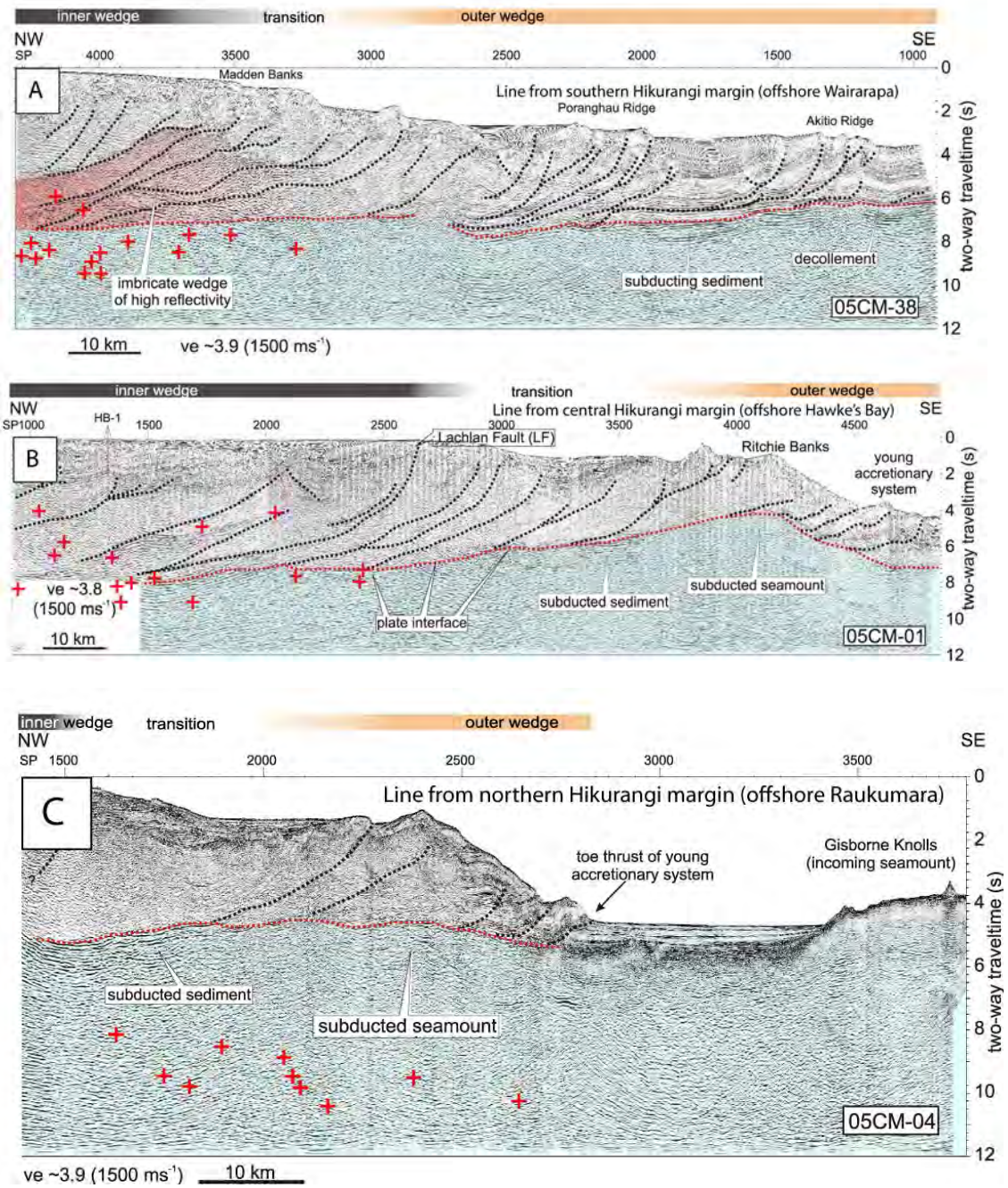

Figure 6 Representative seismic lines from the southern (A), central (B), and northern (C) sections of the offshore Hikurangi margin, adapted from Barker et al. (2009). (A) Seismic reflection line 05CM-38, location Figure 1. Dotted red line marks the decollément/plate interface, with shaded blue transparency for subducting material below. The shaded red transparency indicates an imbricate wedge of high reflectivity material. Red crosses indicates projected positions of earthquakes within 10 km of the section, with depths converted to two-way time using the velocity model discussed in Barker et al. (2009). Barker et al. (2009) interpret the transition from inner to outer wedge (top), to be marked by the break in slope. Numerous splay faults cut the wedge. Young faults toward the toe of the wedge cut a thick section of incoming turbidites, while undeformed sediment can be seen subducting beneath the decollément (see also Barnes et al., 2009). (B) Seismic reflection line 05CM-01, location Figure 1. Note the splay faults cutting the upper plate, including Lachlan Fault displacing the seafloor. Subduction of a seamount has deformed the outer wedge to produce an outer high (Ritchie Banks), with uplifted slope basins landward and a young, narrow accretionary zone seaward. (C) Seismic reflection line 05CM-04, location Figure 1. As with 05CM-01 this margin has been modified by seamount subduction, with a seamount underlying an outer high. Landward of the high are uplifted slope basins, while seaward is a narrow accretionary zone with an oversteepened slope. Note the incoming seamount, as yet unsubducted, and thin sedimentary cover on the downgoing plate compared with further south (Figure 1).

1.0 OVERVIEW OF HIKURANGI MARGIN SLOW SLIP EVENTS AND THEIR RELATIONSHIP TO INTERSEISMIC COUPLING.

The installation of a continuous GPS (cGPS) network in New Zealand since 2002 (www.geonet.org.nz; Figure 5) has enabled the discovery of 15 slow slip events (SSEs) at the Hikurangi subduction margin. Analysis and interpretation of the cGPS data reveal a marked diversity in characteristics of slow slip events in the North Island, with durations varying from 6 days to 1.5 years, equivalent moment release between Mw 6.4-7.2, and recurrence intervals of repeating SSEs on the order of two years to more than five years (*Wallace and Beavan*, 2010). The duration and magnitude characteristics of Hikurangi SSEs appear to be related to the depths where they occur (Figures 6-7). The deepest, longest duration, and largest SSEs occur at the southern Hikurangi margin, near the down-dip limit of deep (down to ~40 km depth), strong interseismic coupling (Figures 6, 8). The shallowest, shortest duration, smallest, and most frequent SSEs occur at the northern and central Hikurangi margin near the down-dip limit of unusually shallow (<10-15 km depth) interseismic coupling (Figures 7, 8).

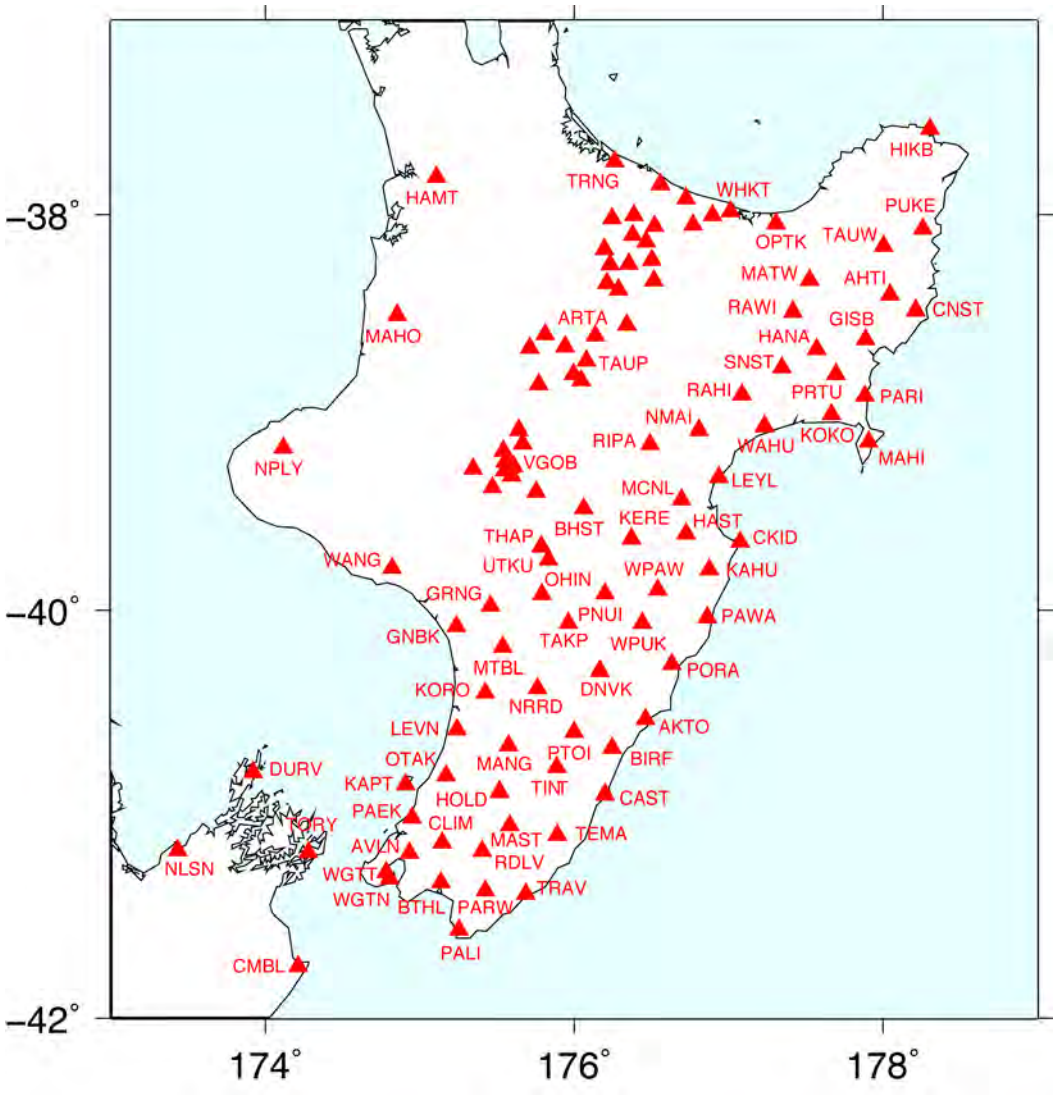

Figure 7 Map showing current configuration of the continuous GPS (cGPS) network in New Zealand (www.geonet.org.nz). Red triangles denote a cGPS site, and site names for most stations are denoted by a four-letter code.

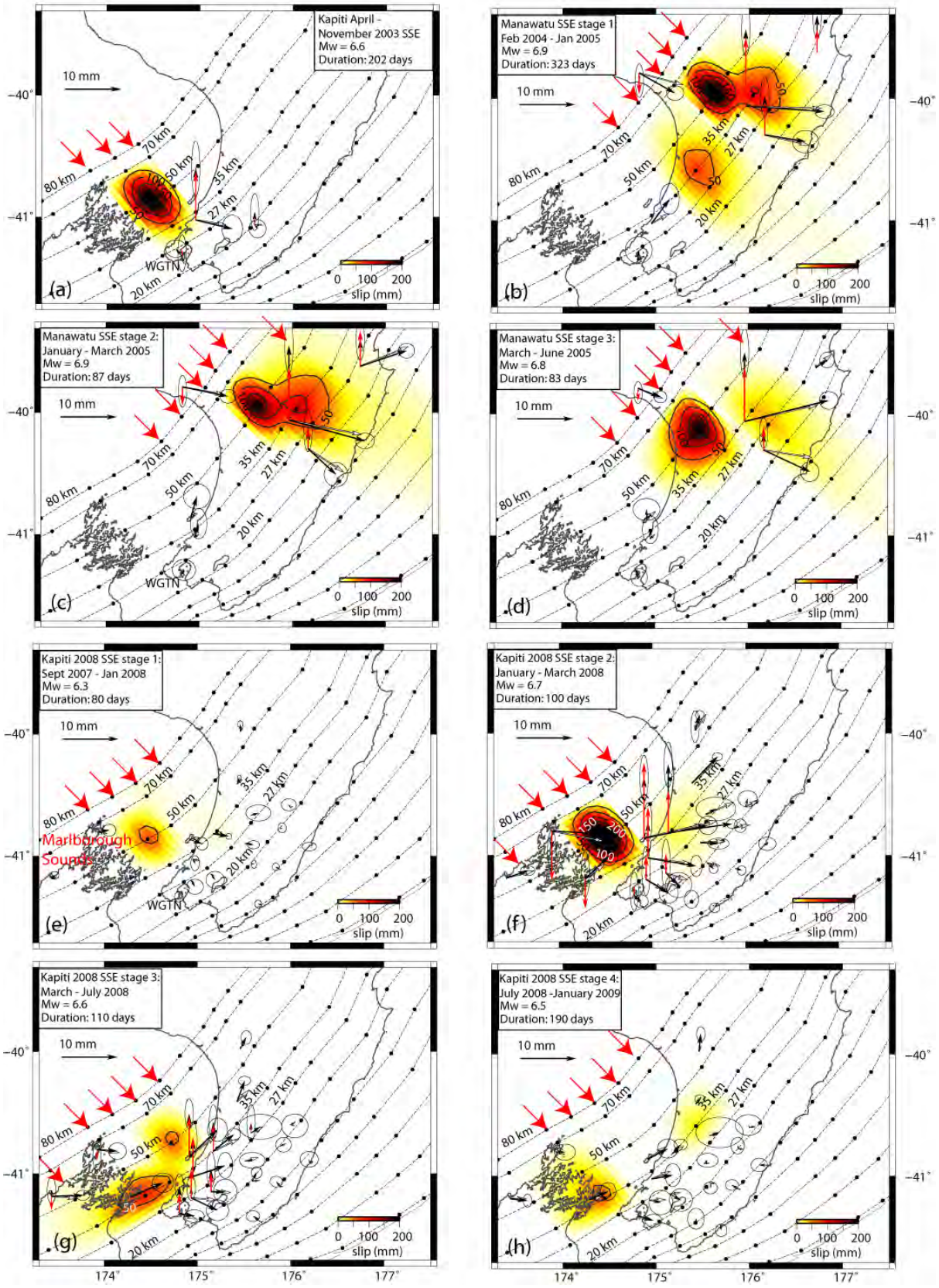

Figure 8 Slip distribution on the subduction interface (in mm), with modelled (white arrows) and observed (black arrows with 1σ error ellipses) horizontal surface displacements at various stages of three major SSEs documented since 2002 in the southern half of the Hikurangi margin. Observed (black arrows with 1σ error ellipses) and model (red arrows) vertical displacements in the SSEs are shown for sites where significant vertical displacements occur. Black dots show nodes defining the subduction interface, and the large red arrows point to the node profiles along which we invert for slip, using a Gaussian parameterization. Subduction interface depth contours for model slip region (black lines) labelled with depth. From Wallace and Beavan (2010).

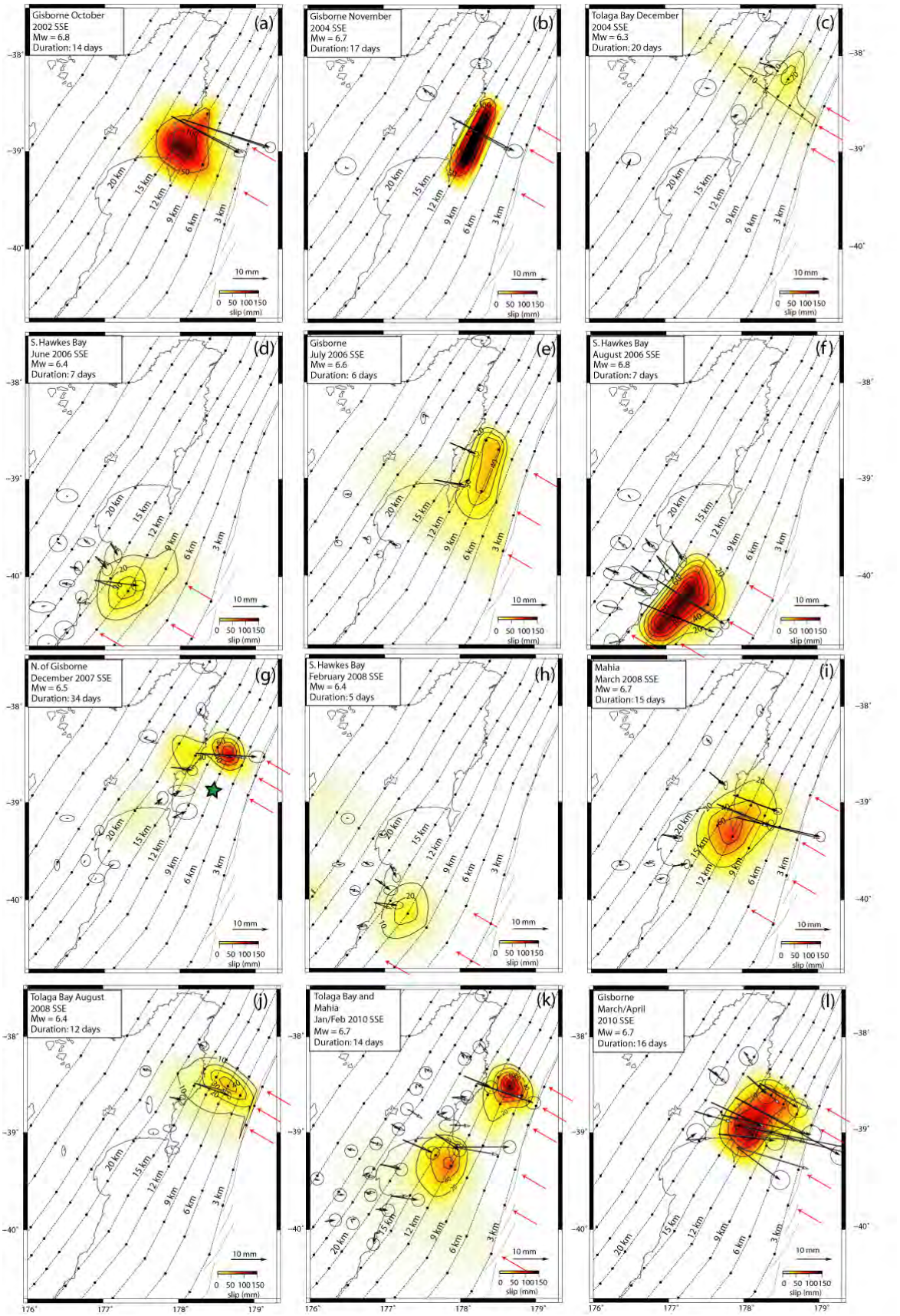

Figure 9 Slip distribution on the subduction interface (in mm), modelled (white arrows) and observed (black arrows, 1σ error ellipses shown) horizontal surface displacements from SSEs documented since 2002 in the northern half of the Hikurangi margin. Black dots show nodes defining the subduction interface, and the red arrows point to the node profiles that we invert for slip on, using a Gaussian parameterization. Subduction interface depth contours for model slip region (black lines) labeled with depth. Green star in (g) shows epicenter of the 2007 Gisborne Mw 6.6 earthquake. From Wallace and Beavan (2010).

In all cases observed to date, Hikurangi margin SSEs occur at the down-dip limit of interseismic coupling (Figure 8a), similar to examples from other subduction margins. The continuous GPS data also show that moment accumulation rates on the interface for the time periods between SSEs are ~40% higher (Figure 8b) than for the period of more than a decade averaging through the SSEs, indicating that SSEs comprise a major portion of the overall moment release budget of the Hikurangi subduction interface.

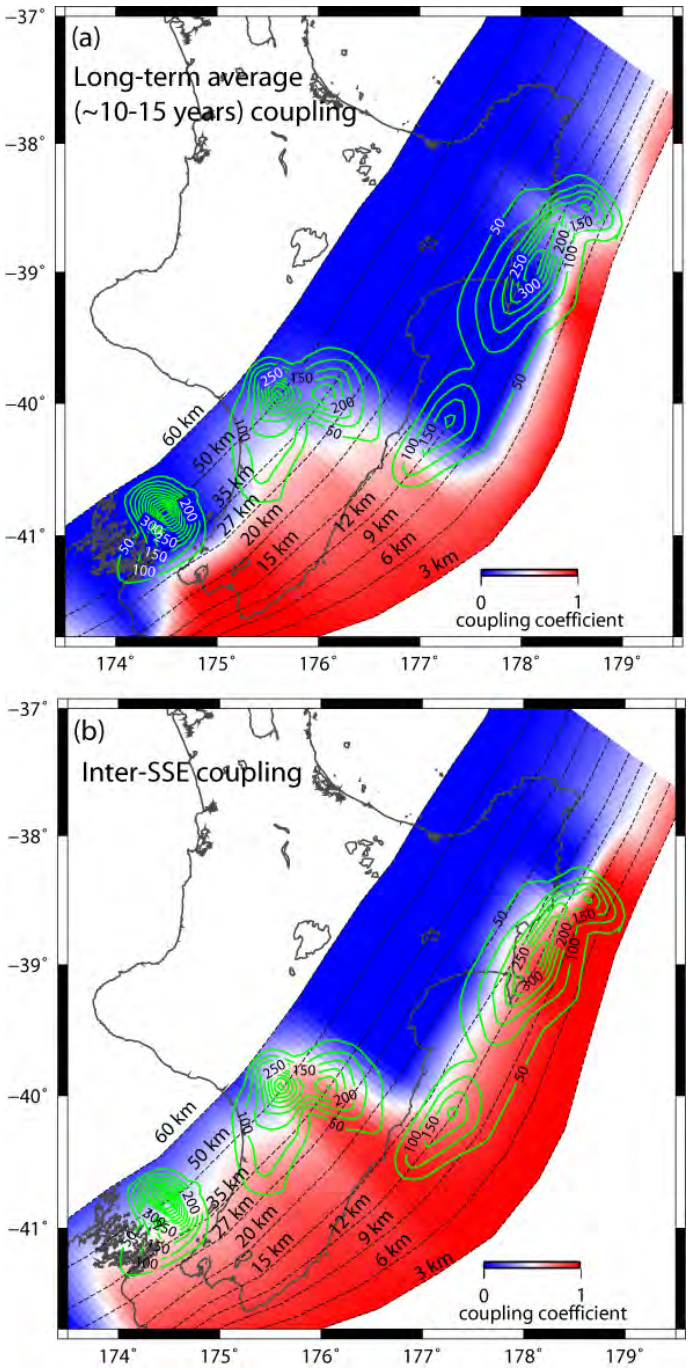

Figure 10 (a) Coupling coefficient on the subduction interface determined from velocities that are averaged through slow slip events (continuous and campaign GPS measurements). (b) Coupling coefficient on the subduction interface during the time period between slow slip events (e.g., inter-SSE period). The inversion for inter-SSE coupling uses the block modelling approach of McCaffrey (2002) that we have also used for the campaign GPS velocities in the North Island (e.g., Wallace et al., 2004; 2009). Green contours show total slip (in mm) detected in SSEs on the Hikurangi subduction interface since 2002. Dashed black line shows depth contours (labelled) to the subduction interface. From Wallace and Beavan (2010).

1.1 RELATIONSHIP OF NORTHERN HIKURANGI MARGIN SSES TO REFLECTIVE PROPERTIES OF THE SUBDUCTION INTERFACE

An intriguing sequence of slow slip events and triggered seismicity occurred offshore the northern Hikurangi margin, between January 2010 and April 2010 (Figures 7 and 9). The first event (lasting two weeks from late January until early February) ruptured two separate patches of the northern Hikurangi subduction thrust, and was followed one month later by rupture of the intervening patch (lasting three weeks from mid-March until mid-April) (Figure 9). The January/February slow slip patches coincide with zones of high amplitude reflectivity (imaged from seismic reflection data; Figures 4c and 9; *Bell et al.*, 2010) near the subduction interface. These high amplitude reflectivity zones are interpreted to be a thick sequence of subducted sediments and where fluid pressures may be elevated locally. The intervening portion of the interface where the subsequent slow slip event (March/April) occurred is characterized by low amplitude reflectivity near the interface. We suggest that the January/February slow slip patches ruptured first, due to the elevated fluid pressures (and decreased resistance to slip) in the source area of those events. The March/April source region is likely to be in an environment where fluid pressures are lower (low amplitude reflectivity zone) so slip was delayed; this later SSE was possibly triggered by static stress transfer from the earlier January/February phase of slow slip.

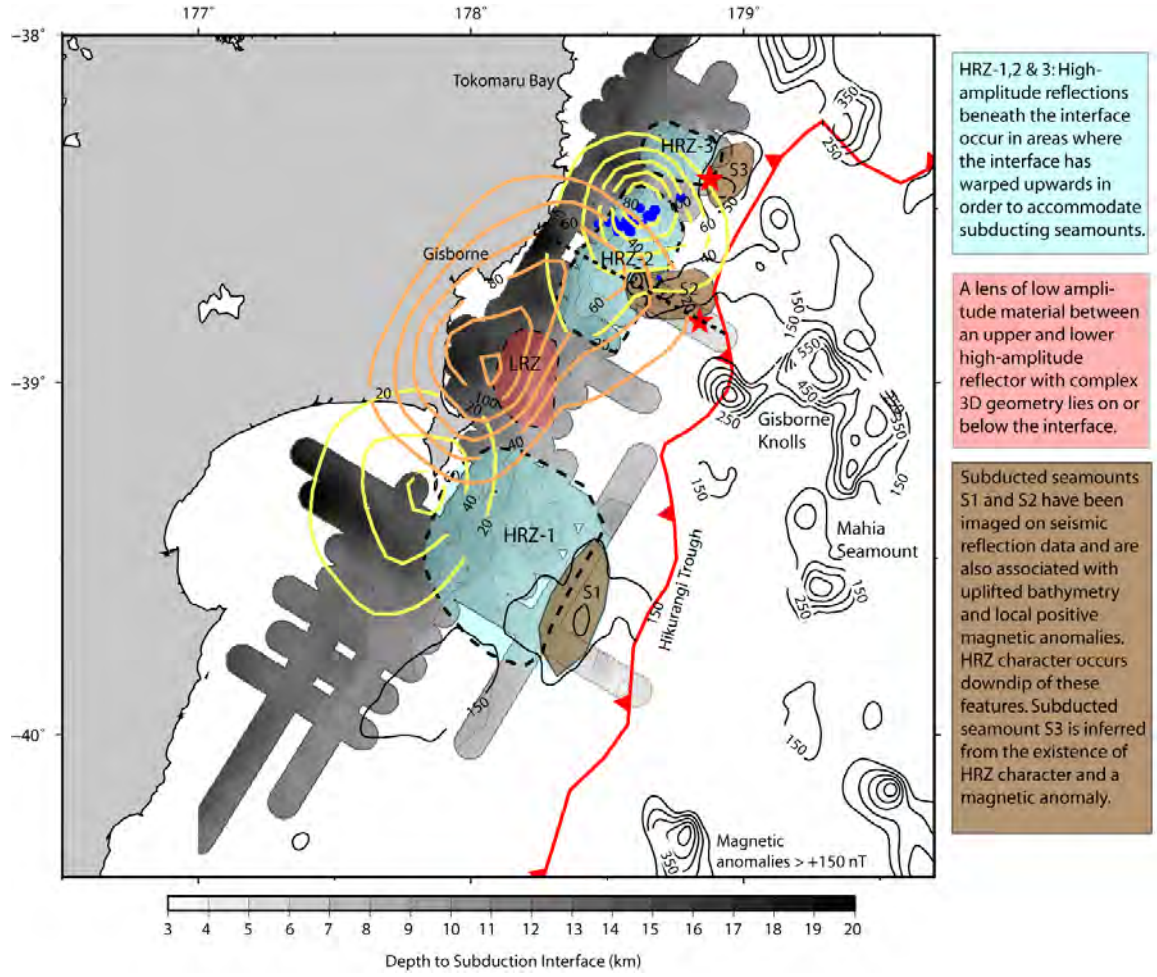

Figure 11 Reflective properties of the subduction interface (see key at right for explanation) at the northern Hikurangi margin and the location of slip on the interface in the January/February (yellow contours) and the March/April (orange contours) 2010 SSEs. Black dashed straight line shows location of seismic line in Figure 4c. Blue dots are locations of triggered seismicity during the January/February 2010 SSE. Red stars are the location two tsunamigenic subduction interface earthquakes (Mw 6.9-7.1) in March and May of 1947. Subduction interface properties from Bell et al. (2010).

1.2 THE ONGOING MANAWATU SLOW SLIP EVENT

On the second day of the fieldtrip, we will be crossing over the source area of the Manawatu slow slip event that occurred in 2004/2005 (Figure 6b-d). A repeat of the 2004/2005 Manawatu slow slip event (Figure 10) is currently ongoing, since mid-2010, suggesting an approximately 5 year recurrence interval for SSEs in the central portion of the Hikurangi margin. Most of the slip in the latest event occurred from early September to end December 2010, and the event appears to be in the process of winding-down (Figure 10). To date, the slip on the subduction interface in this event is > 15 cm in some locations, and has released moment equivalent to an Mw 7.1. There has also been an increase in the number of interface and intraslab earthquakes just up-dip of the slow slip source area over the last year, which we expect are being triggered by the ongoing slow slip event.

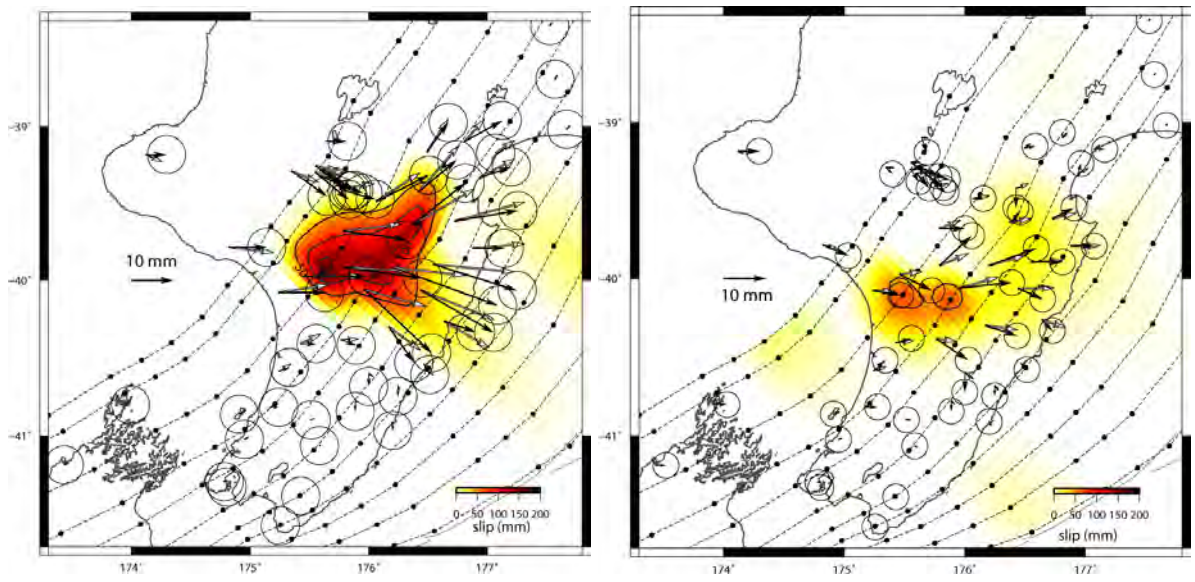

Slow slip between June 2010 and December 2010 Slow slip between January 2011 and July 2011

Figure 12 Slip distribution on the subduction interface (in mm), with modelled (white arrows) and observed (black arrows) horizontal surface displacements for the ongoing 2010/2011 Manawatu slow slip event. Black dots show nodes defining the subduction interface. Subduction interface depth contours for model slip region (black lines).

2.0 OVERVIEW OF THE EAST COAST BASIN GEOLOGY

The East Coast Basin covers both the onshore and offshore area (~75,000 km^2) along the eastern side of the North Island and the northeastern part of the South Island. The northern boundary is arbitrarily defined as lying north of East Cape. The western boundary is the axial ranges of the North Island and the Wairau Fault in the South Island where Mesozoic basement is exposed or sediments are thin. The southern and eastern boundaries of the East Coast Basin are at the Hikurangi Trough, although sedimentary cover extends unbroken onto the Chatham Rise.

The geological history of the East Coast Basin is not yet fully understood and some tectonic interpretations remain controversial (*Field et al.*, 1996, *Mazengarb and Harris*, 1994). For at least a part of the Early Cretaceous, the area was a convergent margin on the northeastern edge of Gondwanaland, but by the latest Cretaceous, when rifting and spreading in the Tasman Sea was occurring, the East Coast Basin was a passive margin. Throughout the Paleogene there was gradual regional subsidence and slow sedimentation, reflecting the post-rift foundering of the New Zealand region.

In the Early Miocene, deformation and sedimentation patterns changed markedly when subduction began in northern New Zealand. Oblique convergence of the Pacific and Australian plates resulted in more than 1,000 km of lithosphere being subducted in the north, while to the south, where strike-slip motion predominated, there has been little or none subducted. During the Neogene the northern part of the East Coast Basin became a classic forearc basin with subsidence and deposition occurring between the subduction trench (the Hikurangi Trough) in the east and a volcanic arc (the TVZ) in the west.

In the north, the onset of subduction was accompanied by obduction of the East Coast Allochthon. South of the allochthon subduction induced compression and formed structures that trend approximately parallel to the present day plate boundary, with uplift, thrusting, oblique-slip and normal faulting occurring at various times during the Neogene.

2.1 BASIN STRUCTURE

The East Coast Basin is structurally complex. There are two main structural domains; the western, inner forearc, comprises most of the onshore part of the basin (*Beanland et al.*, 1998), while the eastern, outer forearc, includes the coastal areas of eastern North Island and most of the offshore parts of the basin (*Lewis and Petinga*, 1993). In Wairarapa and southern Hawke's Bay, the boundary between the inner forearc and the outer forearc is along a range of hills (the Coastal ranges) where Cretaceous basement greywacke crops out. The structural belts are further subdivided into separate structural blocks based on distinct pre-Neogene facies and structural characteristics.

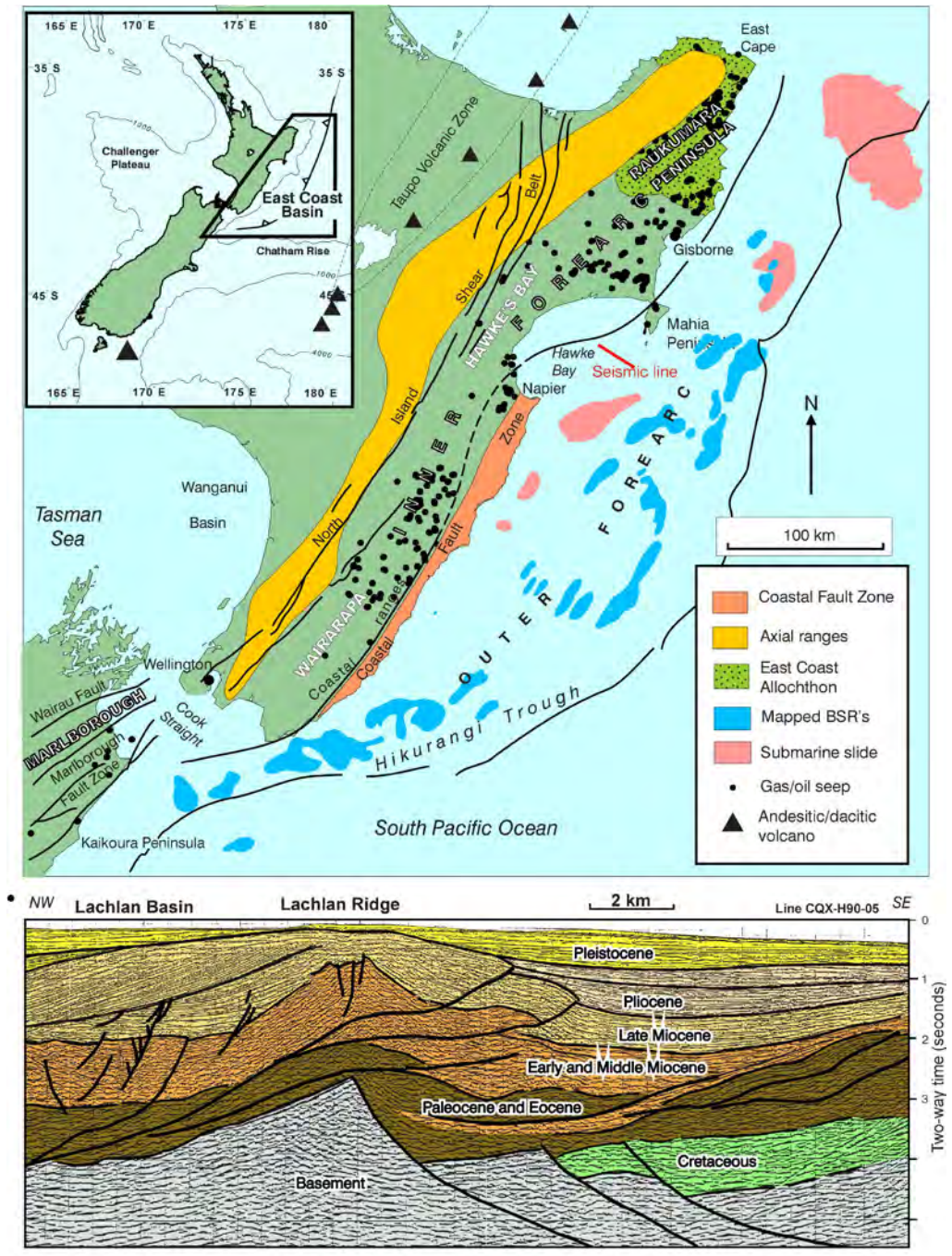

Figure 13 Location map of East Coast and offshore seismic line from Hawke Bay showing the typical reverse faulting and imbricate thrust wedge structure of the region (adapted from Field et al., 1997).

The outer forearc is primarily an imbricate thrust wedge with predominantly east-verging low-angle thrust faults. Late Miocene to Recent deformation is characterised by normal faulting and large-scale gravity collapse toward the trench north of Hawke Bay. In areas to the south, the orientation of faults and folds is much more variable but are generally parallel to the plate boundary. Diapiric processes have also influenced the formation of some Neogene structures. Footwalls of some normal faults are upturned by the intrusion of diapiric muds and shale, and are often associated with seeps of oil, gas, and hot water. The East Coast is one of New Zealand's most seismically active areas and several major earthquakes have been recorded in the last 200 years.

2.2 EAST COAST BASIN STRATIGRAPHY

Basement consists of weakly metamorphosed Triassic to Early Cretaceous greywacke sandstone and mudstone of the Torlesse composite Terrane. The overlying mid-Cretaceous and younger stratigraphy is almost solely described from onshore outcrop and consists of three major elements:

1. Cretaceous rocks ranging from paralic sandstones to bathyal mudstones, deposited in a variety of compressional tectonic settings prior to and during rifting associated with the break-up of Gondwanaland and Tasman Sea spreading. Mid- and Late Cretaceous stratigraphic thicknesses of c. 3000 m have been measured in many places.

2. Latest Cretaceous and Paleogene rocks, mainly mudstone and micritic limestone, deposited at a passive margin. Late Cretaceous and Paleogene sedimentation rates were low throughout the East Coast Basin, and this part of the sedimentary succession is typically less than 1000 m thick.

3. Miocene to Recent rocks dominated by bathyal flysch and mudstone, with intercalated neritic sands and limestones. The maximum known thickness of these strata is more than 5000 m.

3.0 DAY 1: GISBORNE – HASTINGS

3.1 STOP 1/1: KAITI HILL LOOKOUT

The main Kaiti Hill Lookout offers views across the Pacific Ocean, Poverty Bay, the lower Waipaoa River floodplain, and the coastal ranges. On a clear day, Mahia Peninsula (stop 1/3) can be viewed off in the distance to the south.

Looking E-SE over the Pacific Ocean you might imagine a ~25 km wide continental shelf sloping gradually to the shelf break at ~120 m below sea level (Figure 14). 20,000 years ago, at the glacial maximum, the shoreline was out at the margin of a vast coastal plain. From that point, for another ~50 km, the continental slope plunges to ~3000 m below sea level to the deformation front of the Hikurangi Forearc. The morphology of the continental slope, as illustrated by Figure 14 strongly reflects subduction margin processes, and at this location is dominated by the large Poverty Reentrant, postulated to be the result of multiple impacts from seamounts on the incoming Pacific Plate. Approximately 42 km due east, roughly the same distance as to Mahia Peninsula, is the location of the most landward drilling site in the Hikurangi Margin slow slip drilling proposal. Between the shelf break and the coast there are two major fault zones that appear to persist along much of the margin, comprising outer shelf structures (e.g. the Ariel Bank Fault) and inner shelf structures (e.g. the Gable End faults Figure 14). These inner shelf faults are predicted to be responsible for much of the coastal uplift observed along the Hikurangi Margin.

The coastlines north and south of Kaiti Hill are marked by generally steep cliffs and are prone to coastal landsliding. Marine terraces are not preserved anywhere along the coast between Kaiti Hill and Mahia Peninsula, which may reflect high coastal erosion rates, no tectonic uplift, or both. Near Tuaheni Point, at Sponge Bay (Figure 14), an early Holocene marine terrace is exposed, recording an uplift rate of ~2 mm/yr (*Wellman*, 1962; *Ota et al.*, 1988, 1992). The Sponge Bay terrace was formed by estuary infilling during the late stages of post-glacial sea-level rise, and it and lower erosional terraces can be traced intermittently at least as far north as Karaka Bay (Ota et al., 1988, 1992; Wilson et al., 2006, 2007a,b; Clark et al., 2010) (Figure 14). The Sponge Bay terrace is highest (27 m) at Pakarae River mouth, ~20 km northeast of Gisborne (*Wilson et al*., 2006; *Litchfield et al*., 2010a). There, 7 marine terraces record an uplift rate of 3.2 ± 0.8 mm/yr (*Wilson et al*., 2006), which matches well with the slip rate on the likely causative fault, the offshore, northwest-dipping reverse Gable End Fault, situated 5-10 km to the southeast (*Mountjoy and Barnes*, 2011) (Figure 14).

Poverty Bay is a shallow, bowl-shaped (8 x 5 km) bay bound by Young Nicks Head[1] on the southwest side and Tuaheni Point on the northeast side. Both peninsulas are composed of Miocene sedimentary rocks, Young Nicks head is soft, erodible mudstone and Tuaheni Point is alternating mudstone and sandstone. Chirp profiles (Figure 15) show that a sill extends across much of the bay, which is exposed, or just below the surface, and as a result not much sediment delivered from the Waipaoa River mouth (15 Mt/yr, Hicks and Shankar, 2003) is being trapped within the bay.

[1] Young Nicks Head was named by Captain James Cook after 12 year old Nicholas Young who, in 1769, was the first European to sight New Zealand since Abel Tasman's voyage in 1642.

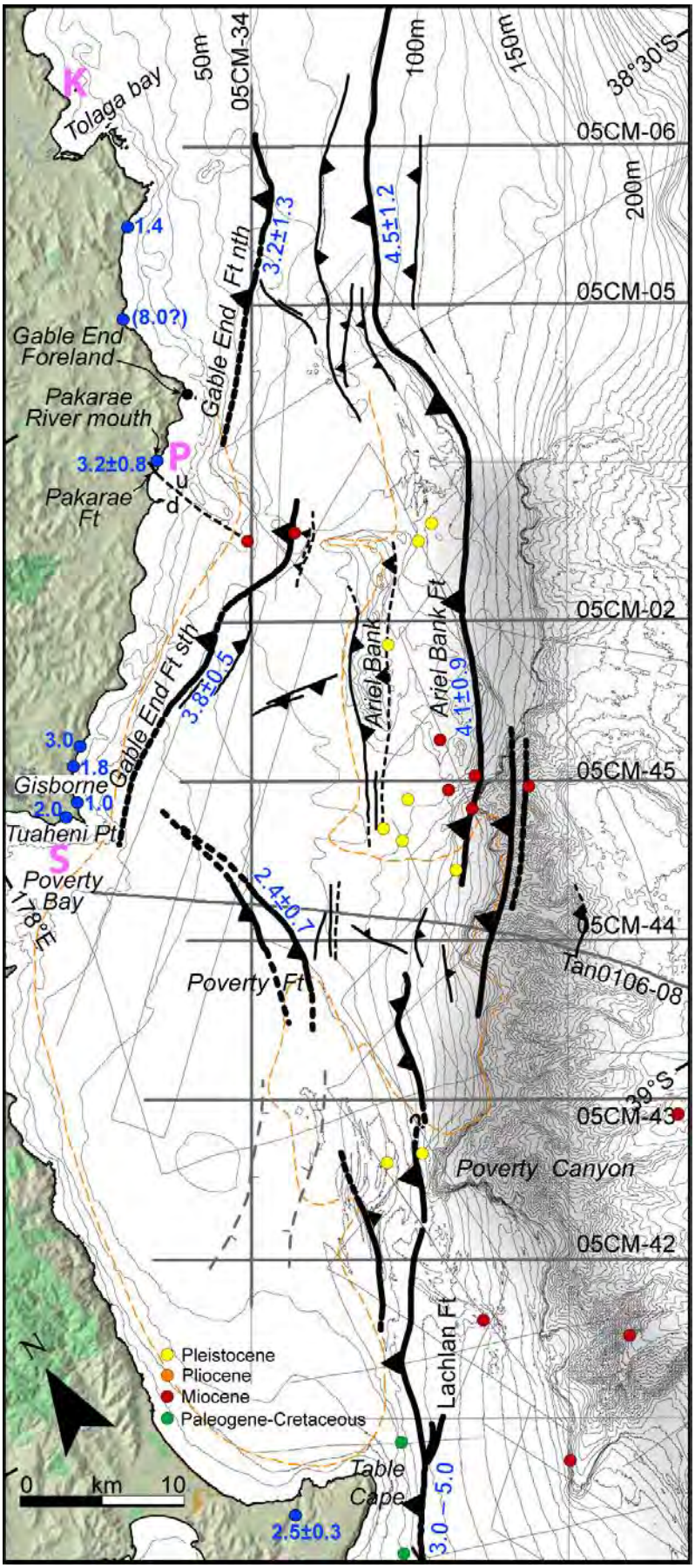

Figure 14 Map of Mountjoy and Barnes (2011) showing a comparison of uplift rates along the coast calculated from marine terraces (bold blue) and slip rates on offshore faults. S = Sponge Bay, P = Pakarae River mouth, K = Karaka Bay sites mentioned in the text.

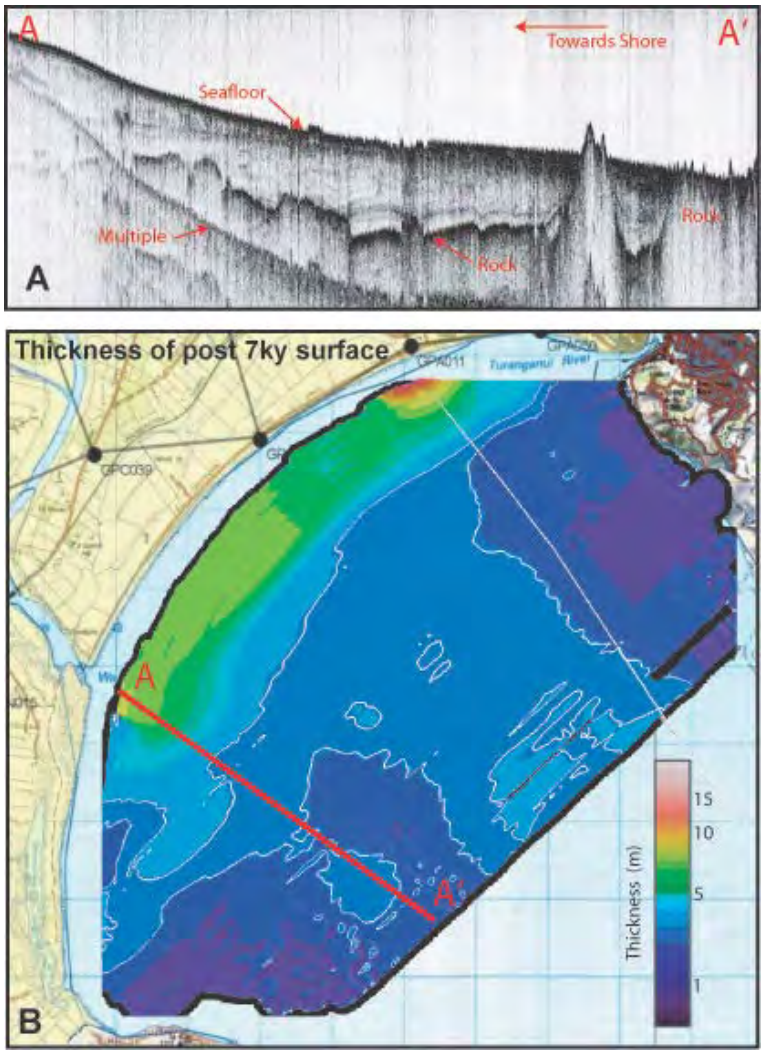

Figure 15 Chirp seismic profiles across Poverty Bay, exemplified in A-A', show rock near the surface of the seafloor and minimal sediment preserved above (J. McNinch, unpubl. data).

Gisborne city is situated at the eastern corner of the triangular shaped coastal plain, the Poverty Bay Flats, which are actively tilting westward and trapping substantial volumes of Waipaoa River sediment (*Brown*, 1995; *Berryman et al*., 2000; *Wolinsky et al*., 2010). The structure controlling the westwards tilt is not understood – there is no evidence for north-striking active faults along the eastern side of the Plains, but evidence that this marks a significant tectonic hingeline is provided by generally higher post-glacial river incision rates in the eastern Waipaoa River catchment (*Marden et al*., 2008).

The hill country surrounding the floodplain is composed predominantly of highly erodible Miocene and Pliocene rocks, with localised early to middle Quaternary lake deposits (*Mazengarb and Speden*, 2000; *Kennedy et al*. 2008). In the headwaters of the Waipaoa River catchment and further north are Paleogene and Late Cretaceous sediments, most of which have been part of the East Coast Allochthon. Few active faults have been mapped in the Raukumara Peninsula (Figure 16), partly the result of poor preservation because of the high erosion rates. Most active faults are interpreted to be normal faults formed as a consequence of the rapid uplift of the Raukumara Range and related extensional strain (*Thornley*, 1996; *Berryman et al.*, 2009). Only one fault has been trenched, the Repongaere Fault (Figure 16), which has a low slip rate (0.1 mm/yr) and long recurrence interval (4490-6900 years), considered typical for the Raukumara Range faults (*Berryman et al.*, 2009).

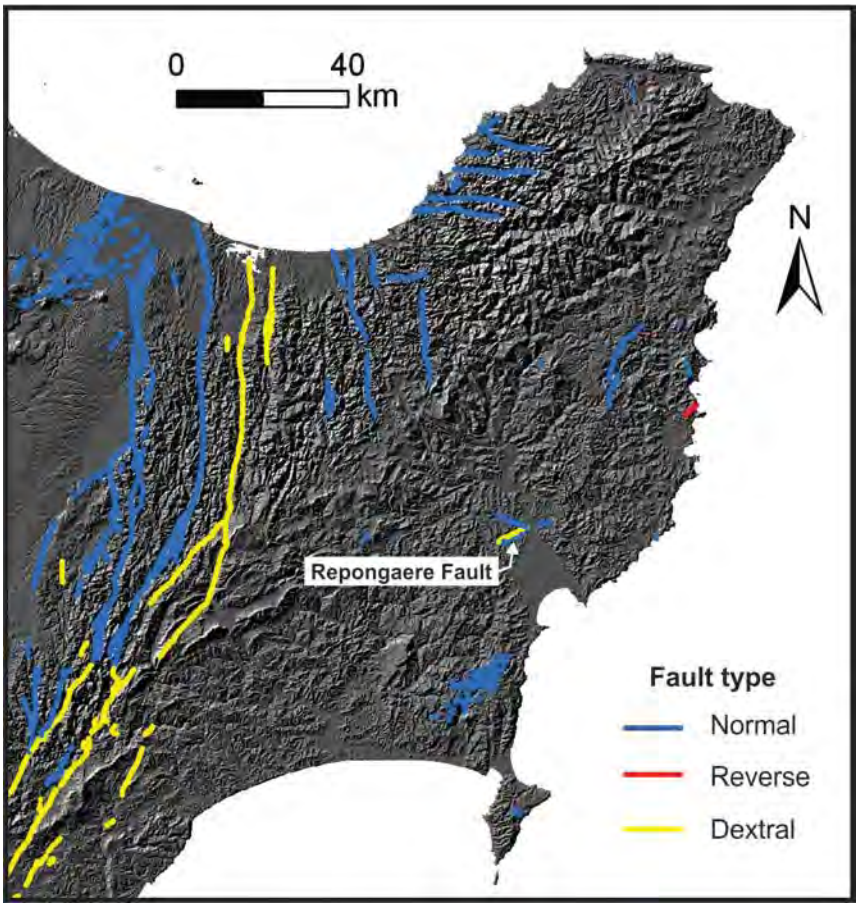

Figure 16 Raukumara Peninsula active faults, from the GNS Active faults database (http://maps.gns.cri.nz/website/af/viewer.htm).

3.2 STOP 1/2: MORERE HOT SPRINGS

The Morere hot springs (Figure 17) were “discovered” in 1889 although the hot waters have been traditionally used by Maori for centuries. Since 1897 the area has been developed as baths and, in earlier times, the waters were also ingested by people suffering from goitre or who were in the last stages of syphilis. In the early 1900s, a bath house was lit by methane from the springs. The baths have a history of being rebuilt after several events of destructive floods, storms and landslides (*Rockel*, 1986). The hot and cold springs are distributed in 55 hectares of a 364 hectare conservation bush reserve known for enclosing one of the last tracts of native bush in the east coast of the North Island. The native trees include rimu, matai, totara, kohekohe, tawa and a large area covered by nikau palm groves.

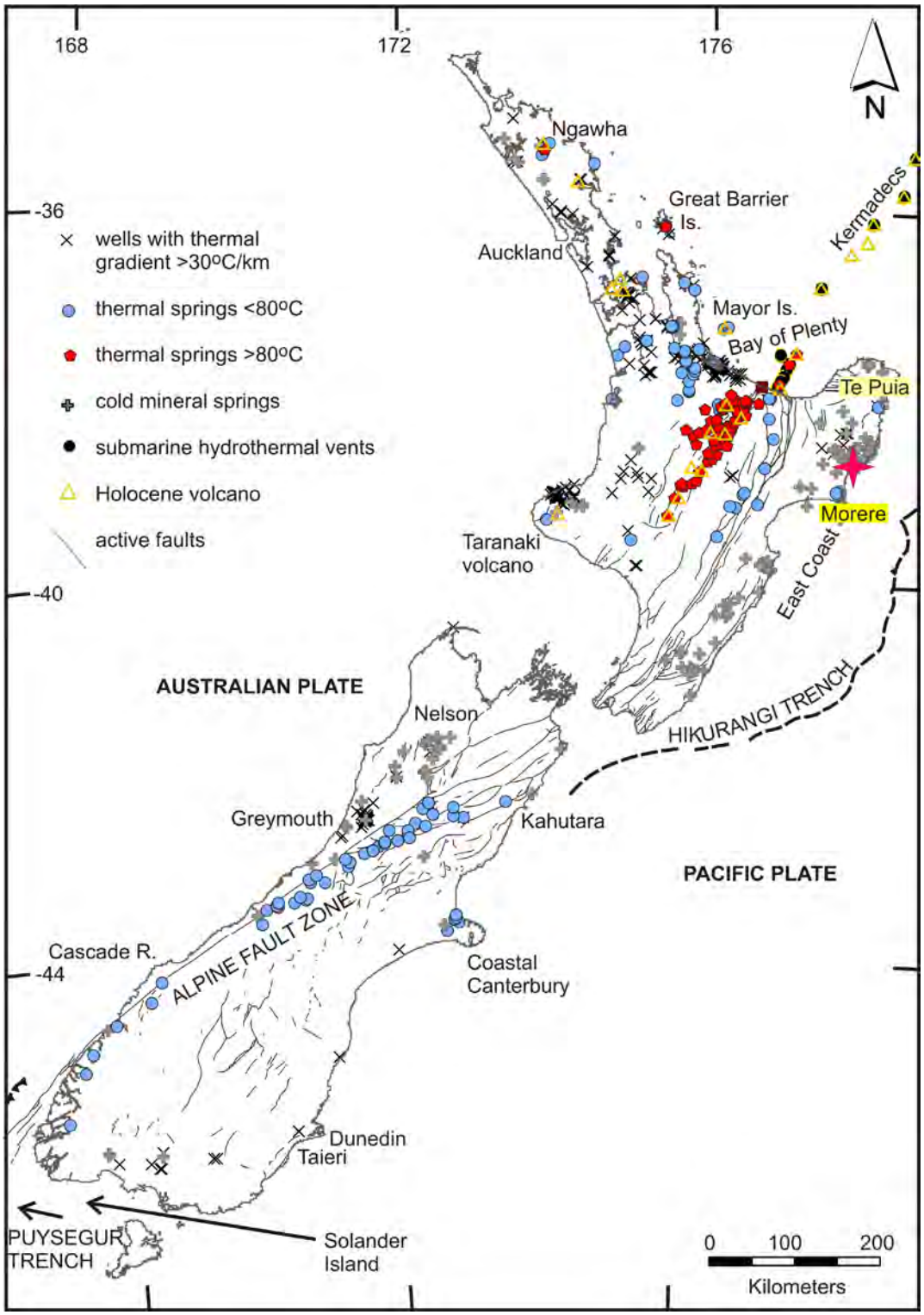

Figure 17 Location of cold and thermal springs in New Zealand including the only two thermal spring systems in the Hikurangi Accretionary Prism in the East Coast of the North Island: Morere and Te Puia. Also shown are Holocene volcanoes, active faults and the location of wells with thermal gradients >30oC/km. Pink star marks the location of Gisborne (adapted from Reyes et al, 2010).

The Morere springs emerge from Middle Miocene mudstones and sandstones on the southern flank of the Morere anticline, on the banks of the Mangakawa Stream (Figure 18). Morere springs overlie a region where the accumulated slow slip on the plate interface, from 2002-2010, is about 150 mm/yr (Figure 23).

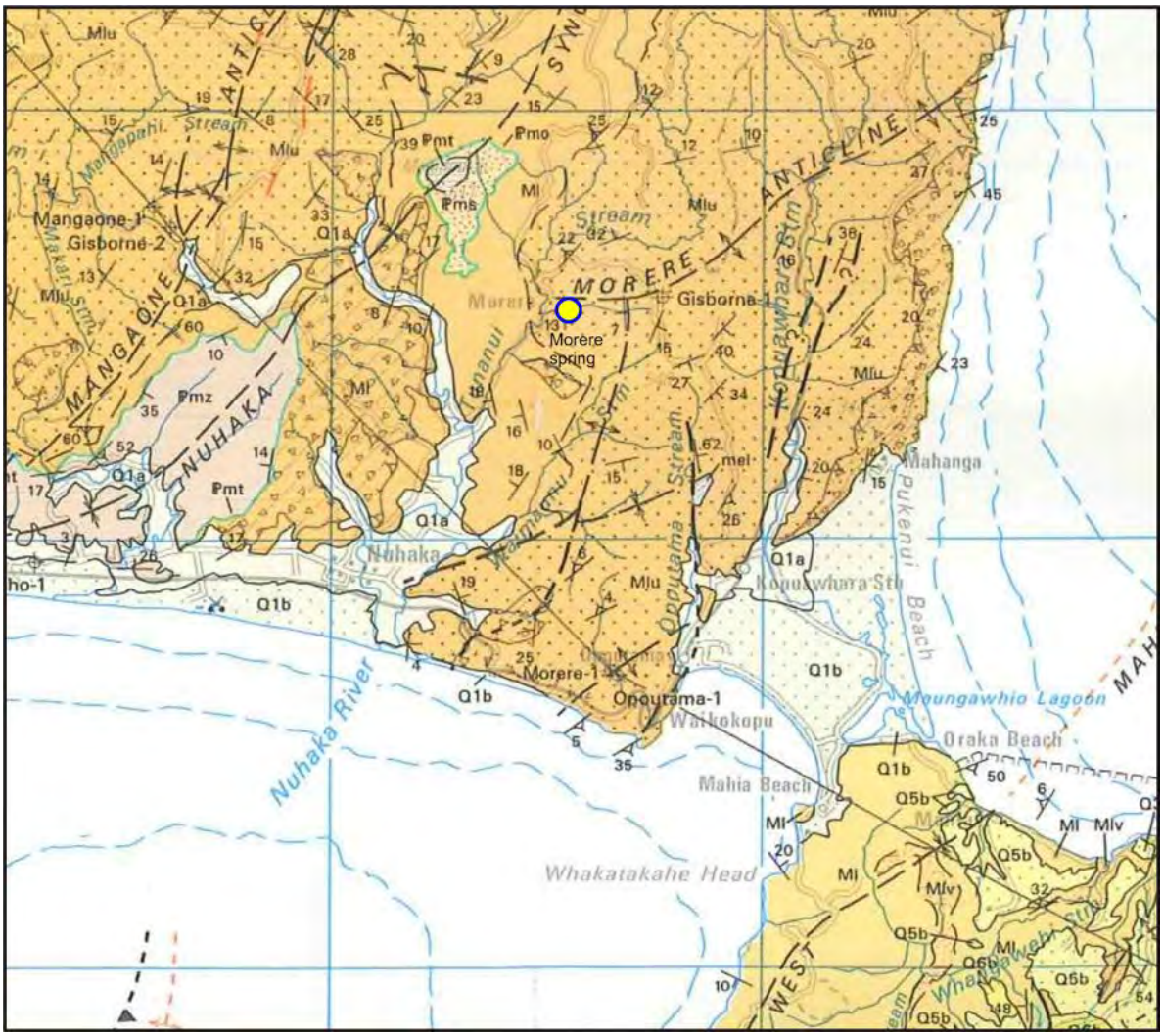

Figure 18 Geology in the vicinity of Morere springs (taken from Mazengarb and Speden, 2000). Yellow circle shows location of Morere springs. Grid is 10 km.

Maximum discharge temperature is 50.6ºC (although as high as 62ºC was reported in the past by Mongillo and Clelland, 1984) and mass flow is about 175 L/min (Table 1). Springs in Morere discharge CH_4 gas and neutral pH Na-Cl aqueous solutions containing high concentrations of Cl, Br, I, B, Ba, Ca, Cs, I, Li, Rb, and Sr, enriched in D and $\delta^{18}O$ with respect to meteoric water (Table 1).

The least diluted forearc subducted waters in the Hikurangi accretionary prism are discharged in Morere, characterised by unusually high Cl, I and Br contents (Figure 19), high Br/Cl, Br/B and I/Cl ratios from porewaters and positive $\delta^{18}O$ contents indicative of about 40% contribution from clay water of hydration (Reyes et al., 2010). The unusually high Cl, Br and I concentrations of Morere springs can be attributed to the central sector of the Hikurangi forearc as being most open to the subduction wedge (*Giggenbach et. al.*, 1993). Gases entrain high amounts of mantle volatiles (34%) probably originating from a fracture plane separating the overriding from the subducting plate (*Giggenbach et al.*, 1993). Forearc subduction zone aqueous solutions heated at depth rapidly ascend along deeply-penetrating permeable fractures in Morere. Apparently, the more permeable the structure and the greater the mass flow in mineral springs of the Hikurangi accretionary prism, the faster the ascent of heated waters to the surface, such that less heat is lost by the rising fluids prior to discharge (*Reyes et al.*, 2010). Temperatures at depth are estimated to be 100 ± 20°C although carbon isotopes imply higher-temperature thermogenic processes at depth (*Lyon et al.*, 1992).

Table 1 Physical characteristics and chemical and isotopic compositions of Morere thermal aqueous solutions, compared to seawater (from Reyes et al., 2010).

Parameters	Morere	Seawater
Elevation (m)	100	0
Discharge T(oC)	50.6	Ambient
Flow (L/min)	175	--
pH(20oC)	6.95	--
Chemical Composition	(mg/kg)	(mg/kg)
Li	4.8	0.08
Na	6847	10870
K	107	504
Rb	0.25	0.08
Cs	0.04	0.0003
Ca	2416	422
Mg	72	1236
Sr	206	5.7
Ba	4.5	0.012
B	37	4.5
HCO3	43	118
SiO2	31	
SO4	0.17	2669
F	1.1	1.3
Cl	16610	19406
Br	63	64
I	41.1	0.06
Isotopic Composition	‰	‰
δD	-12.6	0
$\delta^{18}O$	+4.6	0

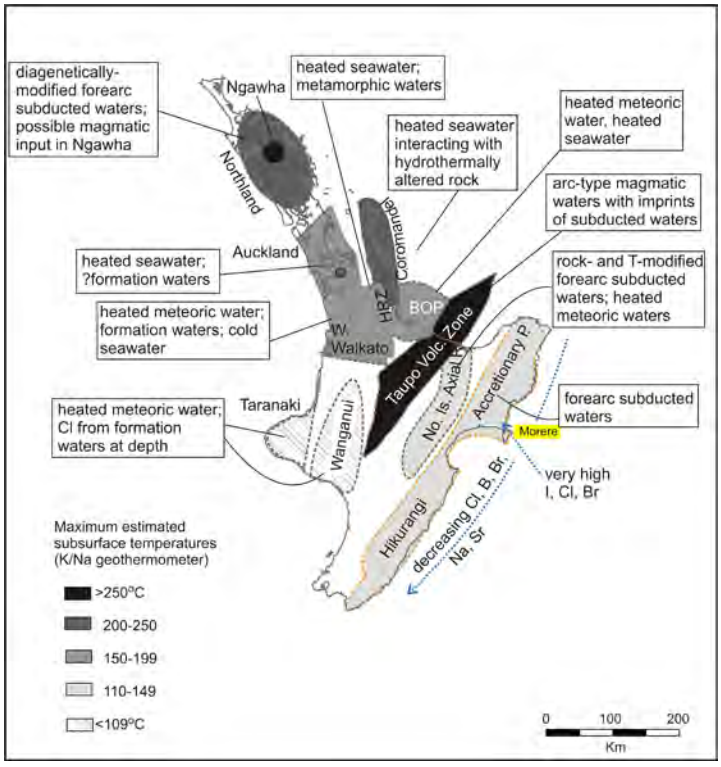

Figure 19 Map of North Island showing variations in chemical compositions of aqueous solutions across different tectonic settings and predicted subsurface temperatures, including the Hikurangi accretionary prism. Morere springs have the highest I, Cl and Br contents along the accretionary prism (adapted from Reyes et al 2010).

3.3 STOP 1/3: MAHIA PENINSULA

One of the most well-known sequences of Holocene marine terraces in New Zealand (and world-wide) is at Mahia Peninsula, North Island, New Zealand. At Mahia we can see at least five coastal platforms that have been coseismically uplifted by the offshore Lachlan Fault during the Holocene (Figures 20, 21). There is also a spectacular sequence of Pleistocene marine terraces (Figure 22) overlying late Miocene volcaniclastic turbidites and Pliocene shelfal limestones. Mahia Peninsula lies directly above a zone of slow-slip on the plate interface (Figure 23).

Mahia Peninsula sits near the boundary between the inner and outer forearcs. Within and east of Mahia Peninsula the outer forearc structure is dominated by structural highs cored by splay faults, paired with inboard sedimentary basins (*Barnes, et al*., 2002; *Henrys, et al*., 2006). The Lachlan Fault is one such splay fault (Figures 23–24) and it is responsible for uplift of the Mahia Peninsula and the Lachlan Ridge (a submarine structural high located southwest along-strike from Mahia Peninsula, *Barnes, et al*., 2002). West of Mahia Peninsula the uplifted inner forearc consists of folded and imbricated Paleogene passive margin and Neogene forearc basin strata abutted against the forearc backstop formed by the Mesozioc greywacke axial ranges.

Mahia Peninsula is composed of Miocene-aged accreted siltstone and sandstone sequences, which have been uplifted and moderately deformed (*Mazengarb and Speden*, 2000). The Peninsula is fringed by up to five mid to late Holocene marine terraces and also displays uplifted early Holocene transgressive estuarine sediments (*Berryman*, 1993a). Berryman (1993a) correlated the Holocene marine terraces around the Peninsula and demonstrated a general westward- (inboard-) tilt (Figure 26). A similar westward tilt across the Peninsula is displayed by the Pleistocene marine terraces. The inland topography of the Peninsula is dominated by Pleistocene marine terraces, which range in age from 40 to 210 ka and form ~40% of the land area (*Berryman*, 1993b).

Complimentary investigation of faunal and sediment zones on the modern shore platform and the excavation of trenches across a sequence of four marine terraces at Table Cape have allowed detailed paleoenvironmental facies mapping of terrace cover beds based on modern analogue samples (*K. Berryman*, unpubl. data). Seven sediment zones and seven macrofaunal zones were delineated on the modern shore platform. Sediment and or macrofauna samples were collected from almost all sedimentary units on the marine terraces and, in most cases, close correlations could be made between the fossil and modern shore platform zones. Extensive dating of terrace deposits and additional age constraint provided by airfall tephras indicates the highest terrace, T1, was uplifted 3500 ± 50 cal. yrs B.P., T2: 1850 ± 50 cal. yrs B.P., T3: 1400 ± 100 and T4: 250 ±100 cal. yrs B.P. A terrace preserved elsewhere on Mahia Peninsula (but not at Table Cape) has an age of 5000-5500 cal. yrs B.P.

Currently there is little overlap in the earthquake records of the mainland coast and Mahia Peninsula; the Opoho and Opoutama sites (next field trip stop) do not contain high-resolution records of the last ~5000 yr, and the Mahia record does not extend back beyond the last ~5500 yr. There is a possibility that an event at ca. 5550 yr B.P. involved subsidence on the mainland coast and uplift at Mahia Peninsula (Figure 26). Further age control, particularly clarifying the timing of the event in comparison with deposition of the Whakatane Tephra, and further records are required to investigate synchroneity more thoroughly.

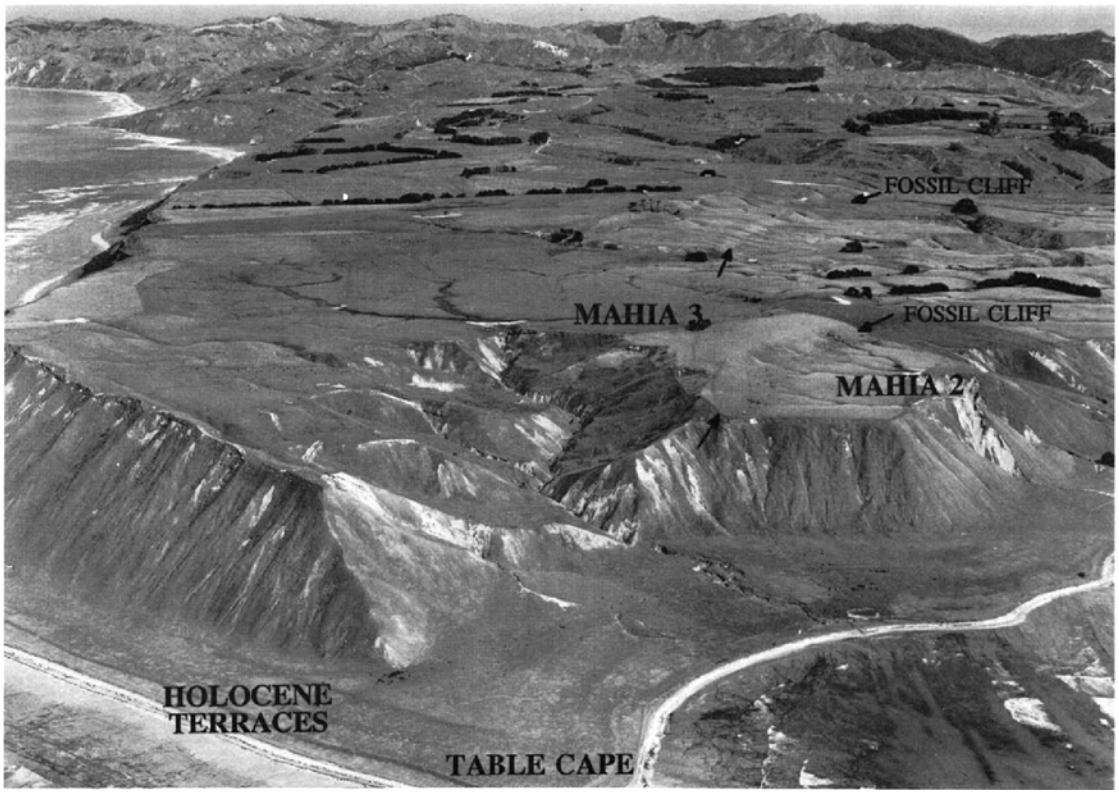

Figure 20 Oblique aerial photo looking west across Mahia Peninsula. In the foreground are uplifted Holocene marine terraces and in the mid-ground are Pleistocene marine terraces. *Photograph*: Lloyd Homer.

Figure 21 Table Cape, Mahia Peninsula. View from the modern marine platform (foreground) looking back towards the Holocene terraces (mid-ground) with the Pleistocene marine terraces in the background. *Photograph*: Kate Clark.

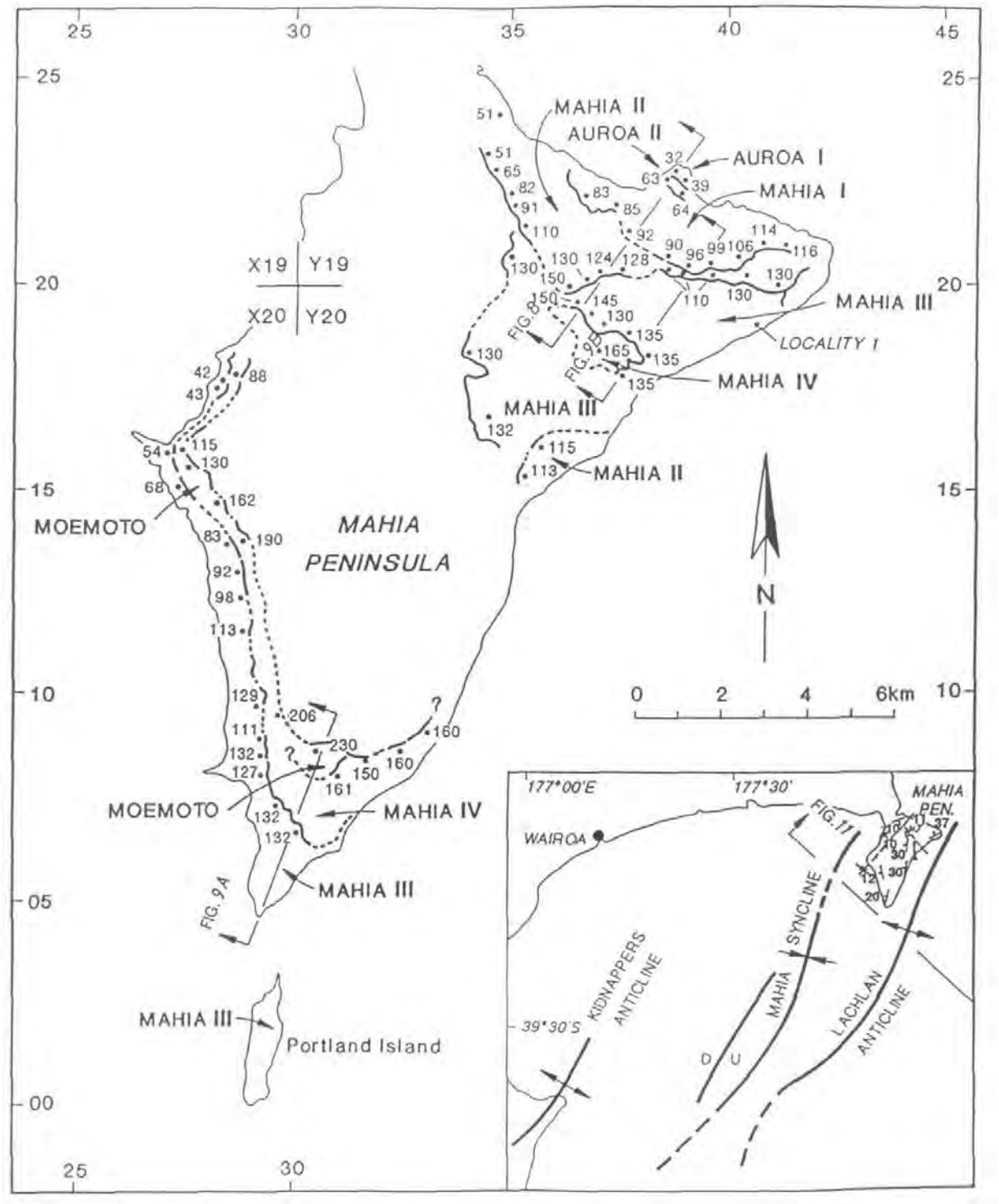

Figure 22 Fossil shorelines and distribution and altitude of late Pleistocene marine terraces at Mahia Peninsula. From Berryman (1993b).

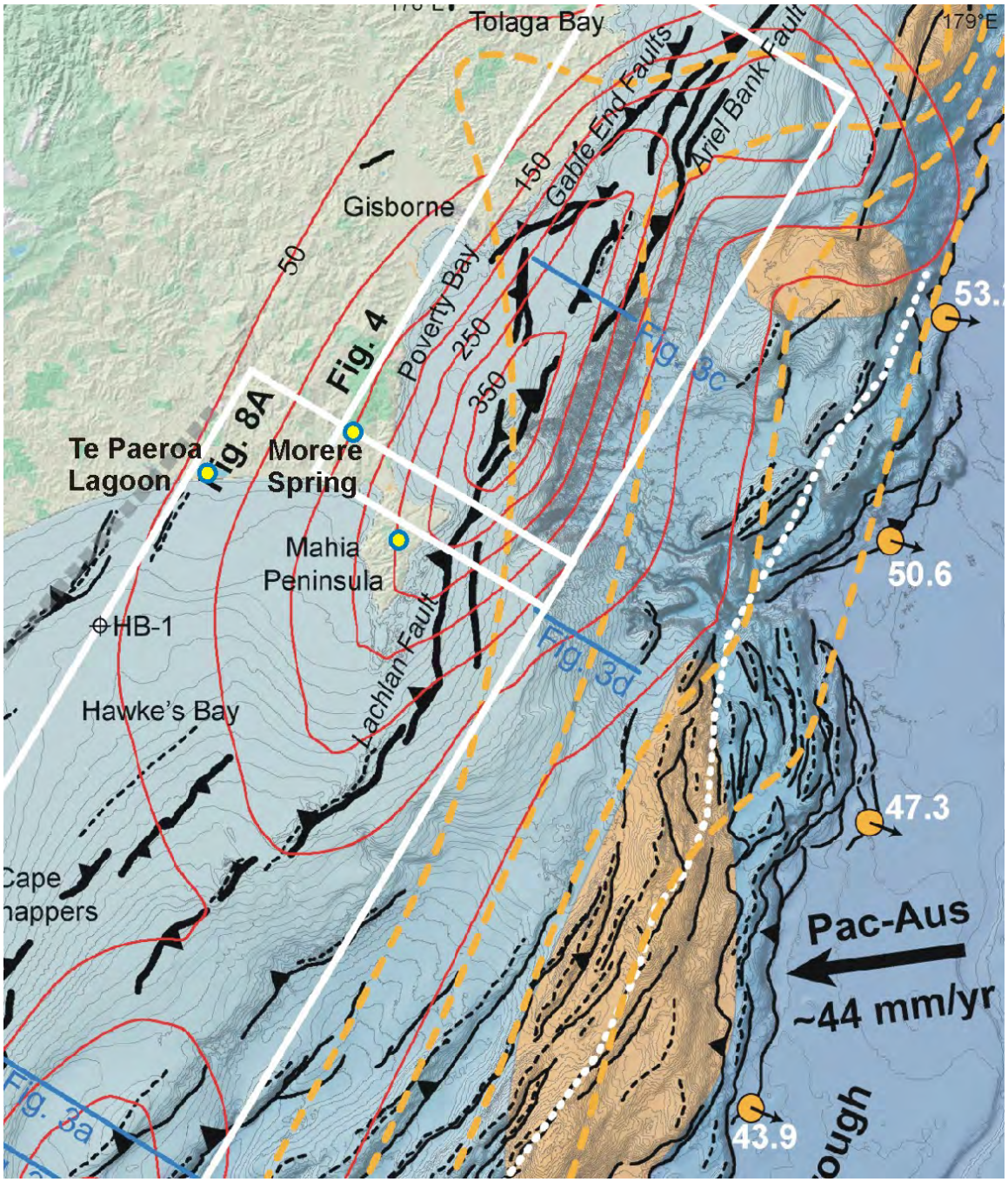

Figure 23 Tectonic setting of Mahia Peninsula in relation to slow slip events. Figure extracted from Mountjoy and Barnes (2011): Main tectonic features of the Hikurangi margin between Cape Turnagain and Tolaga Bay. Black line work shows active fault traces (solid) and fold crests (dashed), dominated by thrust faulting in the offshore fore arc (Barnes et al., 2002; Mountjoy and Barnes, 2011) and onshore by the North Island Dextral Fault Belt (http://data.gns.cri.nz/af/). The dashed white line at midslope is the boundary between the late Cenozoic accretionary wedge and the deforming backstop, after Barnes et al. (2010). Dashed orange lines are contours of interseismic coupling coefficient (8ic), orange dots with associated numbers show total margin orthogonal convergence rates (Wallace et al., 2009), and red contours show 50 mm contours for total recorded slip in slow slip events between 2002 and 2010 (Wallace and Beavan, 2010). Solid orange polygons are the interpreted footprints of seamounts in the incoming Pacific Plate (Barnes et al., 2010; Bell et al., 2010).

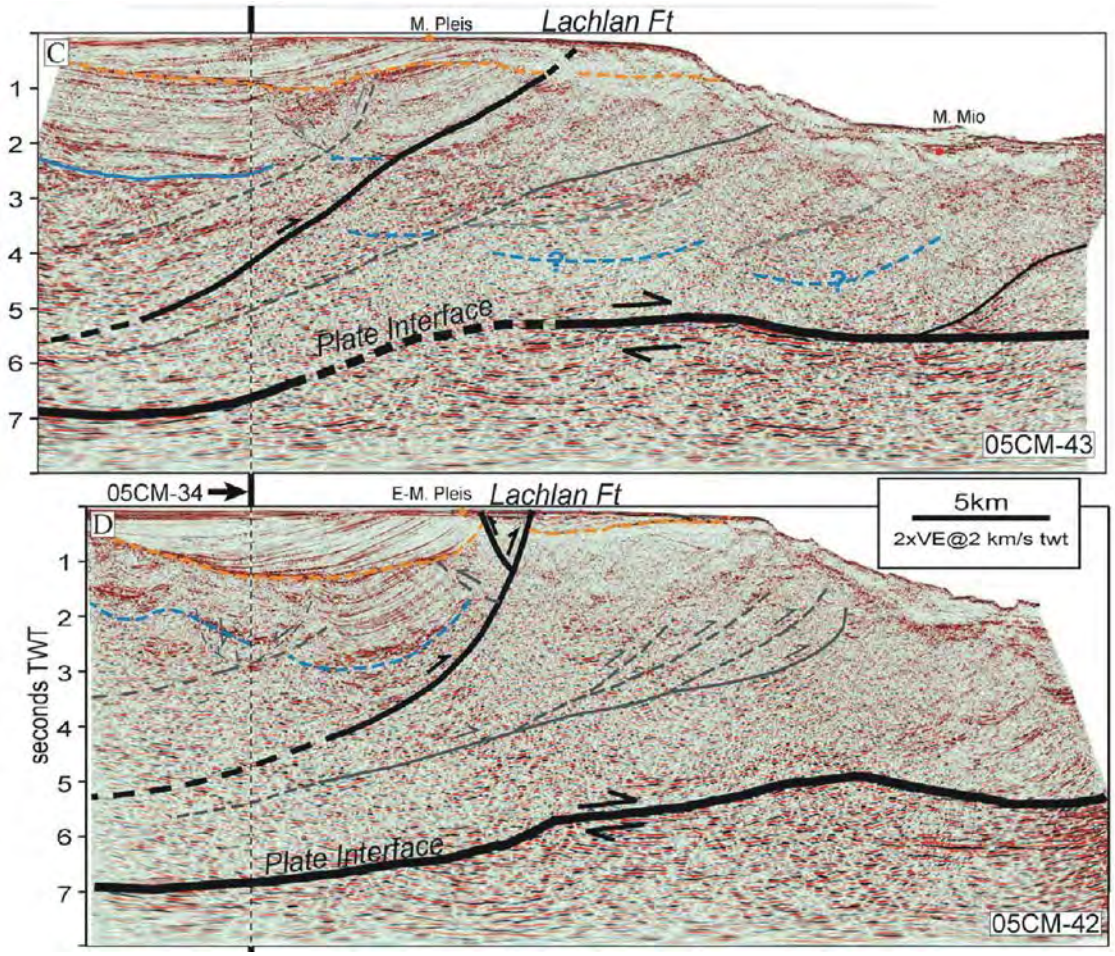

Figure 24 Figure extracted from from Mountjoy and Barnes (2011): Interpreted multichannel seismic profiles illustrating the structure of the Lachlan Fault north of Mahia Peninsula.

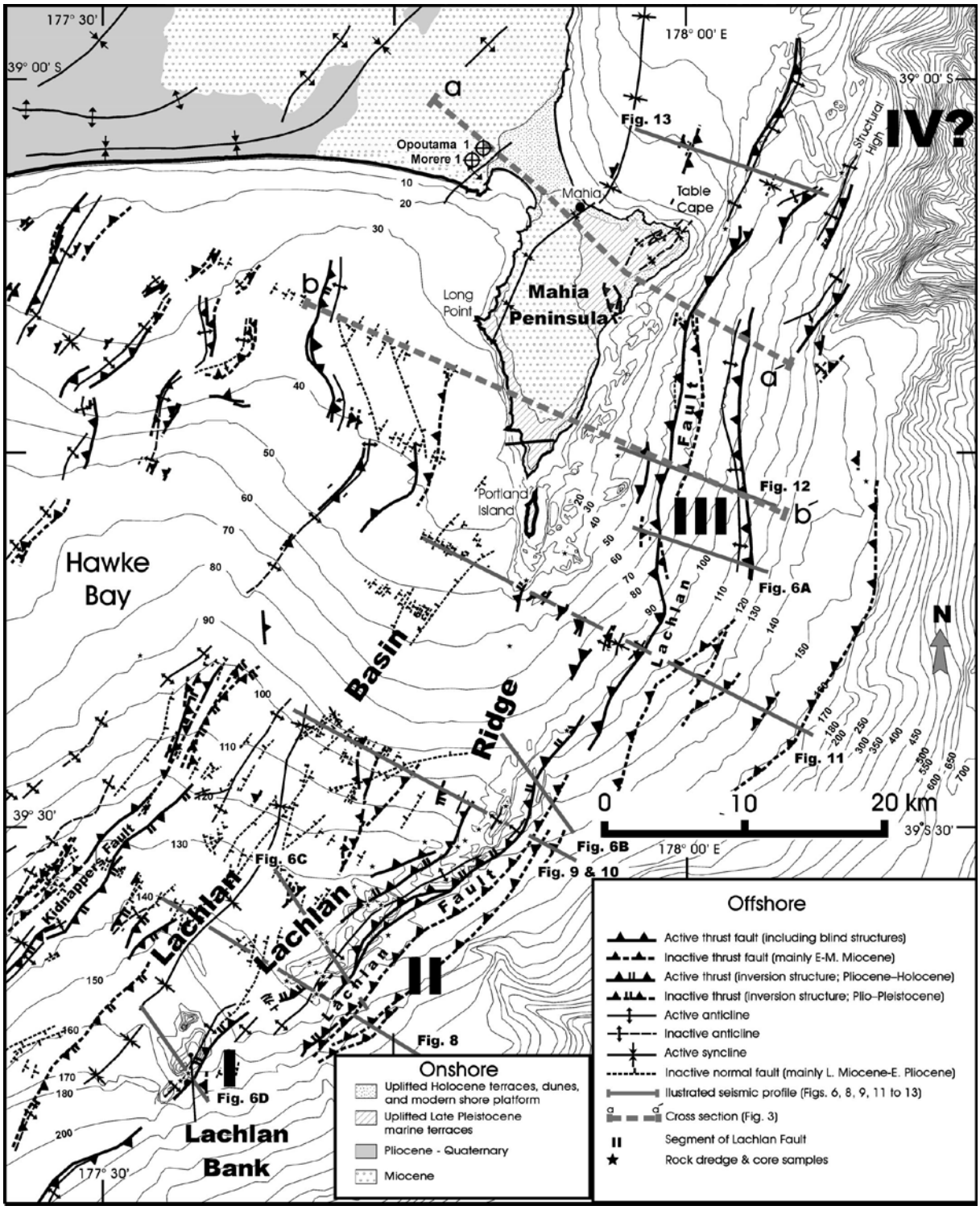

Figure 25 Structural map of Mahia Peninsula, Lachlan Ridge, Lachlan Basin, and adjacent areas. Bathymetry contours are in metres. Large, bold roman numerals are structural segments of the Lachlan Fault. Figure from Barnes et al. (2002).

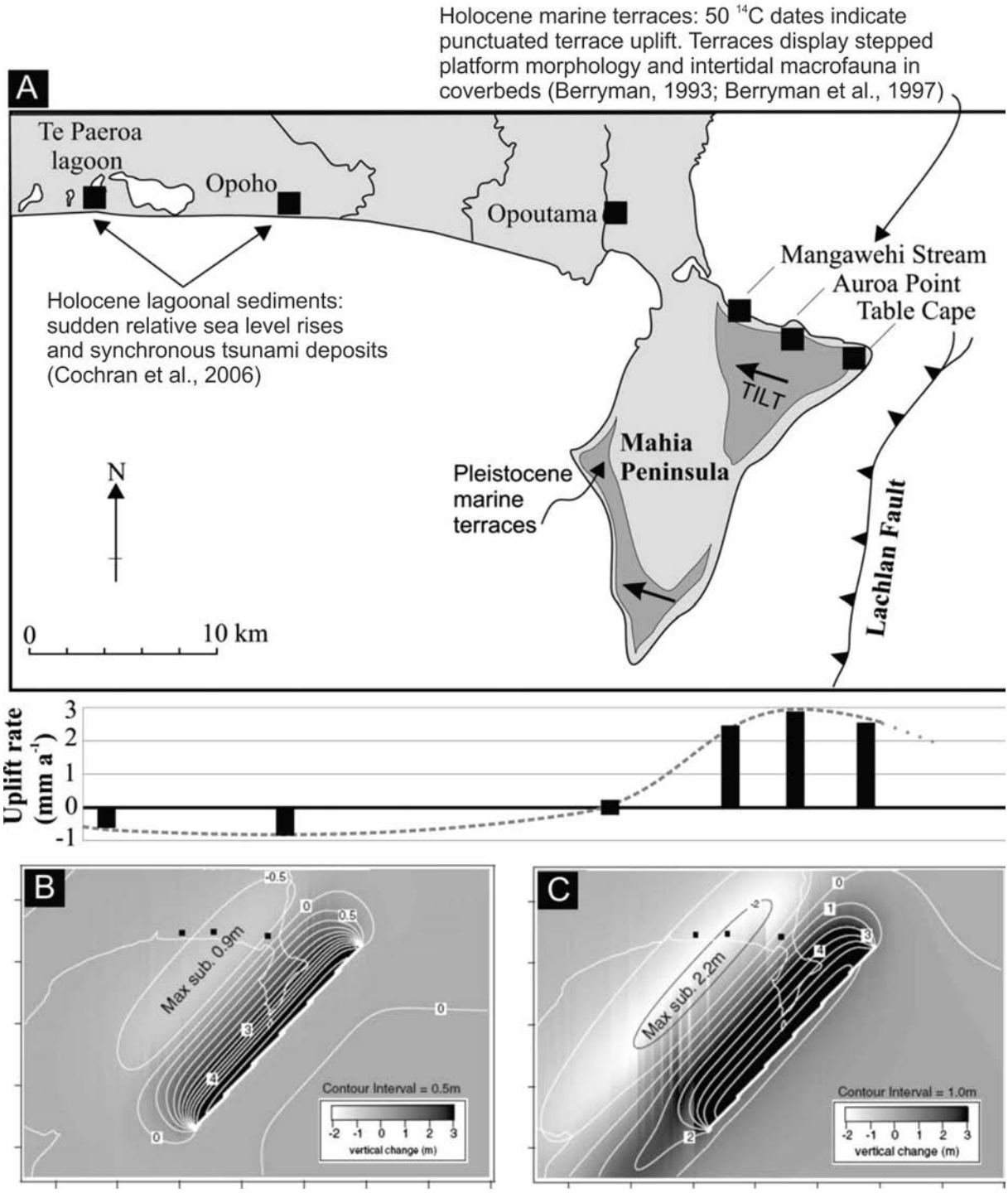

Figure 26 (A) Map and coastal deformation profile across the Mahia Peninsula. Each black square on the map corresponds to an uplift or subsidence rate on the graph below. The uplift rates represent the average rate of deformation over several earthquake cycles since 7 ka, the approximate time of eustatic sea-level stabilisation in the New Zealand region. Data sourced from Berryman (1993) and Cochran et al. (2006); see Table 2. (B) Forward elastic-dislocation model of vertical deformation from 8 m of slip on the Lachlan Fault. (C) Forward elastic-dislocation model of vertical deformation from 8 m of slip on a combination of the subduction interface and the Lachlan Fault. See Cochran et al. (2006) for more details on the modelling parameters. Black dots represent Te Paeroa, Opoho and Opoutama, respectively. Figure from Clark et al. (2010).

3.4 STOP/DRIVE-BY 1/4: WAIROA LAGOONS

Investigation of subsiding parts of the Hawke's Bay coastline (generally in-board of the uplifted zone) have provided evidence for subsidence and marine submergence events throughout the Holocene (*Cochran et al*., 2006; *Hayward et al*., 2006). Subsidence events have provided the most robust geological evidence for the occurrence of preinstrumental plate interface earthquakes in other parts of the world (e.g., Cascadia, Japan, Sumatra and Chile).

Evidence for sudden subsidence in northern Hawke's Bay includes tsunami deposits overlain by chaotically mixed, reworked sediment that appears to have been deposited rapidly at tidal inlet sites 10 km apart at Te Paeroa and Opoho Lagoons (Figures 27–29). We will be driving past both of these lagoons on our way between Mahia and Wairoa (however they may be difficult to see from the road).

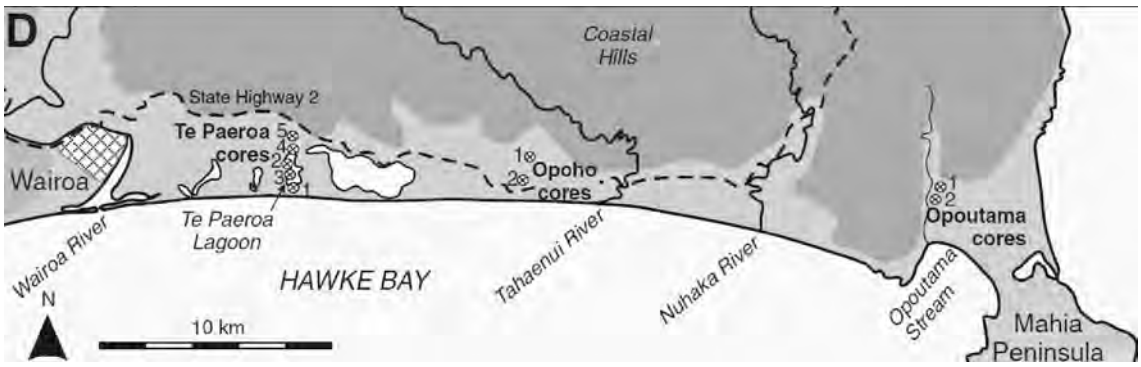

Figure 27 Location of cores collected to study paleotsunami and cosiesmic subsidence in the Cochran et al. (2006) study.

One subsidence event (at about 7000 cal yrs BP) has been correlated between northern and southern Hawke's Bay, indicating either a single long rupture or two or more ruptures that occurred within decades of each other (Figure 30). This event (or pair of events) also coincides with the formation of two landslide-dammed lakes in central and northern Hawke's Bay. Elastic dislocation models that fit the subsidence amplitudes imply ~8 m of slip on the interface that largely occurs offshore, terminating beneath Mahia Peninsula (Cochran et al., 2006; Wallace et al., 2009; Figure 31). If we assume that the subsidence events that occurred at ~7000 cal. years BP in northern and southern Hawke's Bay were indeed synchronous (although the resolution of radiocarbon dating is not good enough to prove this) and occurred on a single structure, then an interface source is likely. Such an event might have affected >100 km of coastline and would have had a magnitude of at least MW 8.0.

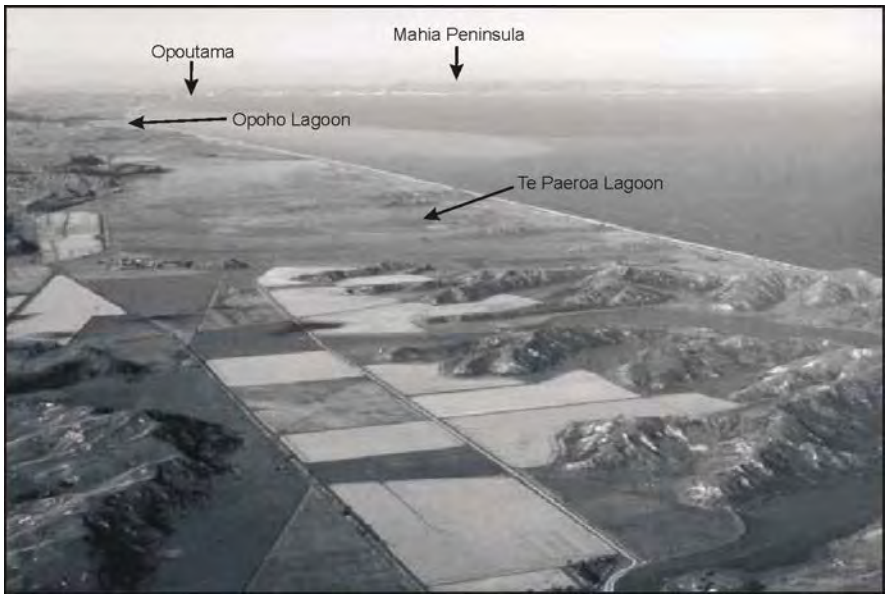

Figure 28 Oblique aerial view of the coastal plain, looking east from near Wairoa. *Photograph*: Lloyd Homer.

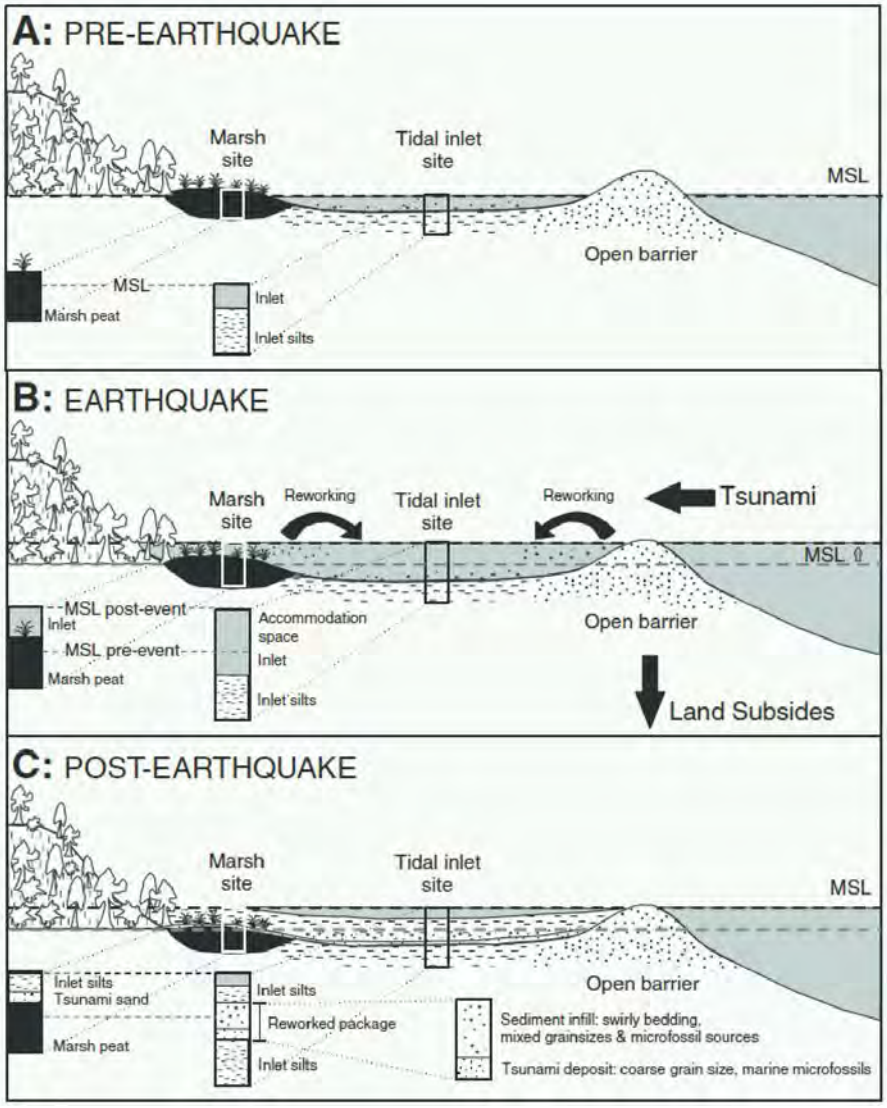

Figure 29 Idealized illustration of the effects on sedimentation of a coseismic subsidence event and tsunami inundation at marginal marsh and central inlet sites. Cores from Te Paeroa Lagoon and Opoho exhibit characteristics in keeping with the tidal inlet site, whereas previous subduction-earthquake geological studies have generally conformed to characteristics of the marsh site. MSL—mean sea level. From Cochran et al. (2006).

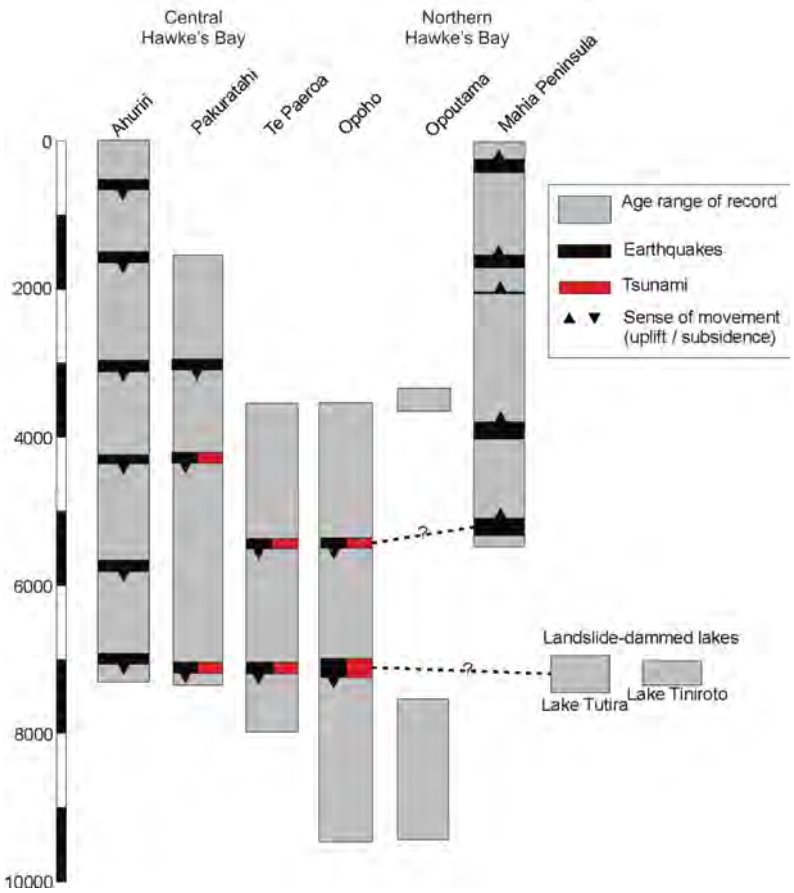

Figure 30 Correlation of Holocene coastal deformation events along the Hawke's Bay coastline. Figure adapted from Cochran et al. (2006) and Wallace et al. (2009). Data from Cochran et al. (2006), Hayward et al. (2006), Berryman (1993a) and Page and Trustrum (1997).

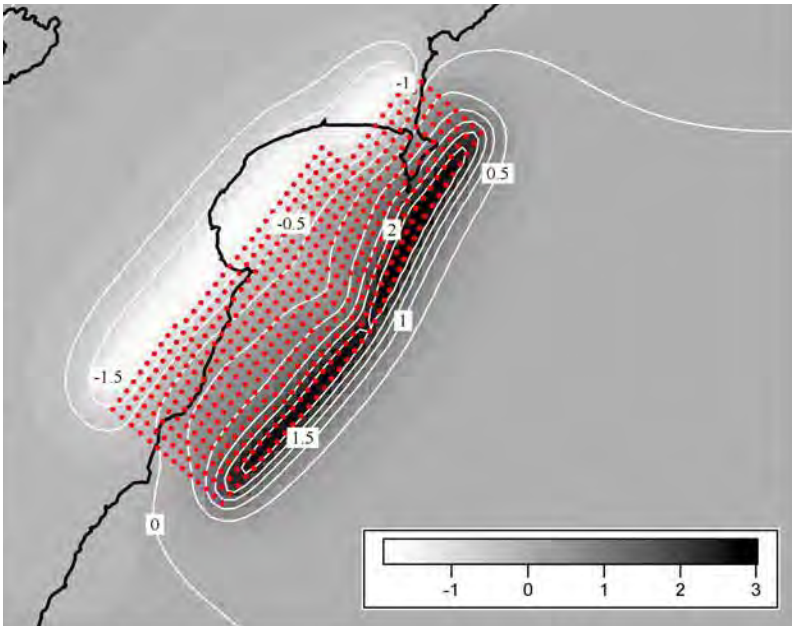

Figure 31 Forward elastic dislocation modeling of subduction interface rupture scenario (8 m slip on subduction interface on patches centered at red nodes) to reproduce 0.5–2 m of coseismic subsidence observed at Te Paeroa and Opoho coastal sites in northern Hawke's Bay, with negligible subsidence at Opoutama and uplift at Mahia Peninsula (Cochran et al., 2006), and subsidence at Ahuriri Lagoon in central Hawke's Bay (Hayward et al., 2006). From Wallace et al. (2009).

3.5 STOP 1/5: MOHAKA RIVER TERRACES

By comparison with the low-lying, embayed, lagoonal Wairoa coastal plain that we've just travelled, the coastline along the northwest side of Hawke Bay is marked by steep cliffs and relatively narrow river mouths. This coastline, which is inboard of the area of the slow slip events, is also devoid of marine terraces.

The Mohaka River is one of several large rivers that have their headwaters in the basement-cored axial ranges, and then drain generally down the dip-slopes of the gently southeast-dipping Neogene forearc basin sequence, into inner Hawke Bay. The headwaters of some of these rivers are also periodically inundated by ignimbrites from the Taupo Volcanic Zone (*Cutten*, 1994; *Segschneider et al*., 2002a,b), which are subsequently reworked down the rivers; pumice is commonly found at the river mouths today.

Active faults in this part of the Hikurangi Margin are generally confined to either the North Island Dextral Fault Belt (NIDFB) in the axial ranges (http://maps.gns.cri.nz/website/af/), or thrust faults in Hawke Bay (Barnes et al., 2002). The latitude of the Mohaka River mouth is approximately where the NIDFB faults start transitioning from being predominantly dextral in the central and southern margin, to being predominantly normal in the north, where they interact with the Taupo Rift (*Mouslopoulou et al*., 2007, 2008, 2009).

Another feature of river mouths in inner Hawke Bay is the presence of flights of fluvial terraces, and the most spectacular of these is at the Mohaka River mouth (Figure 32). These terraces are notable for both their number and their relatively high elevation above river level (Figure 32, 33). At most river mouths around the New Zealand coast (e.g., the Waipaoa River near Gisborne) terraces are buried by post-glacial valley infill marine and fluvial deposits. This is a function of a combination of the primary river gradients at times when sea level was significantly lower than present, and in some cases, such as the Waipaoa and Wairaoa River mouths, subsidence. A survey of the relative height difference between the Last Glacial Maximum terrace, T1, and the present day river level (Figure 33), highlights the anomalously high terraces at the Mohaka River mouth (*Litchfield and Berryman*, 2006).

Figure 32 Mohaka River mouth fluvial terraces. T1-T4 are aggradation terraces with surface ages of ~18 (T1), ~31 (T2), ~55 (T3), and ~90 or ~140 (T4) ka. TpA = 1.7 ka Taupo Alluvium terrace. *Photograph*: Lloyd Homer.

The mechanisms for the relatively high fluvial terraces at the mouth of the Mohaka River are not fully explained, but we suspect it is a combination of tectonic uplift and coastal erosion (*Litchfield and Berryman*, 2006; *Litchfield et al*., 2007; *Litchfield*, 2008). Evidence for tectonic uplift comes from the presence of flights of terraces here, as well as at river mouths to the southwest and northeast. The aggradation terraces formed during cool periods when vegetation was reduced and erosion rates were high (e.g., *Pillans*, 1991; *Litchfield and Berryman*, 2005). Assuming that aggradation filled the valleys to similar levels during each cool period, the presence of flights of terraces suggests that successive terraces have been uplifted out of reach of the river during the next cool period. On this basis, the height difference between pairs of terraces provides a rough measure of uplift rate. The uplift rate calculated from the height difference between the surfaces (treads) of T3 and T1, divided by the difference in age, is 0.6 ± 0.2 mm/yr at the Waikari and Mohaka River mouths, and -0.1 ± 0.1 mm/yr at the Waihua River mouth (*Litchfield*, 2008) (Figure 33b). The rate at the Waihua River mouth indicates it is approximately at the hinge zone between uplift in inner Hawke Bay and subsidence in the north (Wairoa coastal plain). Given the inboard location of inner Hawke Bay, we infer that the uplift is occurring aseismically, as the result of regional, subduction-related processes, such as sediment underplating (Litchfield et al., 2007; Litchfield, 2008).

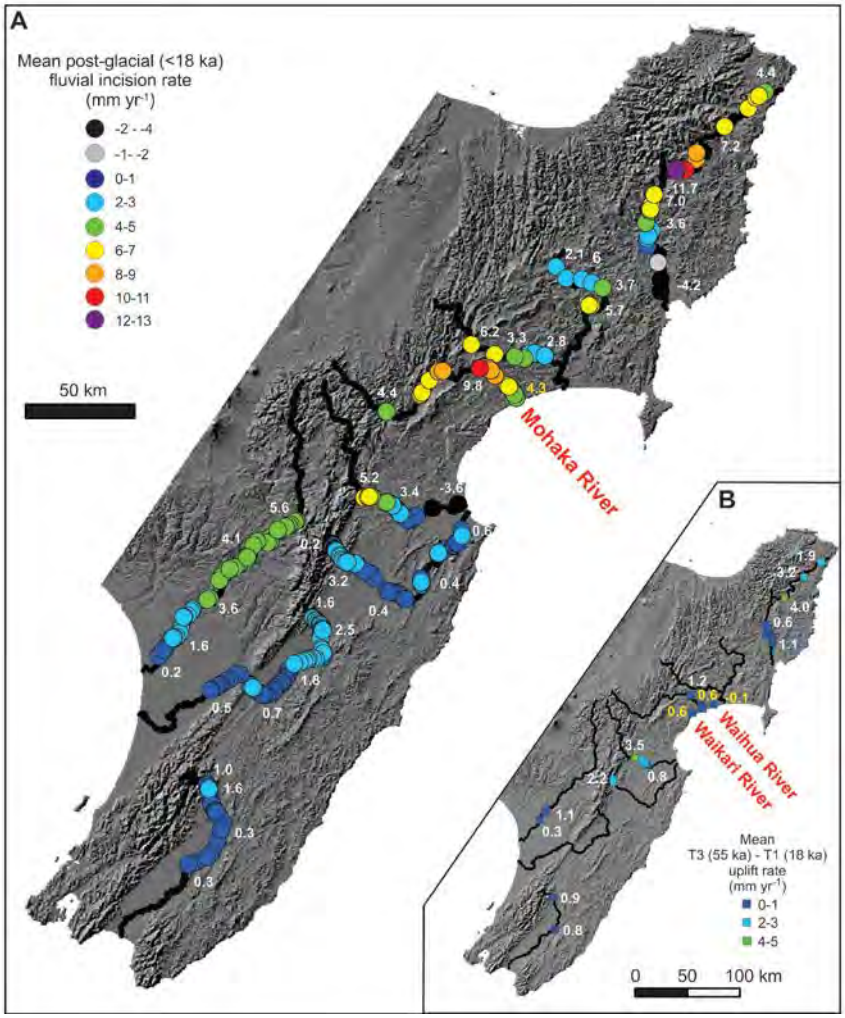

Figure 33 Mean post-glacial river incision rates calculated from the height difference between the LGM fluvial terrace and the present day riverbed. B) Mean uplift rates calculated from the difference between the treads of pairs of fluvial terraces (T3 and T1) assumed to have formed at the same altitude. Adapted from Litchfield and Berryman (2006) and Litchfield (2008).

There are several lines of evidence for relatively high coastal erosion rates along the inner Hawke Bay coastline. The first is that the surveyed historical (~1880 to 1980) rate is relatively high, 0.02 to 0.5 m/year (*Gibb*, 1984), supported by anecdotal evidence from farmers who constantly have to move back their fences! The second is the general geomorphology, with the relatively straight coastline and steep cliffs. Third is the absence of marine terraces, which should be expected to have formed, given the evidence for tectonic uplift outlined above. Finally, the presence of the fluvial terraces perched above the coastal cliff also suggests significant erosion of their downstream continuations. The effect of coastal erosion is to cause a relative drop in base level, which will locally enhance river incision rates, possibly creating knickpoints that propagate upstream. Coastal erosion may be a gradual process, or occur step-wise during large storms or earthquakes; the 1931 Hawke's Bay earthquake (also referred to as the 1931 Napier earthquake) triggered several large coastal landslides along the inner Hawke Bay coast (*Marshall*, 1933; *Hancox et al*., 2002). At the Waikari River mouth to the southeast, an attempt was made to calculate the long-term (7000 years) coastal erosion rate by reconstructing the missing downstream continuation of a fluvial terrace, which suggested a rate of 0.5 ± 0.1 m/yr (*Litchfield*, 2008).

3.6 STOP 1/6: LAKE TUTIRA

Lake Tutira is situated within the gently southeast-dipping Neogene forearc sediments. It is one of a series of landslide-dammed lakes in the eastern North Island, and factors such as its easy access, good historical data (e.g., *Guthrie-Smith*, 1921), and relatively small catchment area (32 km^2) have resulted in it being drilled multiple times for paleoenvironmental studies (e.g., *Page et al*., 1994a; *Page and Trustrum*, 1997; *Wilmshurst*, 1997; *Eden and Page*, 1998; *Gomez et al*., 2002; *Orpin et al*., 2010; *Page et al*., 2010; *Gomez et al*., in press). The high resolution records obtained have resulted in it becoming a key site for Margins Source-to-Sink studies in the eastern North Island (e.g., *Carter et al*., 2010; *Upton et al*., submitted). Most of the results discussed below are from analysis of a long core (27.14 m) taken from the deepest part of the lake (*Orpin et al*., 2010; *Page et al*., 2010). The chronology for upper part was obtained by matching with a short core situated within 10 m, dated by correlation with historical storm and volcanic eruption records, ^{137}Cs, pollen, and diatom analysis (*Page et al*., 1994a). The lower part is dated by twelve tephra layers and three radiocarbon dates.

Radiocarbon dates from wood in the basal sediments date the timing of formation of Lake Tutira, and hence the landslide that formed it (Figure 34), to ~7200 cal. years BP (*Page and Trustrum*, 1997). This date coincides with the timing of a coseismic subsidence event in several cores from the northern and southern Hawke Bay coast (*Cochran et al*., 2006; *Hayward et al*., 2006; *U. Cochran* unpubl. data) (Figure 29). It is therefore tempting to infer an earthquake trigger, possibly even a subduction earthquake event. The 1931 Hawke's Bay Earthquake (see stop 7) triggered several landslides, some of which blocked lakes (Figure 35), although those eventually naturally drained.

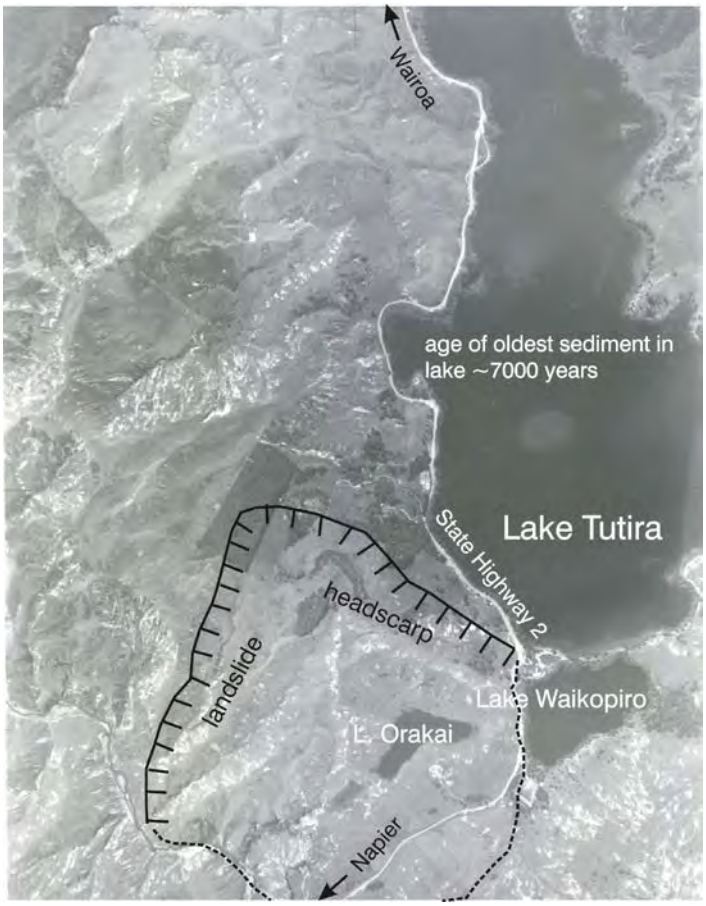

Figure 34 Lake Tutira, which was formed by a landslide damming a stream ca. 7200 yrs BP.

Figure 35 Lake Ngatapa, which was formed by a landslide triggered by the 1931 Hawke's Bay Earthquake. Note the landslides on the slopes in the background. From Guthrie-Smith (1921).

Within the core, multiple sedimentological and paleoecological methods have identified distinct units called homogenites (Figure 36), some of which are interpreted as earthquake-triggered redeposited lake margin sediments (Figure 37) (Orpin et al., 2010). Lake Tutira therefore potentially contains a high resolution paleoearthquake record, but detailed analysis and correlation with paleoearthquakes identified at surrounding sites (e.g., Berryman, 1993a; Cochran et al., 2006; Hayward et al., 2006) has not yet been undertaken.

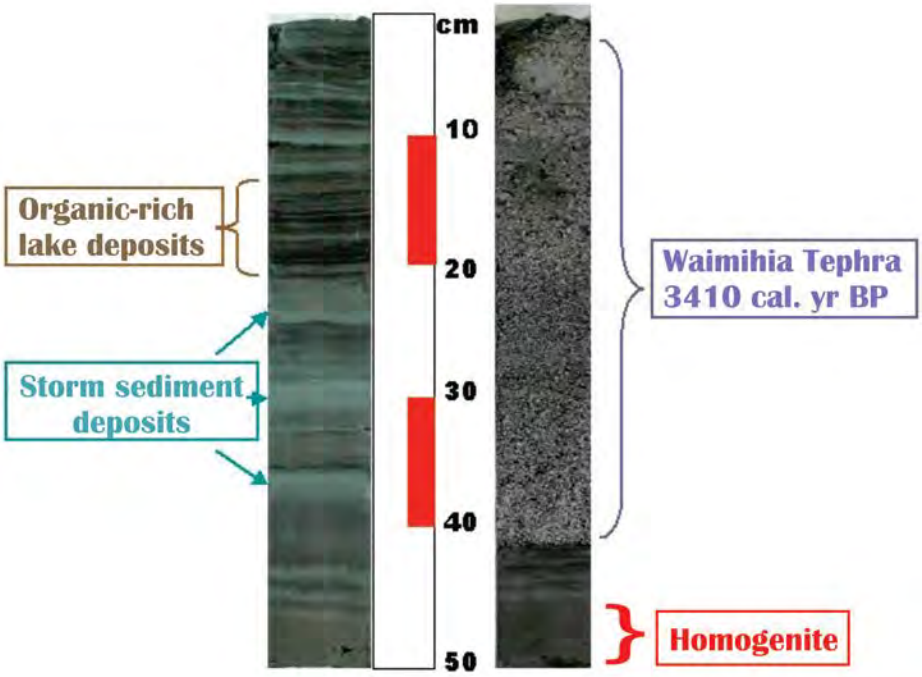

Figure 36 Sections of the 27 m-long Lake Tutira core (LT24) showing homogenites and tephra (right), "background" lake deposits, and storm sediment deposits (left), at a depth of 1191 cm. From M. Page.

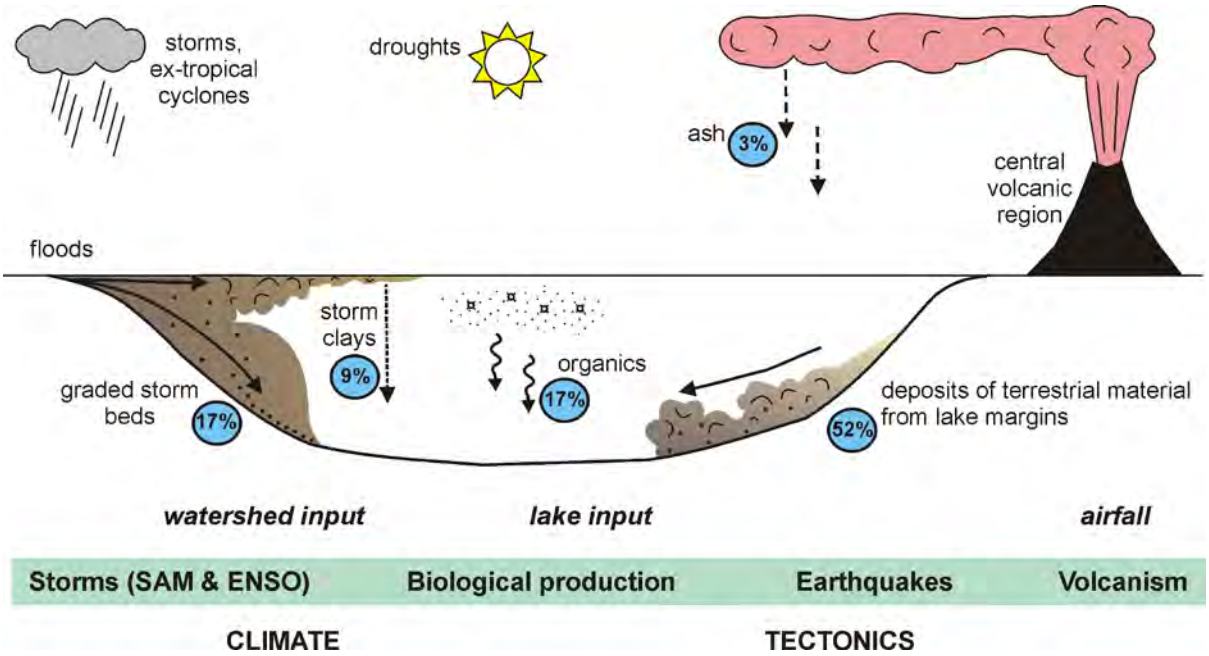

Figure 37 Cartoon summary of sediment input into Lake Tutira derived from the 27 m-long core (LT24). From Orpin et al. (2010)

The other major units of interest, and which have received the most attention, are the storm layers (Figure 36, 37). As mentioned above, the upper storm layers were correlated with historical storms, such as Cyclone Bola in 1988 (Figure 38). Cyclone Bola is the largest storm on record, producing 753 mm of rainfall in 4 days, and thousands of shallow landslides from the highly erodible surrounding mudstone hill country. 56% of the sediment generated by these landslides entered the lake (*Page et al*., 1994b). Relationships between sediment thickness and storm rainfall have been derived from the historical record and, after taking into account reduced sedimentation rates under a fully forested catchment, were used to infer a 7200 year storm record (*Page et al.*, 2010). 1400 storm layers were identified, a frequency of 1 storm every 5 years, with 53 the size of Cyclone Bola (1 in 130 years), and 7 larger than Cyclone Bola. Twenty five periods of major storm activity record the interplay between the El Nino Southern Oscillation (ENSO), Interdecadal Pacific Oscillation (IPO) and the Southern Annular Mode (SAM) (*Page et al.*, 2010; *Gomez et al*., in press).

Figure 38 Lake Tutira and the surrounding hill country immediately after Cyclone Bola. *Photograph*: N.A. Trustrum, March 1988.

3.7 STOP 1/7: AHURIRI LAGOON

Ahuriri Lagoon is the site of several stratigraphic and paleoecological studies that have found evidence for coseismic Holocene subsidence (*Hull*, 1986; *Chague-Goff et al*., 2000; *Hayward et al*., 2006). However, the location is also well known because it was uplifted in the 1931 Ms=7.8 Hawke's Bay earthquake. The 1931 earthquake resulted in uplift 1–1.8 m of Ahuriri Lagoon (Figure 39–41). It enabled the area to be farmed and provided a large flat area for the airport. The southern Hawke's Bay region is inboard of the areas of slow slip on the plate interface.

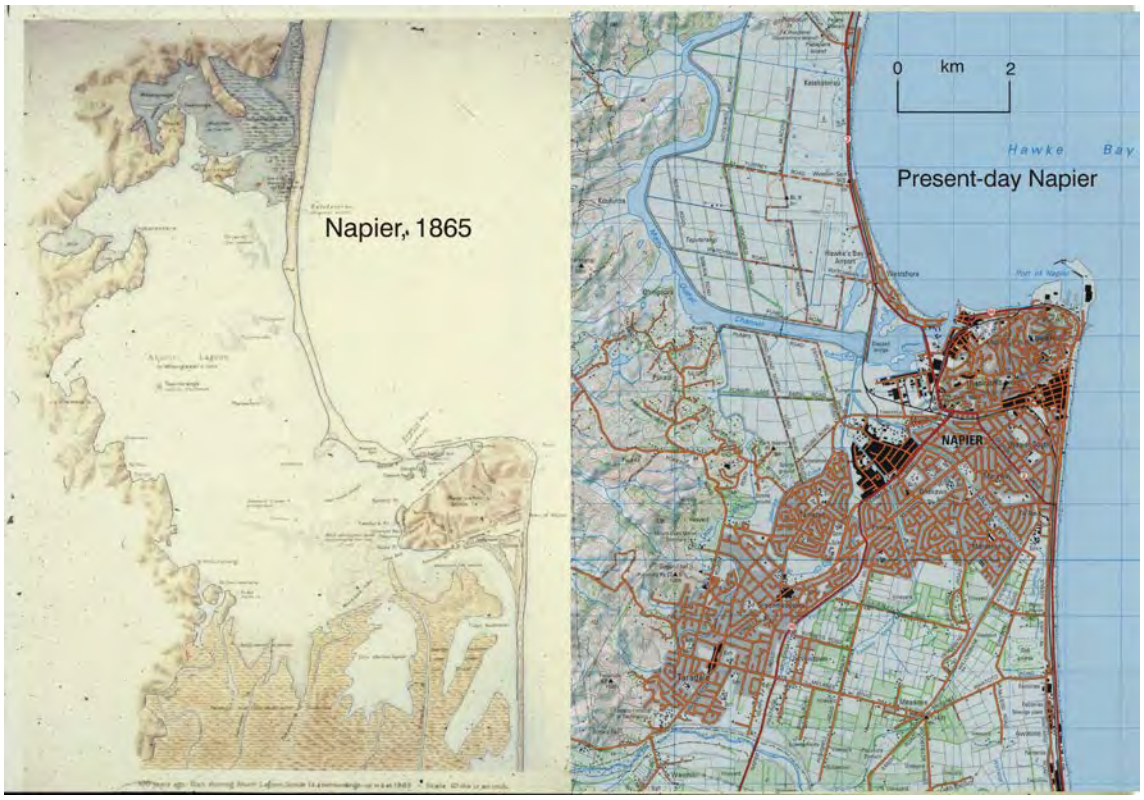

Figure 39 Ahuriri Lagoon before and after the 1931 Hawke's Bay (Napier) earthquake.

Figure 40 View north in 1931 of the western margin of Ahuriri Lagoon. Uplift of about 1 m permanently exposed part of the pre-earthquake lagoon and diverted the Tutaekuri River southward. From Hull (1990).

Figure 41 Stranded boats in Ahuriri Lagoon.

Foraminiferal and diatom assemblages and sediment thicknesses in eleven cores (3-7.5 m deep) from the former bed of brackish-marine Ahuriri Inlet (Figure 42, 43) were examined by Hayward et al. (2006). Microfossil-based paleoelevation estimates were combined with sediment thicknesses, age determinations, the New Zealand Holocene sea level curve, and estimates of compaction, to identify the Holocene land elevation record (LER) of each core (Figure 44). *Hayward et al*. (2006) obtained a record of 8.5 m of subsidence followed by 1.5 m of uplift in the last 7200 cal years.

The following earthquake-related vertical displacement events were identified from the LER plots:

- 1931 AD Hawke's Bay Earthquake, +1.5m displacement
- ca. 600 cal yr BP, ~ -1m
- ca. 1600 cal yr BP, ~-1.7m
- ca. 3000 cal yr BP, -1.4 to -1.8m
- ca. 4200 cal yr BP, ~-1.5m
- ca. 5800 cal yr BP, -0.5m+
- ca. 7000 cal yr BP, -0.6 m+.
- A further ~1–2m of tectonic subsidence is inferred to have occurred during smaller earthquake events during the interval 7000–3000 cal yr BP.

The six subsidence events in the last 7000 years have had a return time of 1000–1400 years in central Hawke's Bay. The tectonic structure responsible for the subsidence events at Ahuriri Lagoon is not confidently known, but it is possible that the subsidence relates to subduction earthquakes. The Ahuriri Lagoon earthquakes at ca. 5800 and ca. 7000 yrs BP may correlate to the ca. 5500 and ca. 7100 yrs BP subsidence events in northern Hawkes Bay (Figure 30). If we assume that the subsidence events that occurred at ca. 7000 cal. years BP in northern and central Hawke's Bay were synchronous (although the resolution of radiocarbon dating is not good enough to prove this) and occurred on a single structure, then a plate interface source is likely. Such an event might have affected >100 km of coastline and would have had a magnitude of at least M_W 8.0 (Wallace et al., 2009). Further work is taking place along the Hawkes Bay coastline to constrain the extent of deformation associated with the ca. 5500 and ca. 7000 year events.

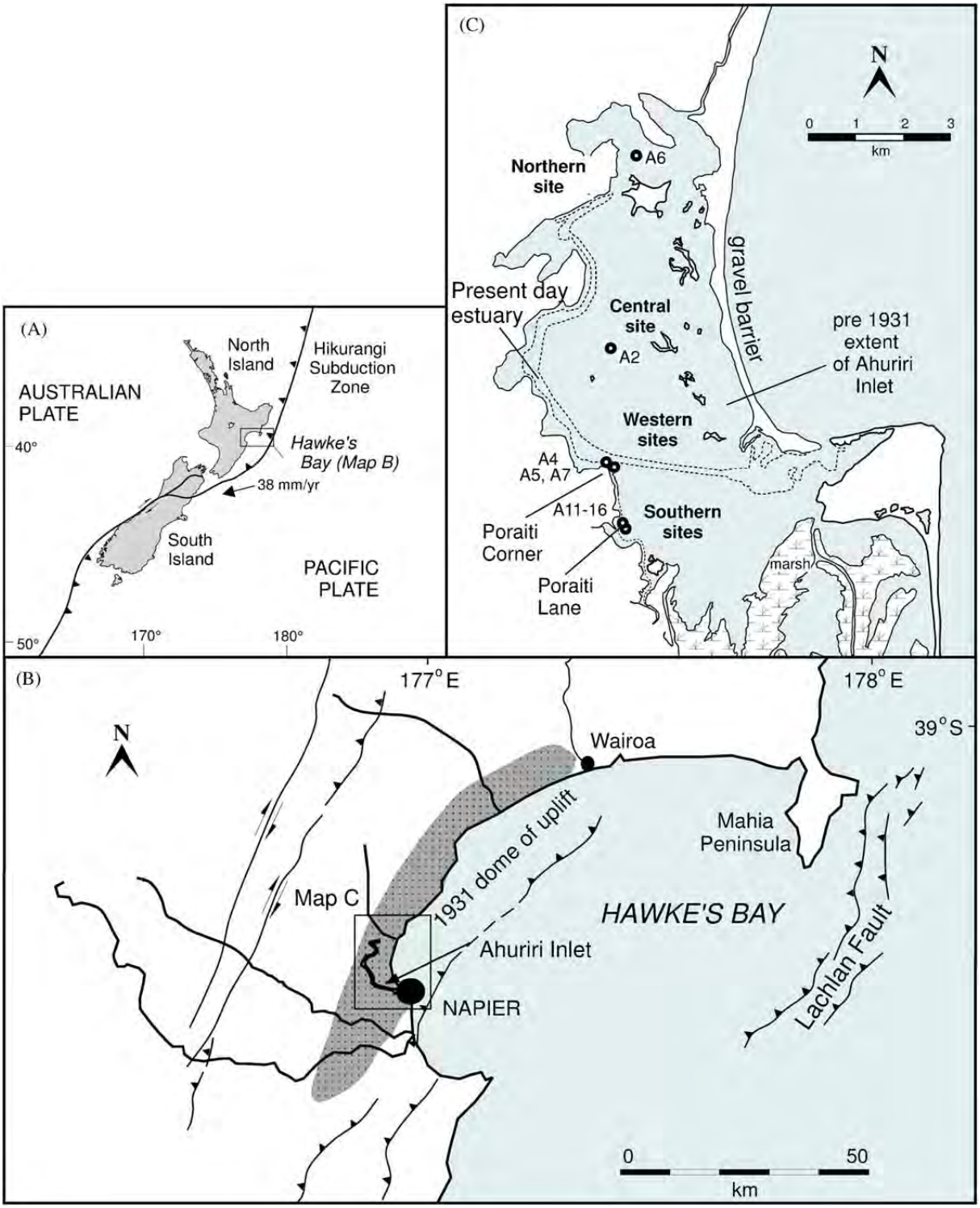

Figure 42 (A) Map of New Zealand showing location of Hawke's Bay above the Hikurangi margin on the Pacific-Australian plate boundary. (B) Map of Hawke's Bay region showing location of major active fault zones (Barnes et al., 2002) and elongate dome of land uplifted during the 1931 Napier Earthquake (Hull, 1990a). (C) Core site locations within the pre-1931 extent of Ahuriri Inlet. The dashed extent of the existing post-1931estuary is also shown. From Hayward et al. (2006)

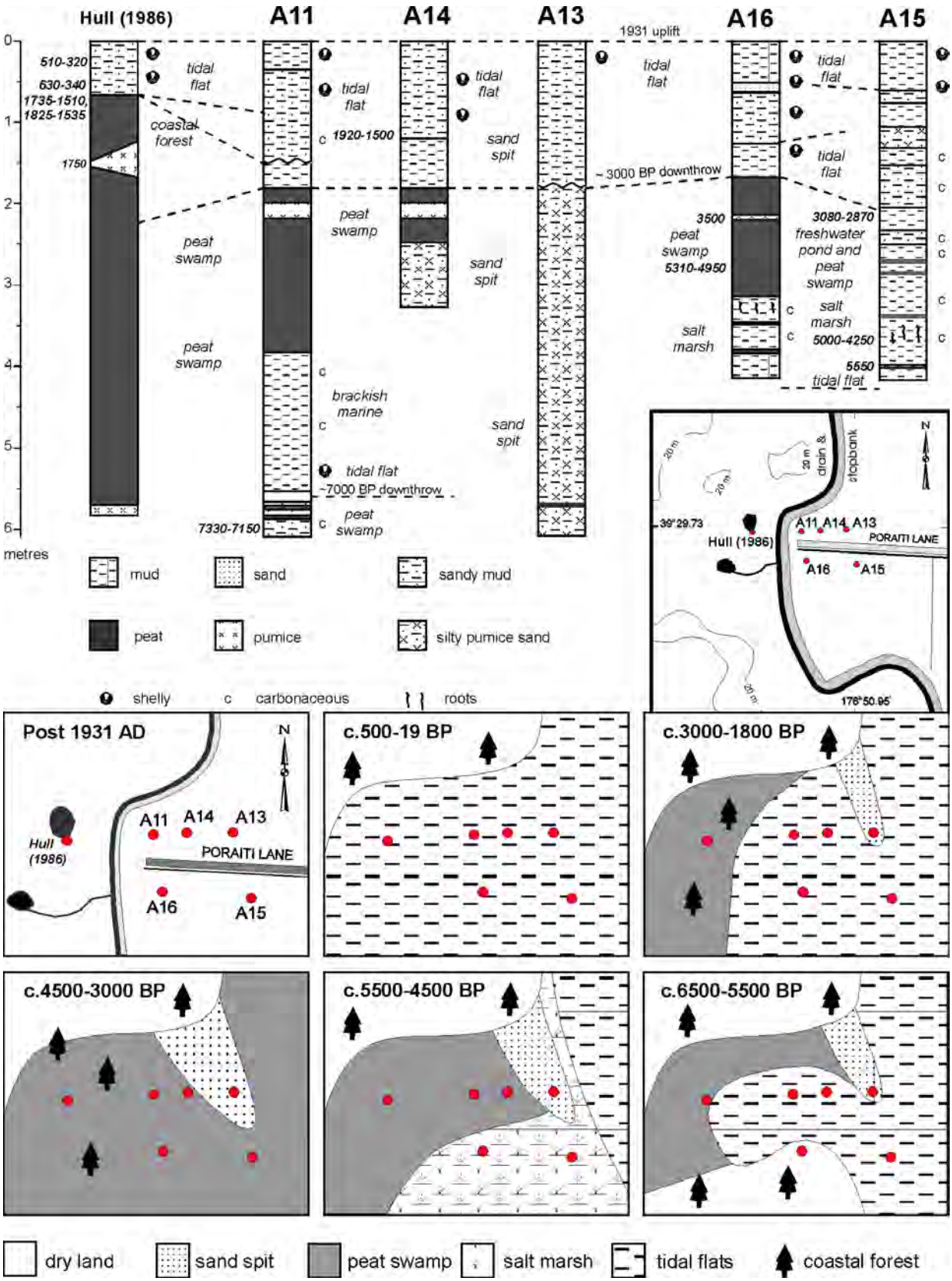

Figure 43 Generalised Holocene lithostratigraphy of five SW Ahuriri Inlet cores plus that recorded in a nearby excavation by Hull (1986). Radiocarbon and tephra ages are shown (in cal yrs BP). Inferred Holocene paleogeographic history of this embayment is shown in six maps at the bottom. From Hayward et al. (2006).

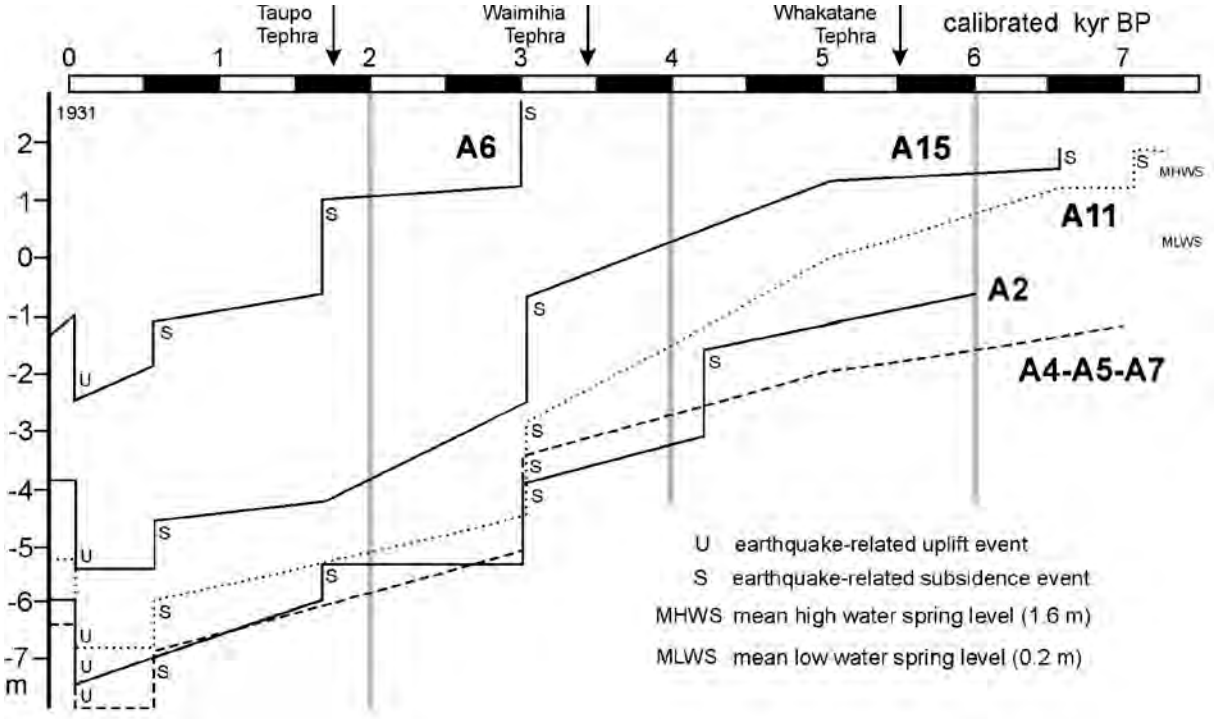

Figure 44 Holocene land elevation history curves for five Ahuriri core sites, based on the indicated elevational record from foraminifera and diatoms, corrected for slight eustatic sea-level change, and adjusted for bedrock depth and lithology-influenced compaction. Accuracy limits on ages assigned to sudden elevational changes have been deleted for simplicity. Adapted from Hayward et al. (2006).

1931 Hawke's Bay Earthquake – Background Information

At 10.47 am on 3 February 1931 local time (2 Feb, 22h 46m UT), a large (Ms=7.8) earthquake struck Hawkes's Bay and was felt throughout most of New Zealand (Figure 45). Within minutes, the business districts of Napier and Hastings lay in ruins and were engulfed by fire. The death toll of 256, mostly in Napier and Hastings, makes this earthquake New Zealand's greatest disaster.

Bullen (1938) judged the earthquake to have been a multiple event, comprising the initial shock, followed by two large events, 6 seconds and 14 seconds later. There were no major foreshocks, and no earthquakes had been felt at Napier for 30 days prior to the February 2 shock (*Adams et al*., 1933). Bullen (1938) located the earthquake at 39.33^{o}S, 176.67^{o} E (±0.2^{o}), 32 km northwest of Napier.

The earthquake had a focal depth between 15-20 km and a surface wave magnitude of 7.8 (*Smith*, 1978). Aftershocks continued throughout 1931, the largest being a M_s 7.3 event on February 13, which appeared to have a similar epicentre but shallower focus than the mainshock (*Bullen*, 1938).

Post-earthquake geological investigations and re-levelling of the Wellington-Gisborne railway, revealed uplift of a >90 km-long, 17 km-wide asymmetric dome, from southwest of Hastings to northeast of the Mohaka River mouth, and a total of 15 km of surface rupture on several faults at the southwestern end of the dome (Figure 45, *Henderson*,1933; *Hull*, 1990).

Coseismic slip was probably in the order of 6-8 m dip-slip and a 4-8 m strike-slip, but after 60 years only the uplift of Napier's former harbour-Ahuriri Lagoon-remains well preserved in the geological record. Present geological techniques for recognising prehistoric earthquakes

would therefore fail to identify the magnitude of deformation associated with this event (*Hull* 1990).

Fault modelling from the observed elevation changes and retriangulation data suggest that the 1931 earthquake occurred on a dextral-reverse fault that dips steeply to the northwest (*Haines and Darby*, 1987), within rocks of the most inboard part of the accretionary prism beneath central Hawke's Bay. Their work suggests that the rupture probably extended upward from the subducted plate interface into rocks of the accretionary prism, but without involving rupture of the interface itself, which is about 20 km beneath the region (*Reyners*, 1980).

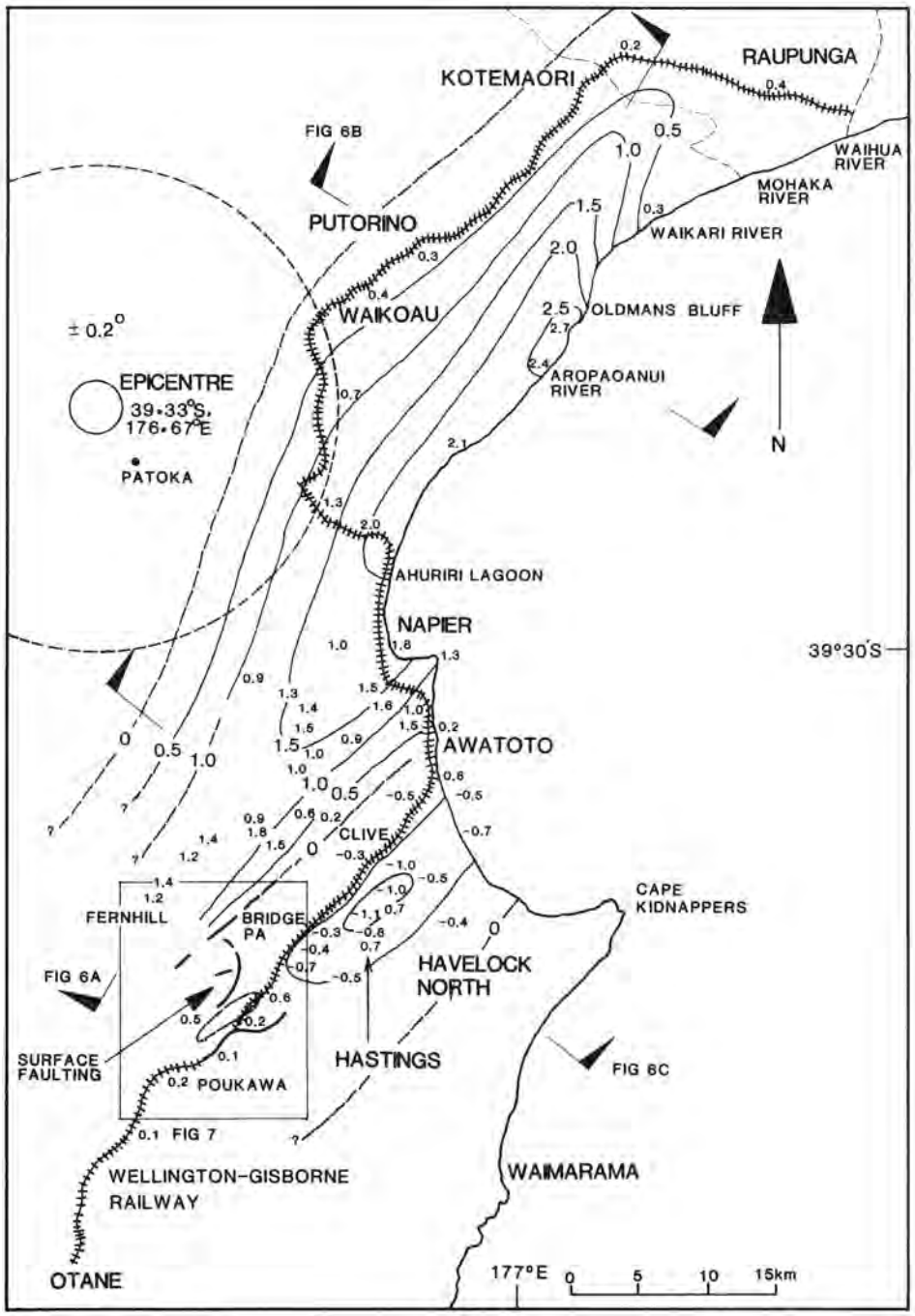

Figure 45 Contours of height change as a result of the 1931 Hawke's Bay earthquake. From Hull (1990).

3.8 STOP/DRIVE-BY 1/8: NAPIER CITY

Within minutes of the earthquake, fire began in three Napier chemist shops in the business district. Firefighters were almost helpless — water pressure faded to a trickle as the reservoir emptied. By mid-afternoon Napier's business area was ablaze and almost 11 blocks of central Napier were gutted (Figures 46–48). Napier was reconstructed largely in the Art Deco style, popular in the 1930's. This is now a big tourist attraction for Napier. The Art Deco style was at the height of its popularity for buildings in 1931 (Figure 49). Its clean simple lines and base relief decoration suited the needs of the new city:

- **Art Deco was fashionable**. With its past destroyed, Napier looked ahead and chose a style associated with Manhattan, the movies and modernism.
- **Art Deco was safe**. With its emphasis on low relief surface decoration, Art Deco forsook the elaborate applied ornament that had fallen from the buildings in the earthquake and caused so many deaths and injuries.
- **Art Deco was cheap**. Its relief stucco ornament was an economical way to beautify buildings during the lowpoint of the Great Depression (www.artdeconapier.com).

New Zealand's art-deco gem that grew from disaster

Nigel Tisdall, The Observer, Sunday 25 October 2009

"Grandad was on the loo when the earthquake struck," says Gill, a chirpy New Zealander who grew up in Napier. In 1931 this genteel port on Hawke's Bay, on the east coast of North Island, was struck by a tremor measuring 7.8 on the Richter scale. It flattened the city just as its children were starting the first day of a new school year. A total of 256 people lost their lives in what remains the country's worst natural disaster — although there were some lucky escapes.

"Our family had an outside toilet back then," Gill recalls, "and Grandad fell into the cess pit, where he was eventually rescued some hours later. The soft landing saved his life."

If you believe clouds have silver linings, Napier's is surely rimmed with neon and chrome, the shiny new materials of the art-deco age. For this was an earthquake that also gave back, tilting the coast up by a couple of metres and draining a huge lagoon that is now filled with fertile farmland, the city airport, and some choice stretches of 30s and 40s suburbia.

Downtown Napier, meanwhile, was quickly rebuilt in a colourful, confidence-raising art-deco style that married symbols of renewal — sunbursts, fountains, flowers — with robustly quake-proof buildings limited to two storeys. Out went brick parapets, gables and heavy facades; in came chrome speed-lines, ziggurats and naked women reaching for the stars.

What's remarkable is that it is still all there. Lovers of art deco will find plenty of individual gems to swoon over in metropolises such as Paris, New York and Shanghai, but Napier is exceptional because it offers such an engaging and strollable concentration of provincial 30s edifices.

According to the local Art Deco Trust, which arranges guided walks and bus tours and produces excellent background literature, the city has 147 art-deco buildings, decorated in styles that include Egyptian, Mayan and Maori. Many have been restored and repainted in cheery pastels, and star turns include the still-thriving 1938 Municipal Theatre, which has its

original chrome and neon fittings, and a cubist carpet faithfully recreated from a pre-earthquake scrap found in the manager's office.

Walk down Tennyson Street and you meet one 1932 joy after another. Here is the curious Scinde Building, once a Masonic lodge; there are the former offices of the Daily Telegraph newspaper with its lotus flower capitals — it's now an estate agent.

Some buildings quietly tell tales about their owners' origins: there are sweet little shamrocks on the Munster Chambers, Scottish thistles on Parker's menswear store. A German national flag, in stucco, flutters above Hildebrandts, the chiropodist.

For many, the most engaging sight is the ASB Building, a 1934 bank adorned with a union of art-deco style with Maori motifs. Look above the modern counters and you see stylised hammerhead sharks, curling fern fronds and whales' tails dancing around the ceiling. In the flamboyant National Tobacco Building in the port of Ahuriri, roses and citrus fruits twirl around its stained glass dome as if to dispel the odium of smoking.

Figure 46 Damage in Napier city following the 1931 earthquake. From Alexander Turnbull Library collection http://www.natlib.govt.nz/collections/highlighted-items/hawkes-bay-earthquake-1931

Figure 47 Fire at the Masonic Hotel. It was later rebuilt in the art deco style. From http://www.teara.govt.nz/en/historic-earthquakes/

Figure 48 Emerson Street after the Napier earthquake. From http://christchurchcitylibraries.com/Heritage/Photos/Disc4/IMG0041.asp

Figure 49 Four examples of Napier Art Deco architecture.

4.0 DAY 2: HASTINGS – WELLINGTON

4.1 STOP 2/1: TE MATA PEAK LOOKOUT

Te Mata Peak (elevation 399 m) lies above the fertile Heretaunga plains of Hawke's Bay. It is part of a prominent dip slope of outcropping mid-Pliocene limestone on the west flank of the Elsthorpe Anticline. On a clear day from the lookout at the summit, the Ruahine, Kaweka, Tewaka, and Maungaharuru ranges from the western horizon, with the volcano Ruapehu visible in the distance. Beyond the sweep of mountains and across the curve of Hawke Bay, Mahia Peninsula and Portland Island jut into the Pacific. Southwards lie the coastal hills, while meandering across the plains flow the Tutaekuri and Ngaruroro rivers, and around the base of the Peak, the Tukituki river flows along the crest of Elsthorpe Anticline.

Prior to European times, vegetation in the park was fire-induced bracken and manuka with native grasses in clearings. Today the predominant vegetation is short tussock grassland with a wide variety of introduced trees and shrubs in the valleys and on the lower ridges. Since 1927, thousands of native and exotic trees and shrubs have been planted throughout the area.

Te Mata Peak offers an excellent vantage point to view the main elements of deformation of the upper plate at the latitude of Hawke's Bay. To the west the Axial Ranges from the spine of the North Island and reflect uplift associated with reverse slip at depth on faults that bound their eastern margin. The main oblique slip faults of the North Island Dextral Fault System (NIDFS), which can be mapped for 100s of kilometres, lie within the ranges and in places bound their eastern margin (*Beanland*, 1995). East of the ranges in the region that encloses Te Mata Peak the structures are dominated by steep reverse faults and associated folds, while still further east offshore thrusts and folds dominate. Deformation that produced the structures that we see in the landscape today is primarily post 2 Ma (e.g., *Nicol et al*., 2007). Pre 2 Ma structures are mainly contractional.

Figure 50 View from Te Mata Peak looking north along the western limb of the Elsthorpe Anticline: *Photo S.Henrys*.

The Legend of Te Mata (from http://www.maori.org.nz)

Legend has it that the hill is the body of Maori Chief, Te Mata O Rongokako (the face of Rongokako). Looking from Hastings, the gargantuan bite can be seen, as can the body of the powerful Chief forming the skyline. Many centuries ago the people living in pa (fortified villages) on the Heretaunga Plains were under constant threat of war from the coastal tribes of Waimarama. At a gathering at Pakipaki (5 km south of Hastings) to discuss the problem, the solution came when a wise old woman (kuia) sought permission to speak in the marae. "He ai na te wahine, ka horahia te po, " she said. (The ways of a woman can sometimes overcome the effects of darkness). Hinerakau, the beautiful daughter of a Pakipaki chief, was to be the focal point of a plan. She would get the leader of the Waimarama tribes, a giant named Te Mata, to fall in love with her, turning his thoughts from war into peace. The plan succeeded, but she too fell in love.

The people of Heretaunga, however, had not forgotten the past and with revenge the motive, demanded that Hinerakau make Te Mata prove his devotion by accomplishing seemingly impossible tasks. The last was to bite his way through the hills between the coast and the plains so that people could come and go with greater ease. Te Mata died proving his love and today his half-accomplished work can be seen in the hills in what is known as The Gap or Pari Karangaranga (echoing cliffs).

Legend has it that his prostrate body forms Te Mata Peak. At sunset one can often see, in the mists that stretch from the crown of Kahuraanake, the beautiful blue cloak with which the grieving Hinerakau covered the body of her husband before leaping to her own death from the precipice on the Waimarama side of the peak. The gully at the base of the cliff was formed when her body struck the earth.

4.2 STOP 2/2: POUKAWA FAULT

Background to the Poukawa Fault Zone

The Poukawa Fault Zone (PFZ) is a broad zone of NE-striking, active reverse-slip faulting that extends from near Waipukurau in the south to as far as Napier in the north. Blind faulting across the Heretaunga Plains (and offshore) during the 1931 Hawke's Bay Earthquake has been associated with the northern end of the PFZ (Figure 51; *Kelsey et al.*, 1998). About 15 km of surface ruptures from the 1931 earthquake are located in the Bridge Pa to Poukawa area at the southern end of the plains (Hull 1990). En route from Te Mata Peak we will pass by the 1931 rupture zone, an old tilted meander loop of Poukawa Stream and Lake Poukawa itself, on our way to Stop 2/2 near Otane.

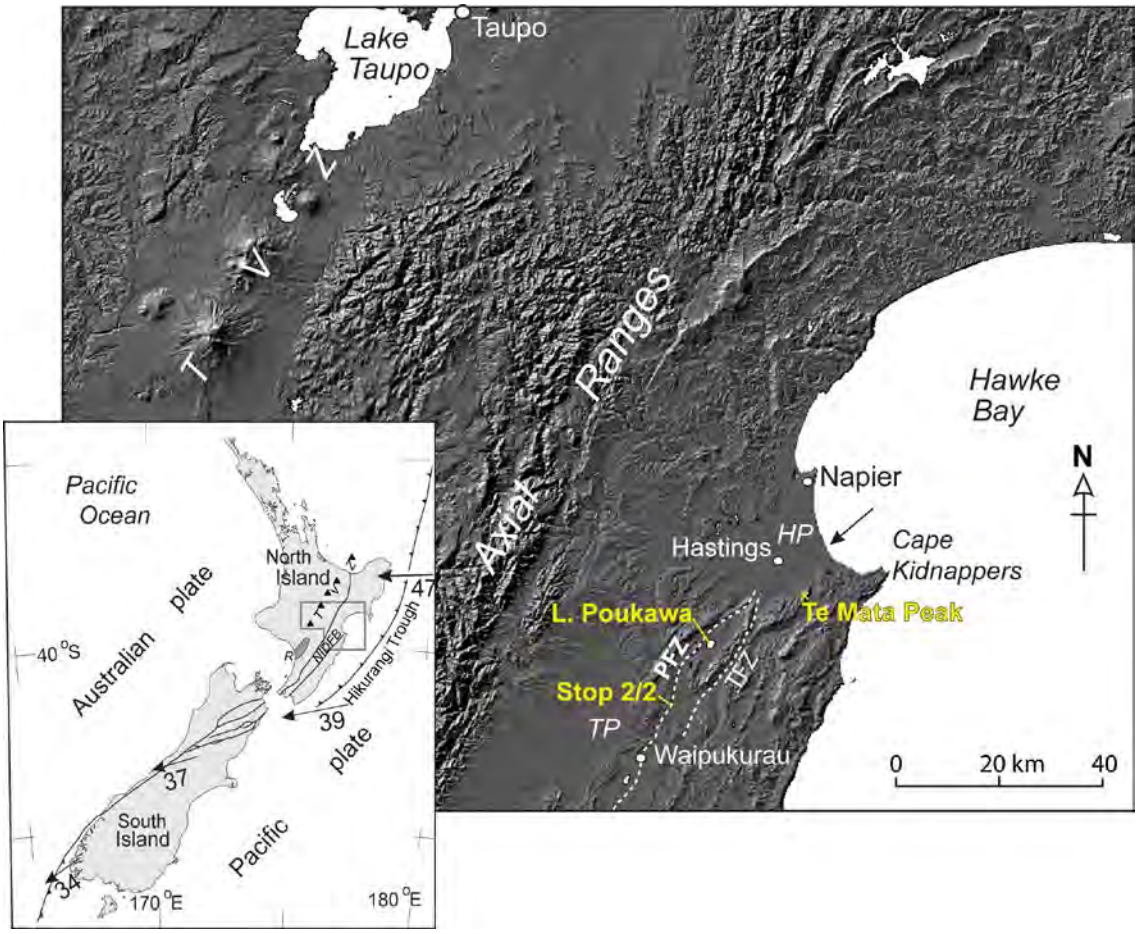

Figure 51 Digital Elevation Model (DEM) of the Hawke's Bay region and central North Island. The Poukawa (PFZ) and Tukituki (TFZ) fault zones are active zones of reverse faulting within the Hikurangi forearc. HP and TP are the Heretaunga and Takapau plains.

Tilted Meander Loop

Spectacular evidence of recent deformation in the Lake Poukawa area is preserved as an uplifted and tilted meander loop of the ancestral Poukawa Stream, located on an actively growing anticline at Pakipaki. Limestone of Pliocene age (2.4 Ma) dips 22–25° NW in the west limb of the fold, while the floor of the ancestral channel dips 6–8° NW (Figure 52). The age of the meander loop is unknown, but the loop is related to the present drainage pattern and presumably is not older than the latest Pleistocene (<0.5 Ma). This deformation is associated with active folding of the Kaokaoroa Range associated with reverse faulting along the Tukituki Fault Zone (*Kelsey et al.*, 1995; 1998) (Figure 53).

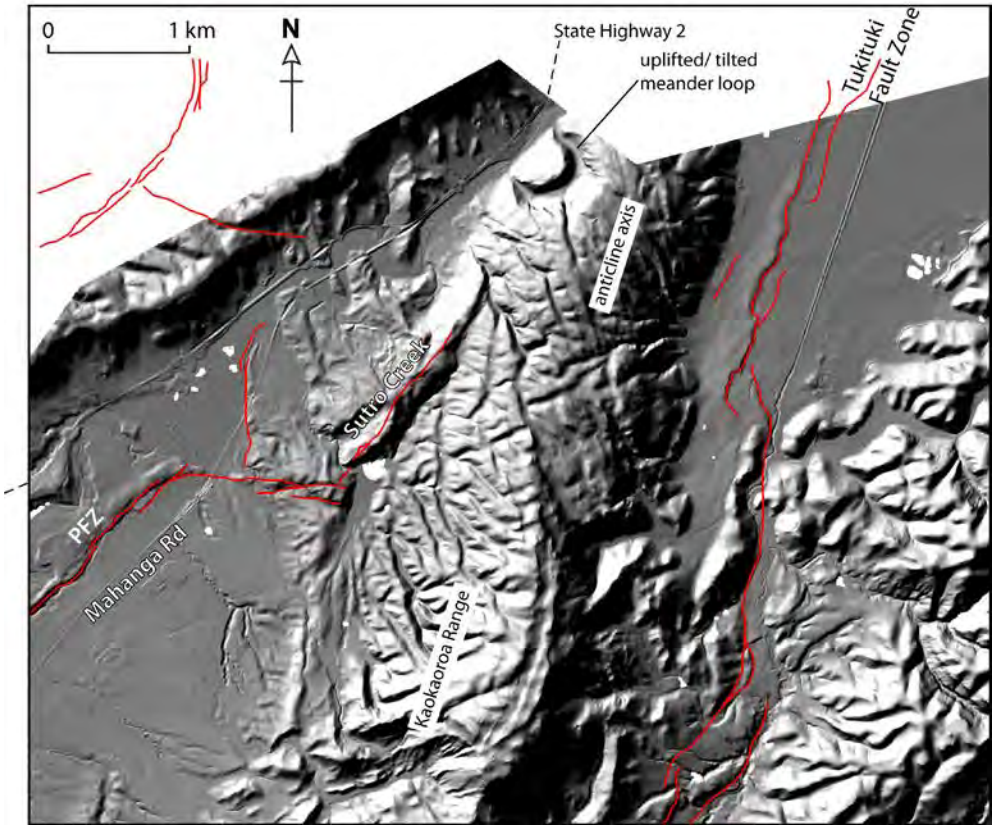

Figure 52 Clipped LiDAR DEM image of the transition from southern edge of the Heretaunga Plains to the northern edge of the Poukawa Depression. The 1931 earthquake ruptured traces of the Poukawa Fault Zone (PFZ) adjacent to Mahanga Rd and Sutro Creek (Hull, 1990). Tilted meander loop is deformed on the back of the Kaokaoroa Range and Tukituki Fault Zone.

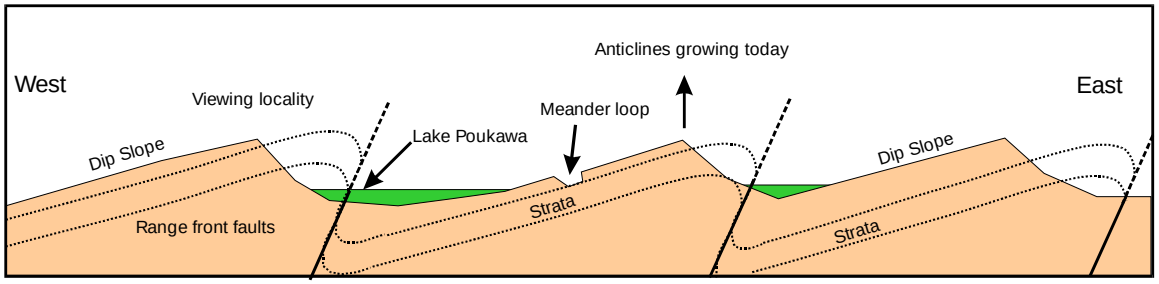

Figure 53 Idealised cross section of contractional deformation (actively growing anticlines) across central Hawke's Bay associated with the Poukawa Fault Zone (at left) and Tukituki Fault Zone (centre right). Synformal basins such as that which Lake Poukawa occupies are typical of this setting.

Lake Poukawa

The Poukawa Depression represents an elongate basin that has formed between ridges capped by Pliocene (3.0-3.4 Ma) shelf limestones. There is no evidence that a major river has ever flowed through this depression, so the basin presumably has evolved as a result of folding and uplift on northeast-striking thrust and oblique-thrust faults. Faults are believed to accommodate oblique-slip displacement beneath the basin, and studies of tephra and peat layers offset within the depression indicate progressive vertical displacements during the last 7000 radiocarbon years, with average return periods of 500-1500 years (*Froggatt and Howorth*, 1980).

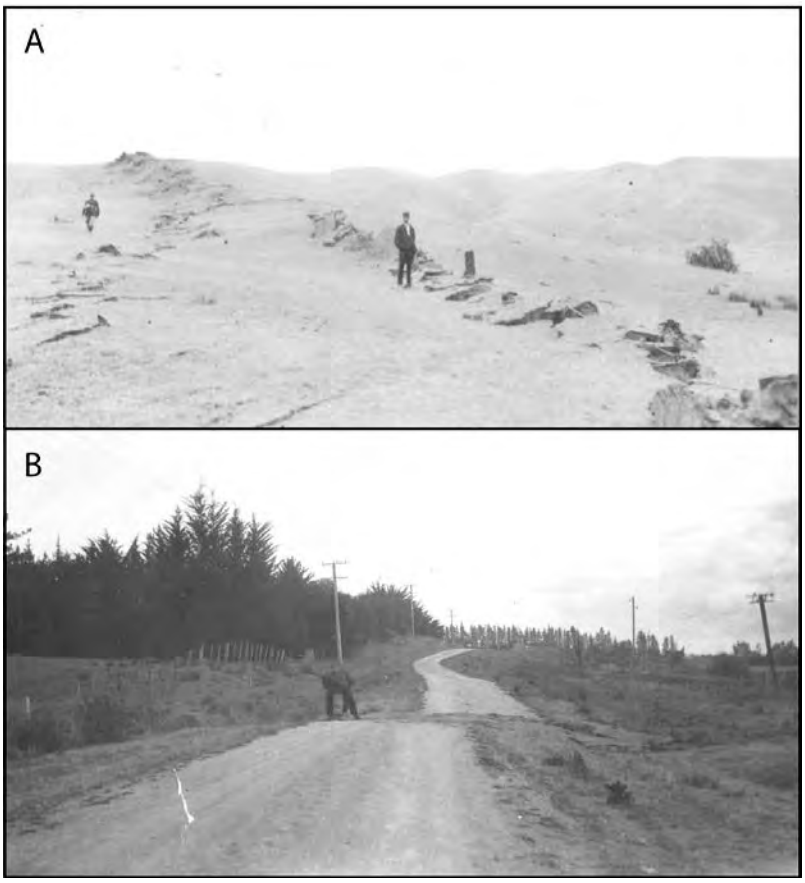

Figure 54 Surface ruptures related to the 1931 Hawke's Bay earthquake south of the Heretaunga Plains. (A). Strike-slip style moletrack showing 1.8 m dextral movement near Mahanga Road. (B) Right-lateral displacement across Mahanga Rd near Lake Poukawa. From Henderson (1933).

Depending on time and weather constraints, Stop 2/2 will visit the Poukawa Fault Zone (PFZ) at Argyll Road (large scarp, trenches) or Otane (scarp, toilets) in central Hawke's Bay. The LiDAR image (Figure 55) clearly shows a number of active fault and fold traces that deform a young valley-filling alluvial surface. The beauty of such a marker surface is that it be dated and the amount of deformation across it can be discerned from precise Digital Elevation Models (DEMs). The active scarps, and indeed the width of the zone of deformation, in this area are characteristic of contractional deformation across the PFZ. Paleoseismic and stratigraphic studies were undertaken at the Argyll trench site and Kaikora Stream by *Kelsey et al.* (1998). Further studies have been undertaken here and particularly in Otane to consider the location and likelihood of future surface rupture as a hazard to that village (*Langridge et al.,* 2006).

In this part of the PFZ there is an active, range-bounding reverse fault that uplifts Whangai Formation rocks in the Raukawa Range. This trace is called the Argyll Road trace, after the impressive 4-5 m high scarp where this road crosses it.

Three trenches were excavated at this site by *Kelsey et al.* (1998). In Argyll trench 2 (Figure 56) a series of alluvial deposits were sorted into packages that separate out four possible earthquake rupture events. These data are consistent with the number of inset terraces preserved behind the fault scarp within the canyon of Kaikora Stream. No datable material was located in this trench. However, the gravels that dominate the lower 2/3 of this trench have been correlated with alluviation of Kaikora Stream associated with the Last Glacial Maximum (Q2; c. 15-12 ka). In addition, Argyll trench 3, which was excavated through a smaller scarp across a post-LGM fan, yielded a radiocarbon date of 9486 ± 120 yr

BP within gravels, which is consistent with the construction of a Holocene fan across the Argyll Road trace. These data yield a preliminary recurrence interval of 3000-3800 yr for this trace. Fault dip in the trench is c. 35° which favours a low-angle thrust style of faulting.

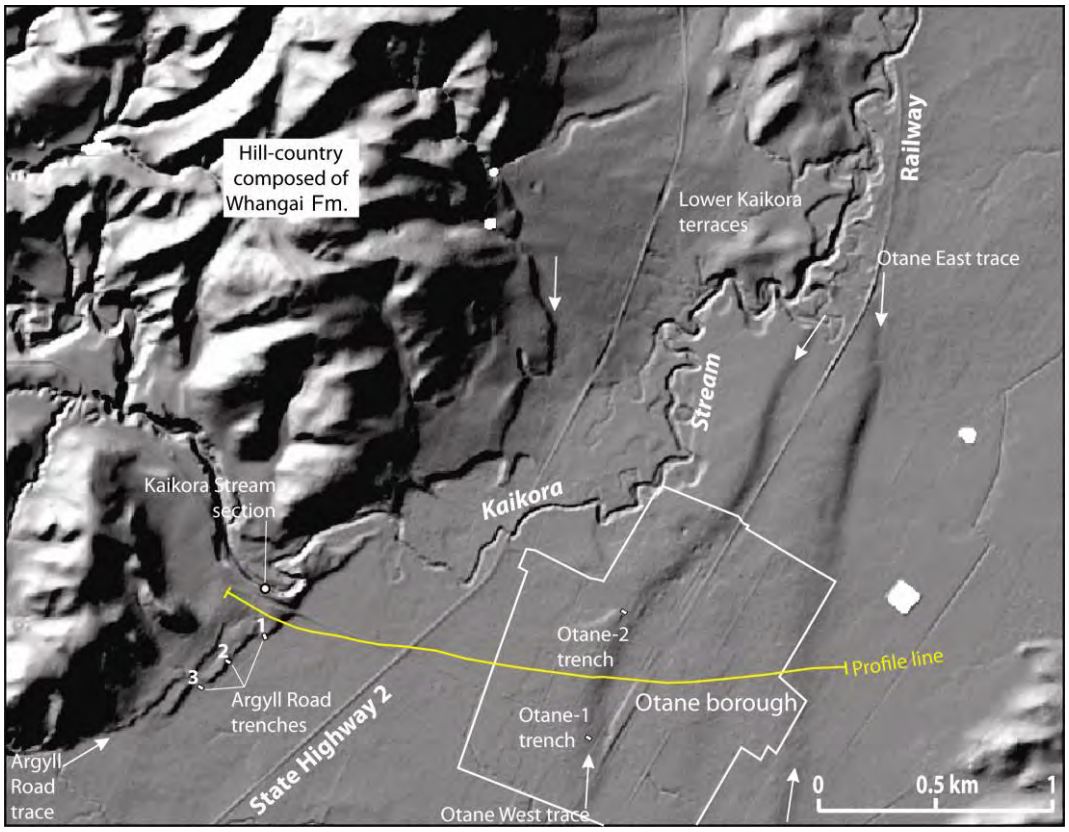

Figure 55 LiDAR DEM of the Otane area in central Hawke's Bay. Active reverse faulting is associated with several traces of the Poukawa Fault Zone (PFZ). Several trenches have spanned both the Argyll Rod and Otane West traces. A topographic profile (yellow) is shown in cross-section in Figure 56.

In 2005 a trench was excavated into the upper part of the scarp of the Otane West trace in the village (Figure 55). The Otane-2 trench showed rather monotonic, weakly bedded gravels with a thick, well-developed soil formed in overbank deposits. No faulting was observed in the trench, however, the consistent 4° slope of the ground surface and underlying unit contacts is considered to be related to active deformation across the Otane West scarp. A single OSL date of 15.2 ± 1.5 ka was obtained from a sandy unit within gravels near the base of this trench (Figure 56). This date confirms that the widespread surface in the area is indeed the LGM alluvial surface.

A 2 km-long profile across Figure 55 includes deformation associated with both the Argyll Road trace and three further fault/fold traces within Otane borough. A total of ~14 ± 2 m of vertical deformation of the LGM surface can be summed across this area in cross-section (Figure 57). Using an age of 12-15 ka for the abandonment of this surface produces a vertical slip rate of 0.8-1.3 mm/yr for the Poukawa Fault Zone. This equates to a dip slip rate of 1.2-2.7 mm/yr across the zone.

These results show that a substantial portion of the upper plate strain within the eastern strand of the North Island Dextral Fault Belt (NIDFB) is accommodated through active reverse-slip faulting across a broad zone, which includes the Poukawa Fault Zone.

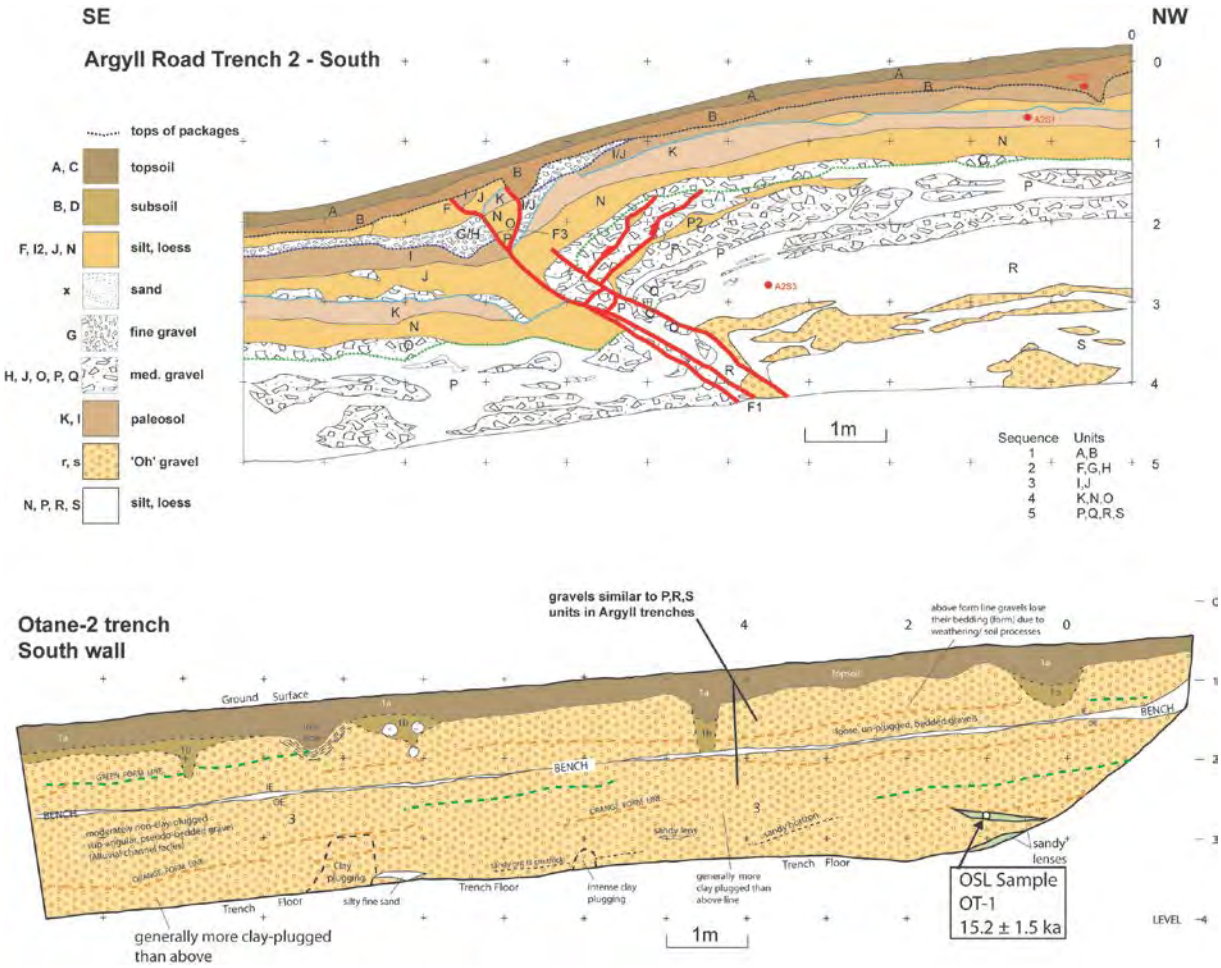

Figure 56 Trench exposures across the Argyll Road and Otane West traces of the Poukawa Fault Zone. The Argyll 2 trench indicates active reverse faulting associated with four late Quaternary faulting events. The tilted sediments in the Otane-2 trench were deposited during the LGM as shown by the OSL date.

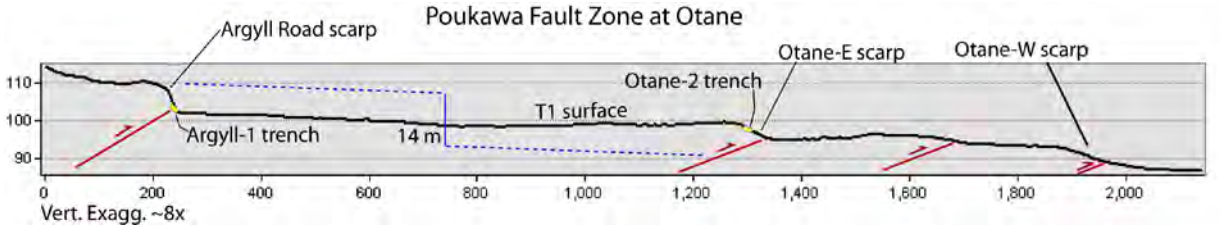

Figure 57 Cross-section across the Argyll Road and Otane West traces of the Poukawa Fault Zone using the LiDAR DEM. The two trenches discussed above are indicated. Vertical and horizontal units are metres.

4.3 STOP 2/3: MOHAKA FAULT

The Mohaka Fault is part of the North Island Dextral Fault Belt (NIDFB) (also referred to as the North Island Fault System). The NIDFB is the principal strike-slip fault system in the eastern North Island, which has formed in response to oblique subduction of the Pacific Plate. Oblique relative plate motion produces a margin-parallel component of motion of 26-33 mm/yr, which is mainly accommodated by regional vertical-axis rotations of the deforming Hikurangi margin relative to stable Australian Plate, and by strike-slip faulting in the upper plate, with little or no strike-slip on the subduction thrust (*Wallace et al*., 2004). The NIDFB accommodates between 20 and 70% of the margin-parallel relative plate motion (*Beanland*, 1995; *Wallace et al.*, 2004).

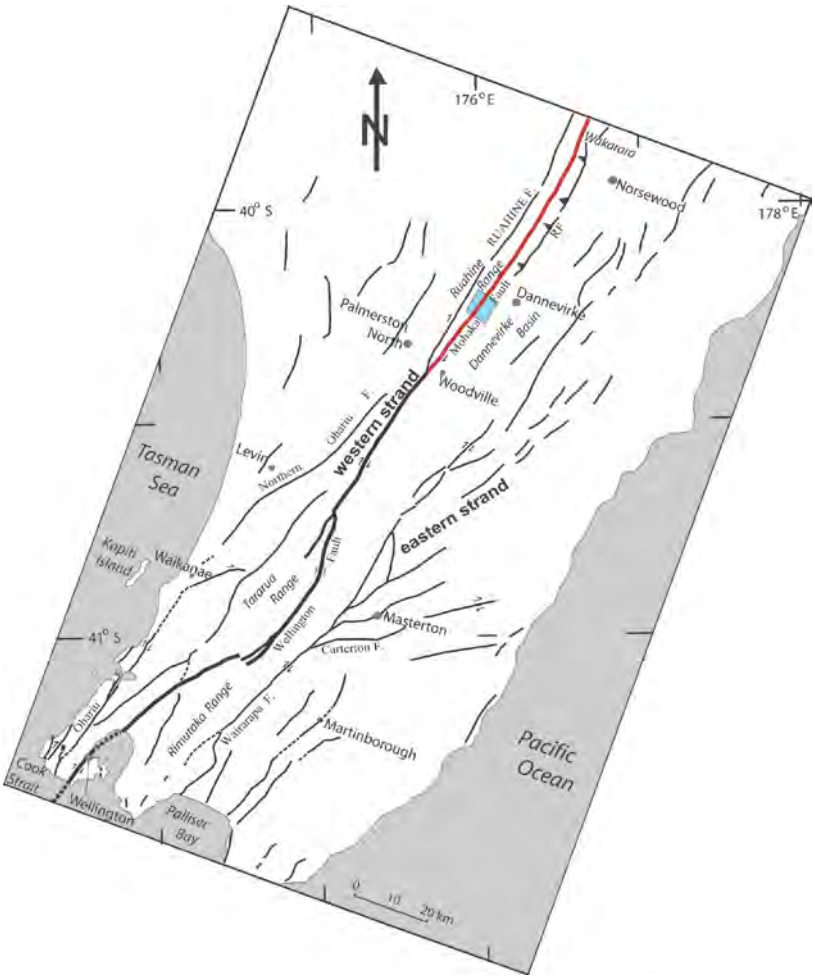

Figure 58 Simplified active fault map of the southern North Island. The two strands of the North Island Dextral Fault Belt (NIDFB) are highlighted by the Wellington (bold) and Mohaka (red) faults (western) and Wairarapa-Makuri-Poukawa faults (eastern). The area of Stop 2/3 is shown by a blue box, which is on the southern edge of the Manawatu slow slip event. RF, refers to the Rangefront Fault.

The NIDFB comprises two main strands, here referred to as the eastern and the western strand (*Beanland*, 1995) (Figure 58). The western strand traverses rugged terrain of Mesozoic greywacke basement along much of its length, both exploiting pre-existing terrane boundaries and mélange zones and cutting across these structures to define their own path (*J. Begg, pers. com.* 2005). The eastern strand, which includes the Wairarapa Fault, extends for approximately 250 km, from the Wairarapa region in the south to southern Hawke's Bay in the north, where it is mainly a reverse-dextral fault system (*Beanland*, 1995; *Kelsey et al.*, 1995). The western strand is approximately 500 km long and traverses the

North Island from Wellington to the Bay of Plenty coastline (*Langridge et al*., 2005; *Mouslopoulou et al*., 2007).

The active NIDFB has accommodated up to 5-8 km of strike-slip during the last 1-2 Ma (*Beanland,* 1995; *Kelsey et al*., 1995; *Nicol et al*., in review). North of Stop 2/3 in the Wakarara area, the total dextral-slip across the Mohaka Fault may be around 2-3 km based on the offset of the bedrock and long-lived river systems. Aggregated late Quaternary dextral strike-slip rates across the two main strands of the NIDFB (i.e. eastern and western) range from ~18 mm/yr in the south, near Wellington (*Beanland* 1995; *Van Dissen and Berryman* 1996; *Langridge et al*., 2005) to ~4 mm/yr in the north, near the Bay of Plenty. During the late Quaternary, the southernmost ~400 km of the NIDFB has chiefly carried dextral strike-slip and only minor reverse or normal-slip (typical horizontal:vertical slip ratios are 10:1) (*Beanland,* 1995).

Figure 59 Google Earth image of the trace of the Mohaka Fault (indicated by arrows) along the range-front of the Ruahine Range. Stop 2/3 is located at the end of Baker Rd where a prominent riser (or) is displaced across the fault. The Trotter's graben site (TG) was trenched to date past earthquakes.

Stop 2/3 visits a classic offset terrace site along the most active onland dextral-slip fault in the central North Island, at Maungapukakakahu Stream (Figure 59). The Mohaka Fault is the northern continuation of the Wellington Fault through the central part of the onshore Hikurangi margin. Along with the Ruahine Fault, the Mohaka Fault splits from the Wellington Fault just south of the Manawatu River gorge between Palmerston North and Woodville (Figure 58). Stop 2/3 can be accessed by turning off Top Grass Road onto Baker Road, west of Dannevirke (Figure 59). At the end of Baker Road, the Mohaka Fault provides an imposing site where a late Quaternary terrace riser is offset horizontally and vertically across the fault. Sites like this offer the opportunity to estimate late Quaternary geologic rates of slip for important faults within the Hikurangi margin. Data from these sites go into both seismic and geodetic models of how the island deforms (e.g. *Stirling et al.*, 2002; *Wallace et al.* 2004).

Maungapukakakahu Stream ('M' Stream) is a small mountain stream that emerges from the Ruahine Range across the Mohaka Fault, which is characterised by two active traces at this locality. A RTK-GPS topographic map was constructed at the site using a vehicle and backpack set-up (Figure 60). 'M' Stream formerly constructed broad alluvial terraces during late Quaternary times. Augur holes and soil pits were dug into the terrace surfaces to conform their cover bed stratigraphy. Like other alluvial terrace sequences around the North Island, these terraces have been correlated to the alluvial chronology of the Rangitikei River (*Milne,* 1973; *Litchfield and Rieser*, 2005).

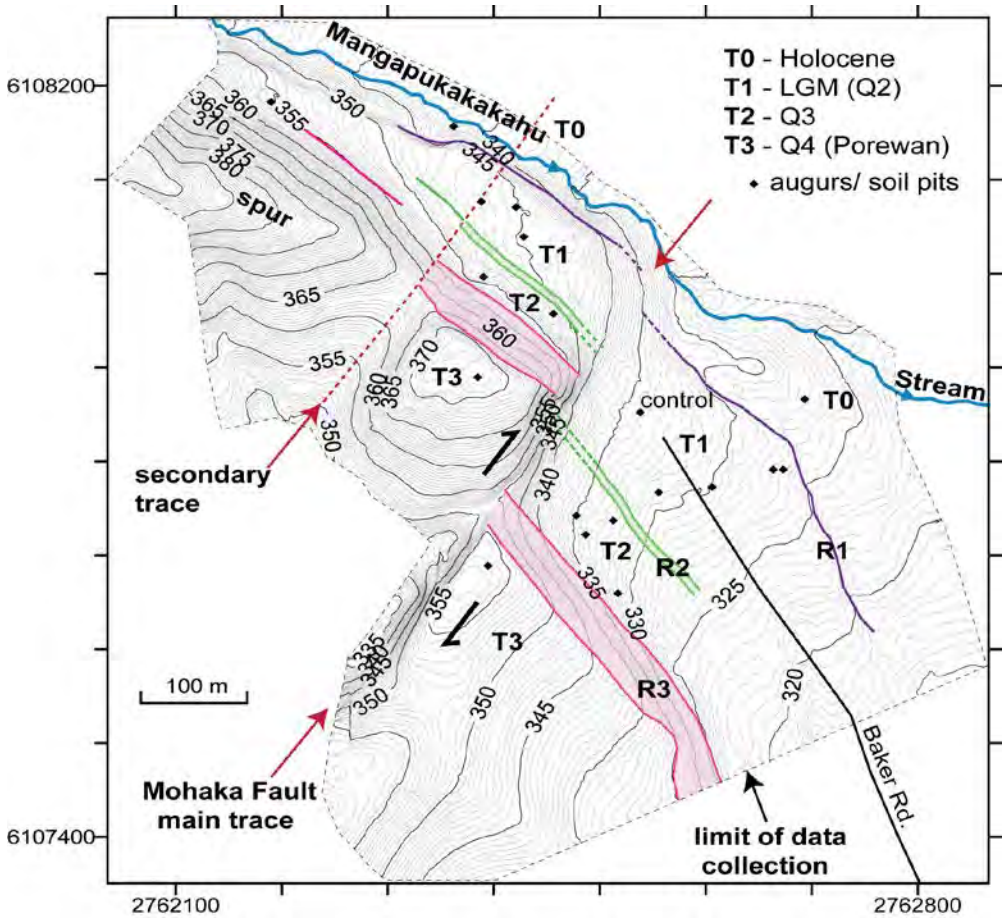

Figure 60 RTK-GPS map of the alluvial terraces (T0-T3) at Maungapukakakahu Stream offset across the Mohaka Fault. Elevations in metres; contour interval is 0.5 m. Risers cut against these terraces (R1-R3) are used to measure the slip and estimate dextral slip rates. LGM, refers to the last glacial maximum.

The highest terrace at the site (T3) is correlated with the Porewan terrace, which is an aggradation terrace that formed during Marine Isotope Stage 4 (Q4). R3 is the very high (15-20 m) erosional riser cut into T3 (Figure 61). Augur holes in the terrace immediately below R3 showed the presence of Kawakawa Tephra (Kk; c. 27.1 ka) in loessic cover deposits, while augur holes in T3 showed the presence of two loess units, the upper of which contained the tephra. T2 has therefore been correlated to the Ratan terrace and MIS stage 3 (Q3). The vertical separation between T2 and T1 is only 0.5-1 m, i.e. R2 is a subtle linear marker. However, the coverbed stratigraphy of T1 lacks tephra and thus this terrace is correlated with the widespread Ohakean terrace, which formed during and following the Last Glacial Maximum (LGM; Q2). T1 is separated from T0 by a 1-1.5 m high riser (R1) which drops down onto T0, the Holocene alluvial surface. T0 exhibits only a thin soil formed on overbank deposits.

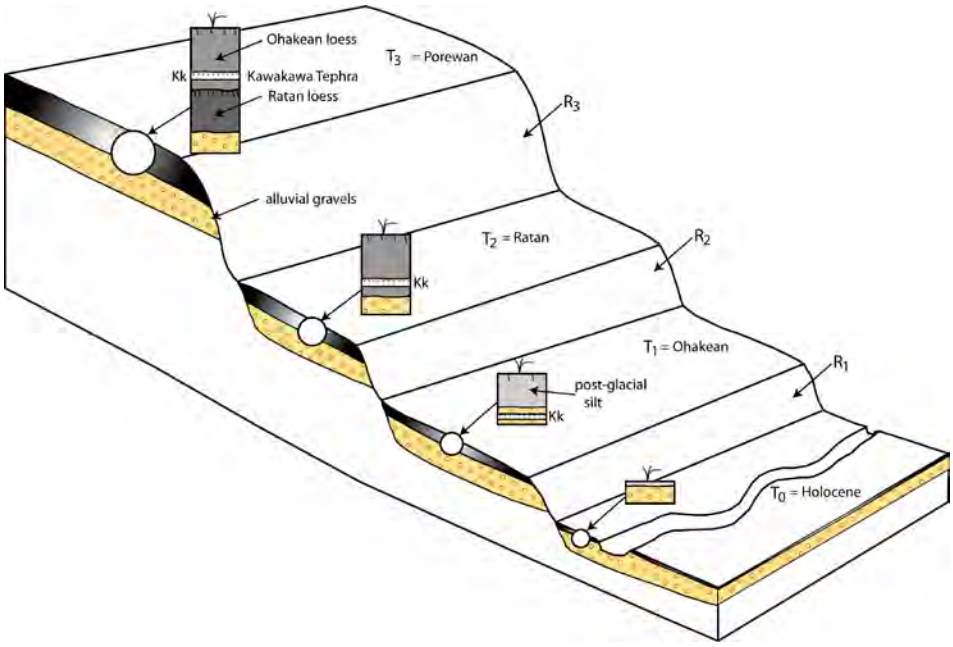

Figure 61 Stratigraphic model of the flight of late Quaternary alluvial terraces and their cover deposits at Maungapukakakahu Stream.

Dextral offsets have been estimated for the three terrace risers preserved at 'M' Stream. Riser R3 is displaced by ~135 ± 10 m across the main trace of the Mohaka Fault and a further 18 ± 5 m across the secondary trace that occurs ~200 m to the NW of us. The true vertical component of motion here is small (~5-10 m down-to-the-east). R2 is displaced by a total of ~80 ± 10 m and R1 is displaced by ~32 ± 6 m across the Mohaka Fault. The displacement of R2 and R1 across the secondary trace is difficult to estimate. To estimate slip rates for these piercing lines we assume that the risers were cut near the beginning of each climatic phase. Abandonment of the higher terrace coincided with downcutting and erosion of the higher terrace edge to form the riser. Later, the lower terrace aggraded and filled in against the edge of the cut riser. Assuming a constant slip rate over the last ca. 60 ka, yields a preliminary minimum slip rate of 2.3-3.2 mm/yr for the Mohaka Fault at this site. The Ruahine Fault, 5 km to the west, carries a dextral slip rate of ~1-2 mm/yr (*Beanland and Berryman,* 1987). Therefore the horizontal component of slip for the western strand of the NIDFB in this area is ~4-5 mm/yr, which is only slightly less than recorded on the northern part of the Wellington Fault south of the Manawatu Gorge (5-6 mm/yr; Langridge et al., 2005). In addition, it has recently been recognised that both active reverse to dextral-reverse slip faulting occurs outboard (2-5 km) of the Mohaka Fault on the Rangefront, Wakarara and Pukenui faults (Figure 58; http://data.gns.cri.nz/af/). Some of these structures can be observed between Dannevirke and Saddle Road as evidenced by broad scarps and uplifted late Quaternary alluvial terraces.

At stop 2/3 we will also briefly discuss the Mohaka Fault at the Trotter paleoseismic site, which is located 3 km to the SW of 'M' Stream on Fairbrother Road (Figure 59). On the Trotter's farm the fault is characterised by two active traces that form a graben across a T1 (Ohakean) surface. The two traces converge to the northeast where a duck shooting pond has been constructed (Figure 62). Following abandonment of the T1 surface, a riser R1 was cut against this surface by a branch of Oruakerataki Stream. Later, Holocene aggradation formed the T0 terrace (Figure 62).

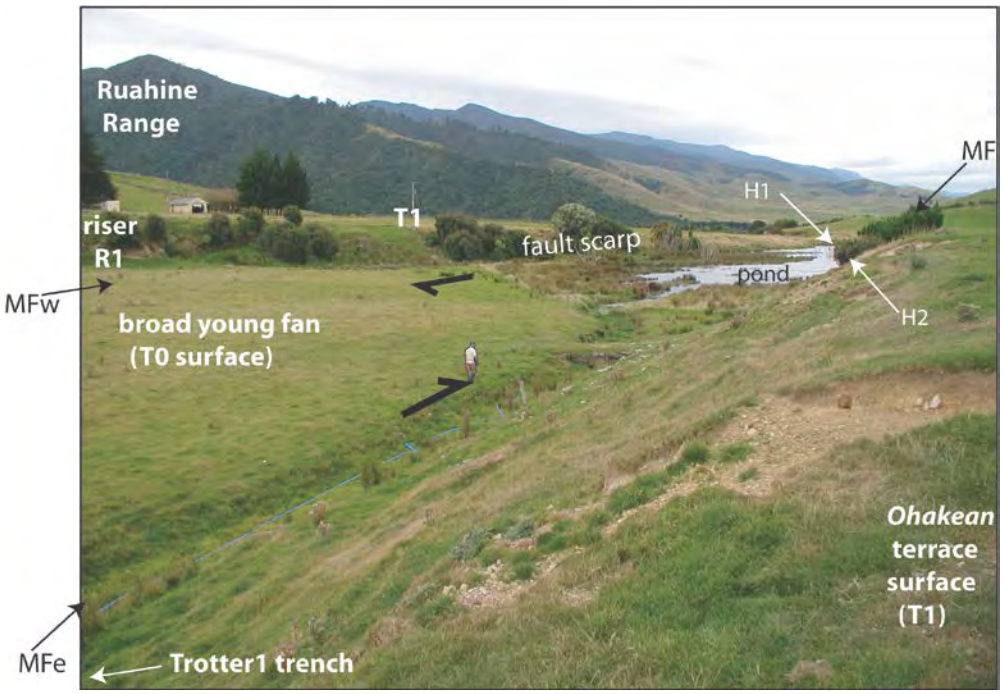

Figure 62 The Trotter graben site along the Mohaka Fault. Two active traces, a western (MFw) and eastern (MFe) converge near Hanson's H1 trench. GNS opened two trenches at this site in 2003. The photographer is standing above the dextrally-offset equivalent of R1 seen in the distance.

Riser R1 is dextrally displaced by 40 ± 2 m. Using the same age bounds for the timing of the formation of R1 (15-12 ka) yields a slip rate of 2.5-3.5 mm/yr, which is consistent with the results from 'M' Stream. Estimates of single-event displacement for the Mohaka Fault from small offset surface features (channels) in this region are 5 ± 1 m. In terms of earthquake recurrence interval this produces a range of 1140-2400 yr. Trenches excavated at this site by Hanson (1998) and Langridge (unpublished data) to date pre-historic earthquakes support such a short recurrence interval.

These data highlight the importance of the Mohaka Fault in terms of seismic hazard and its role in the upper plate deformation within the eastern North Island and across the Hikurangi plate margin.

4.4 STOP 2/4: SADDLE ROAD

Saddle Road crosses the Axial Ranges at their lowest point within the central North Island. On a good day this stop provides a view of the relatively low strain region in the Wanganui and Taranaki basins to the west with the higher strain inner forearc region to the east. The location of the high-strain zone is approximately coincident with the down-dip end of the locked plate interface, as inferred from GPS data. The low strains observed in the geological record of the overriding plate suggest that locking of the plate interface is an interseismic phenomena with slip on the subduction thrust occurring during large magnitude earthquakes. The concentration of high strains in the geological record may reflect preferential loading of faults above the down-dip end of the interseismically locked plate interface which ultimately triggers slip and leads to the accommodation of relatively high permanent strains at this location in the overriding plate.

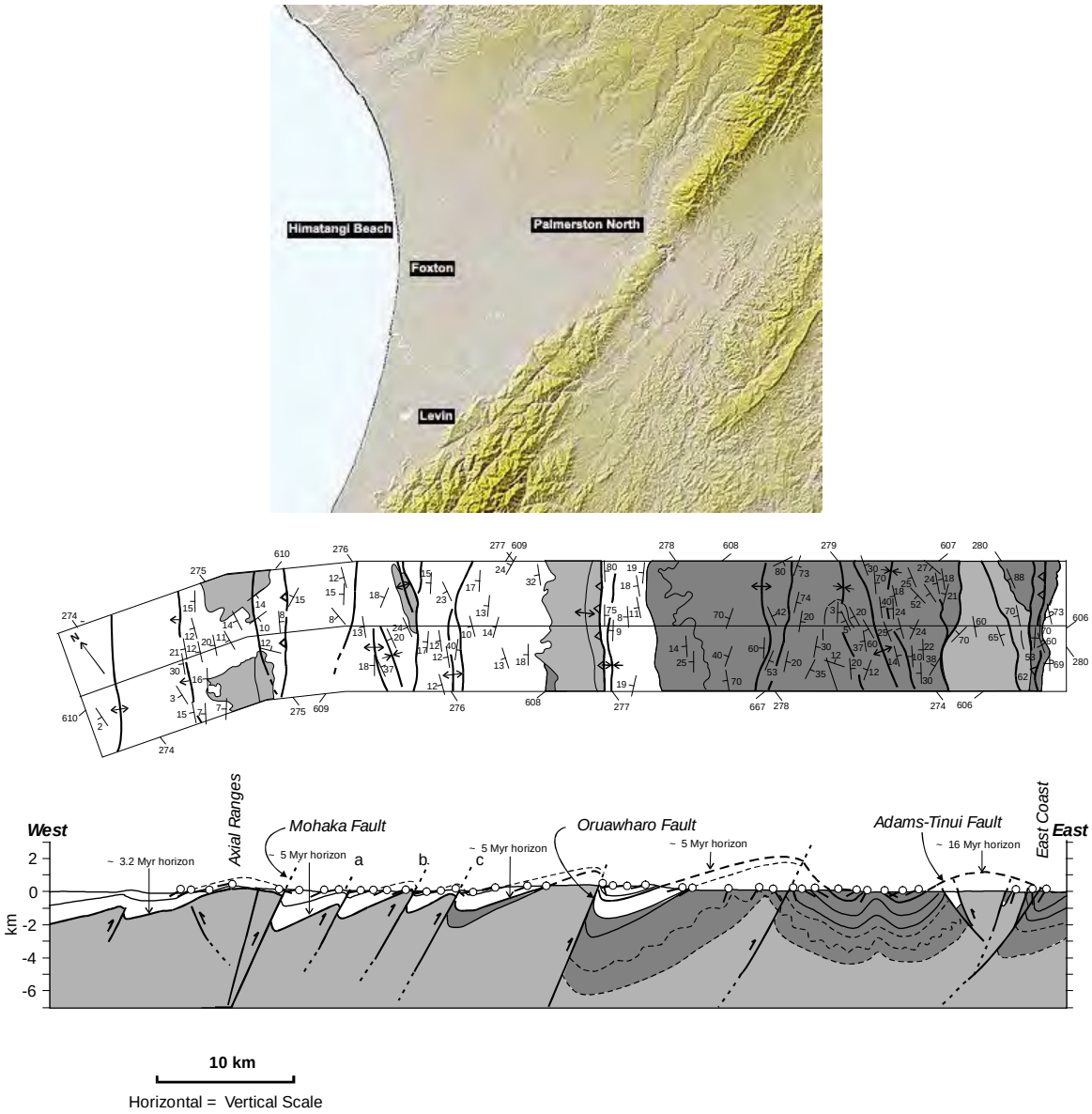

Figure 63 Map and cross-section constructed from outcrop data through East Coast forearc. Tadpoles on cross section indicate bed dips in the plane of the section. Ornamentation in map and cross section indicate distribution of Torlesse basement (light grey), sedimentary rocks of Cretaceous to Miocene in age (dark grey) and Pliocene to Quaternary strata (white). From *Nicol and Beavan* (2003).

The Saddle Road area is the only location where Tertiary sedimentary strata can be traced across the Axial Ranges. Here Pliocene-Pleistocene strata rest on greywacke basement rocks and indicate the presence of an anticline, the hinge of which coincides approximately with the range crest. At the highest point on Saddle Road marginal marine siltstones and conglomerates crop out and range in age from ca. 2.5-3.0 Ma.

In contrast, south of the Manawatu Gorge at the wind farm, non-marine conglomerates of about 1 Ma in age rest directly on basement (i.e. older Pliocene strata were removed prior to deposition of this unit). These observations together with the apparent uniformity in the thickness of ca. 2.5-3.0 Ma strata across Saddle Road suggest that the most recent period of accelerated uplift of the ranges probably commenced between 1 and 2.5 Ma (*Beanland*, 1995; *Trewick and Bland*, 2011). This timing is consistent with the onset of the influx of basement detritus into basins east of the ranges (e.g., *Nicol et al*., 2002, 2007).

The presence of non-marine conglomerates high up on the ranges suggests that a river(s) once flowed across the ranges at the wind farm. The difference in altitude between non-marine river-deposited conglomerates on the top of the range and the active bed of the Manawatu River in the gorge is inferred to principally reflect uplift of the ranges in the last 1 Myr. First order estimates suggest that the ranges at Saddle Road experienced uplift rates of about 0.5-1 mm/yr over the last 1-2 Myr. Debate continues as to whether uplift is occurring today.

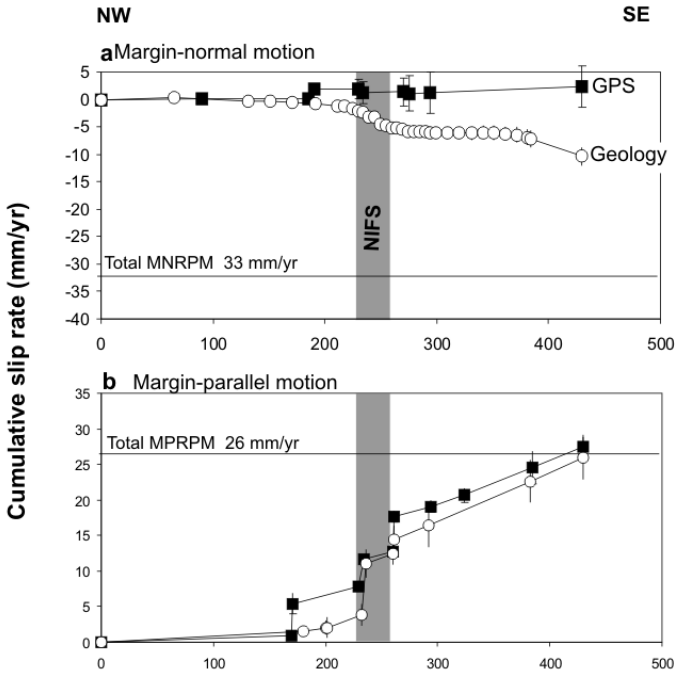

Figure 64 Margin-parallel and margin-normal upper plate deformation measured from GPS (filled squares) and Geological strain markers up to 5 Ma (open circles). From Nicol and Wallace (2007). These figures show that the GPS and geology are mismatched with neither being similar to the margin-normal plate motion, while margin-parallel (strike-slip faulting and vertical axis rotations) is similar for both data sets and comparable to the far-field plate rate. The mismatch of margin-normal deformation arises because most of this deformation occurs on the subduction thrust and is not resolved in the upper-plate signal.

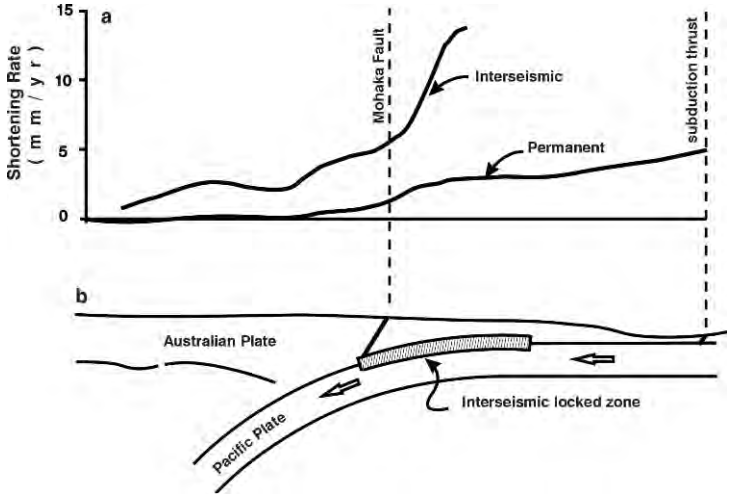

Figure 65 a) Diagram showing profiles of cumulative shortening rates (in mm/yr) from geological and GPS data across the central Hikurangi margin. b) Plate boundary cross section indicating the location of the inferred interseismic locked zone relative to the Mohaka Fault and the high strain zone in the overriding plate. From Nicol and Beaven (in prep).

Figure 66 Tararua Wind Farm. From http://en.wikipedia.org/wiki/Tararua_Wind_Farm

4.5 STOP 2/5: WANGANUI BASIN – AT A BEACH OR ON THE PAEKAKARIKI HILL LOOKOUT

From Saddle Road on the crest of the Axial Ranges we drive westwards into the Wanganui Basin. The South Wanganui Basin is early Pliocene to Recent in age. Subsidence in the basin has been inferred to arise from high friction on the top of the subducting Pacific Plate (i.e. the subduction thrust) some 40-60 km beneath, which produces a downward pull and flexure of the overriding Australian Plate resulting in formation of the Wanganui Basin (*Stern et al.,* 1992). Displacement on reverse faults within the basin (see Tan 16 seismic reflection line) and uplift of the axial ranges at the eastern edge of the basin may also have contributed to basin formation through crustal shortening and lithospheric loading (e.g. *Lamarche et al*., 2005). Through the Pliocene and Pleistocene the centre of subsidence has migrated southwards while there has been a concomitant regional uplift along the northern margin of the basin (*Stern et al*., 1992; *Kamp et al.*, 2004; *Nicol*, 2011).

The greatest subsidence is in a roughly bowl shaped depression offshore of Wanganui city. On seismic reflection lines the floor of the basin is rugged with up to 2000 m relief, which is interpreted to reflect paleotopography and reverse faulting (e.g., *Anderton*, 1981; *Holt and Stern,* 1994; *Lamarche et al.*, 2005; *Nico*l, 2011). In the late Miocene prior to the onset of basin formation parts of the basin were the site of mountain ranges up to 2 km in altitude (*Nicol*, 2011). The basin subsided rapidly (e.g., <3 mm/yr) during the early Pliocene and reached bathyal depths (>200 m below sea level) by ~4 Ma. The resulting depression was filled with sediments which, from ~3 Ma, were predominantly deposited in shelf and shallow-water environments. The resulting basin fill is up to 5 km thick and may have contributed to basin formation via loading of the lithosphere and compaction of basin strata.

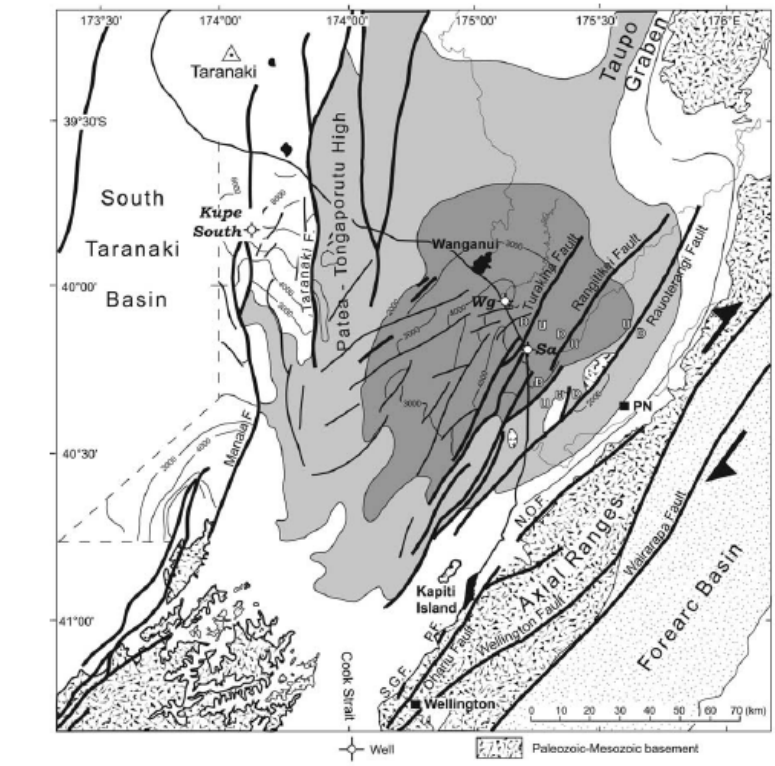

Figure 67 Structural setting of the south Wanganui Basin (From Lamarche et al., 2005; modified from Anderton, 1981). Thin contour lines are depth in metres to top basement with grey shading enhancing 1000 and 2000 m contour lines. Basement faults are shown along with up (U) and down (D) movement directions. Thick red lines show the location of the seismic lines Tan 16 (west northwest) and EA-2 (north northeast). N.O.F, North Ohariu Fault; S.G.F., Shepards Gully Fault; P.F., Pukerua Fault PN; Palmerston North city.

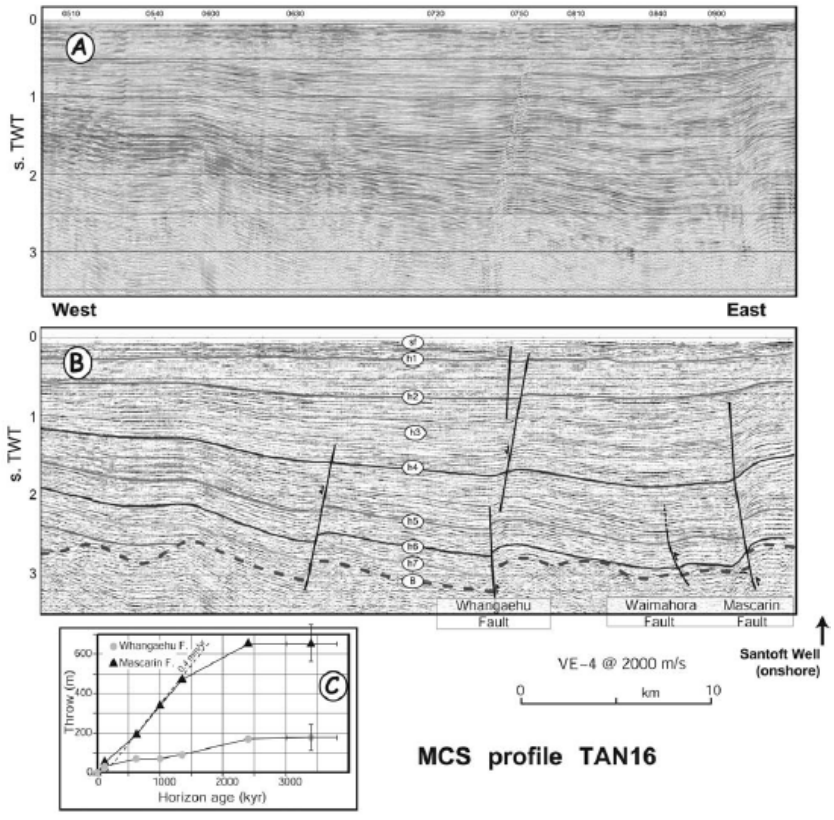

Figure 68 Uninterpreted (A) and interpreted (B) seismic reflection profile (Tan 16) seismic line oriented west-northwest approximately normal to the main faults in the basin (Lamarche et al., 2005). Mapped reflectors range in age from about 3.6 Ma to 120-260 ka. Graph shows shows the accumulation of throw on faults in the section and indicate that faulting commenced between 2 and 1.5 Ma.

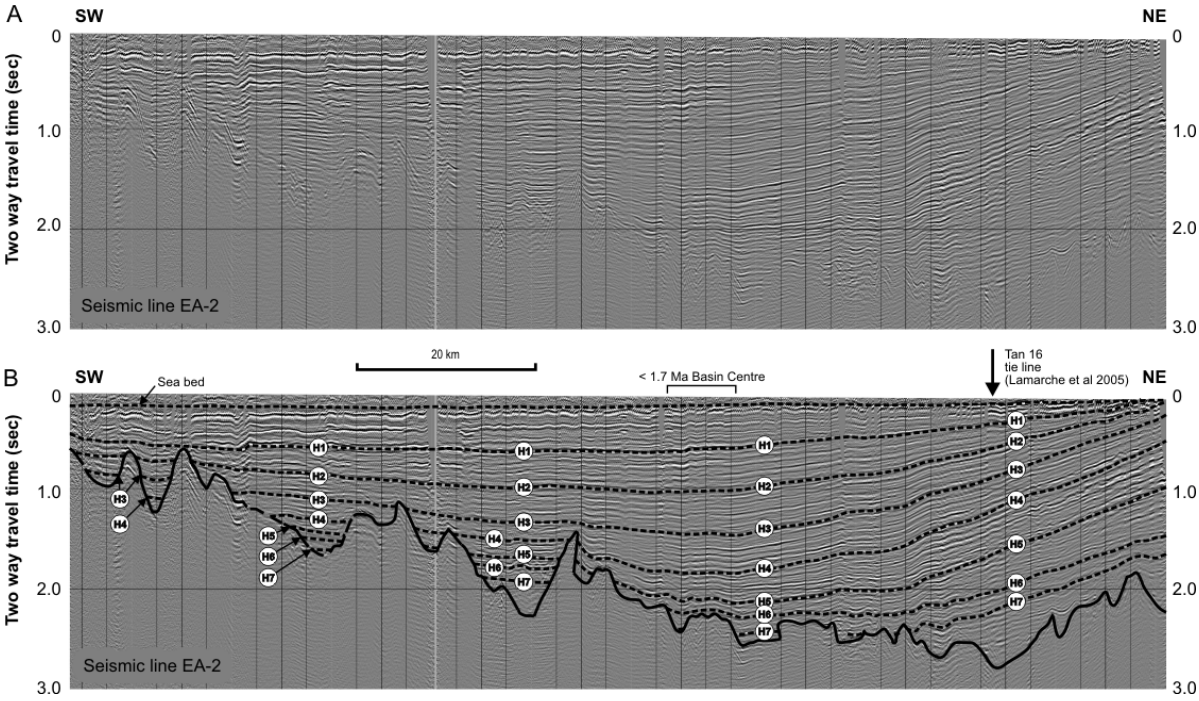

Figure 69 Uninterpreted (A) and interpreted (B) seismic reflection profile (line EA-2) oriented north-northeast across the offshore Wanganui Basin. From Nicol (2011). Eight seismic reflectors (H1-H7 and top basement) have been interpreted in the seismic line with the age and location of the H1-H7 reflectors from cross line Tan 16 of Lamarche et al. (2005). Mapped reflectors range in age from about 3.6 Ma to 120-260 ka and provide a record of basin evolution over this time period.

4.6 STOP 2/6: OHARIU FAULT

The Ohariu Fault is one of the major dextral strike-slip faults of the southern North Island Dextral Fault Belt (NIDFB) (Figure 70). Together, these faults accommodate ~70% of the total Hikurangi margin-parallel motion (*Van Dissen and Berryman*, 1996). The southern NIDFB faults are inferred to extend up from the subduction interface, which is at 20-25 km depth. The Ohariu Fault, one of the westernmost southern NIDFB faults, lies at the western edge of the currently locked part of the interface, and above the southeastern edge of the Kapiti slow slip events (Figure 8).

The Ohariu Fault extends from within Cook Strait in the south (*Pondard and Barnes*, 2010), along valleys (e.g., Ohariu Valley, Porirua Harbour, Transmission Gully) cut into the basement-cored axial ranges, to just north of Waikanae. There deformation continues via a step-over to the Northern Ohariu Fault (Figure 70). The Ohariu Fault accommodates almost pure dextral strike-slip, although locally it is upthrown on either the northwestern (e.g., this site, Muaupoko Stream valley) or southeastern (e.g., Ohariu Valley) side. With a slip rate of ~1 mm/yr (*Heron et al*., 1998), the Ohariu Fault displays the third fastest southern NIDFB fault, after the Wairarapa (~12 mm/yr; Grapes, 1991; Carne et al., 2010) and Wellington (~6.5 mm/yr; *Berryman*, 1990) faults (Figure 70). Single event displacement averages 3.7 m and estimated magnitudes are M_w 7.1 to 7.5 (*Heron et al*., 1998; *Stirling et al.*, submitted).

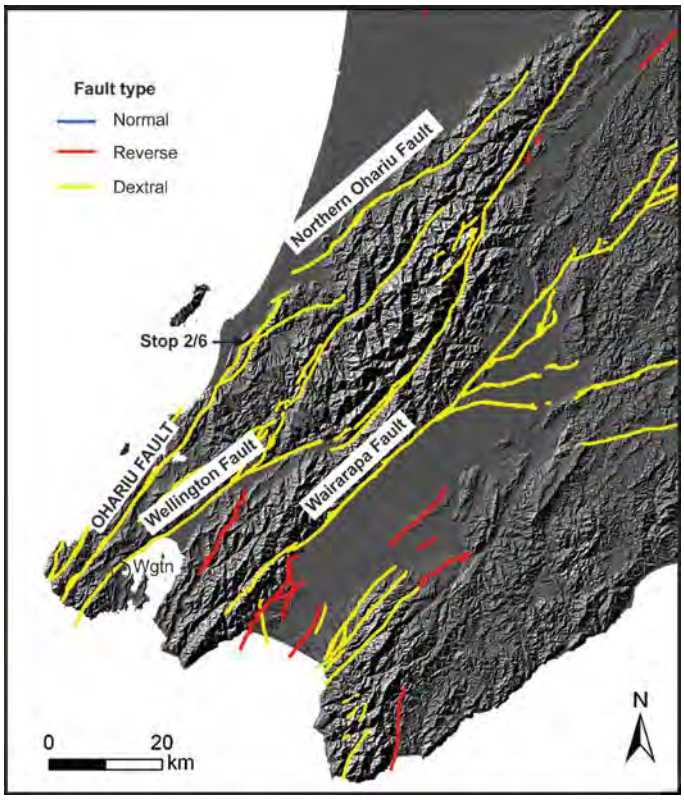

Figure 70 Onshore active faults in the southern North Island (http://data.gns.cri.nz/af/). Wgtn is Wellington city.

The Ohariu Fault is situated within one of the more rapidly growing parts of the Wellington region, the Kapiti Coast District. As a result, the fault has received quite a lot of attention, such as for planning of subdivisions like Nikau Lakes in Muaupoko Stream valley, near Paraparaumu. In Nikau Lakes subdivision the fault consists of a ~5 m high single scarp, trimmed by a small tributary of Muaupoko Stream, which runs along the base (Figure 71). Four trenches were excavated on the downthrown side of the degraded scarp, exposing a fault zone up to 4.5 m wide in three trenches (*Litchfield et al.*, 2004). Trench T00/1 proved the most useful for dating the most recent surface rupture event, with undisturbed peats overlying an event horizon (Figure 72). Combining the radiocarbon dates at this site with those from 10 other sites to the northwest and southeast tightly constrain the timing of the most recent event to 1050-1000 cal. yr BP (*Litchfield et al.*, 2004, 2006, 2010b).

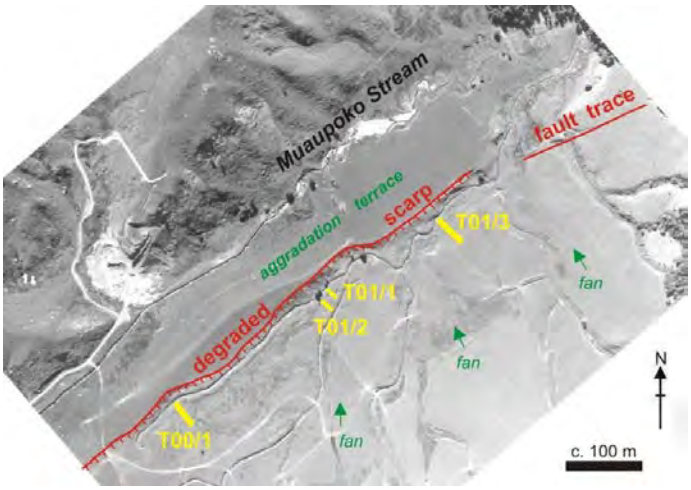

Figure 71 Trench sites along the Ohariu Fault in Muaupoko Stream valley (Nikau Lakes subdivision). From Litchfield et al. (2004).

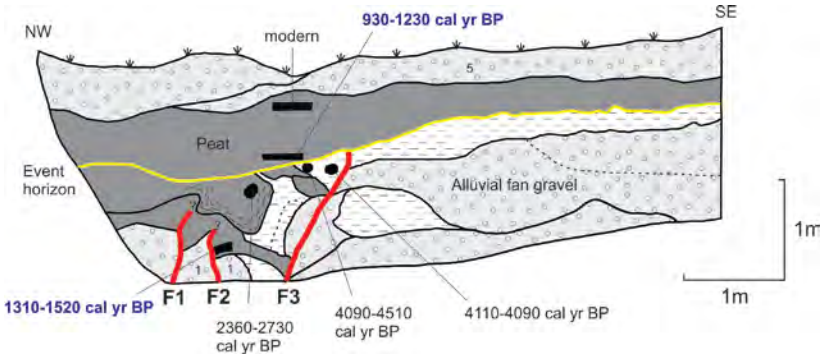

Figure 72 Log of trench T00/1 in Muaupoko Stream valley (Nikau Lakes subdivision). The radiocarbon ages that constrain the timing of the most recent event, marked by the yellow event horizon, are shown in bold blue. From Litchfield et al. (2004).

Constraining the timing of older events, and hence the Ohariu Fault recurrence interval, has proved problematic, with a number of trenches containing unconformities spanning thousands to tens of thousands of years (*Heron et al*., 1998; *Litchfield et al*., 2004, 2010b). Our best estimate of recurrence interval to date comes from MacKays Crossing ~8 km to the southwest of Nikau Lakes. There, a statistical analysis of multiple parameters (inter-event times from three events in the MacKays Crossing trench, mean slip rate, single event displacement, and their uncertainties) was used to constrain a mean recurrence interval of 2200 years, but minimum and maximum 95% confidence interval limits are 800 and 9000 years, respectively (*Litchfield et al*., 2006). The recurrence interval is important, because it forms the basis of a guideline for building on or close to New Zealand's active faults, with a cutoff between class I and II of 2000 years (*Kerr et al.,* 2003).

A trench in Ohariu Valley ~25 km to the southwest has also revealed a young (post-310 cal. yr BP), small (decimetre) rupture event (*Litchfield et al.,* 2010b). This may be either a small primary Ohariu Fault rupture, or a triggered event associated with a large earthquake on a nearby fault (e.g., the Wellington, Wairarapa, or Awatere Faults) (Figure 73). Interactions between central New Zealand faults have also been studied by Pondard and Barnes (2010) and Robinson et al. (submitted).

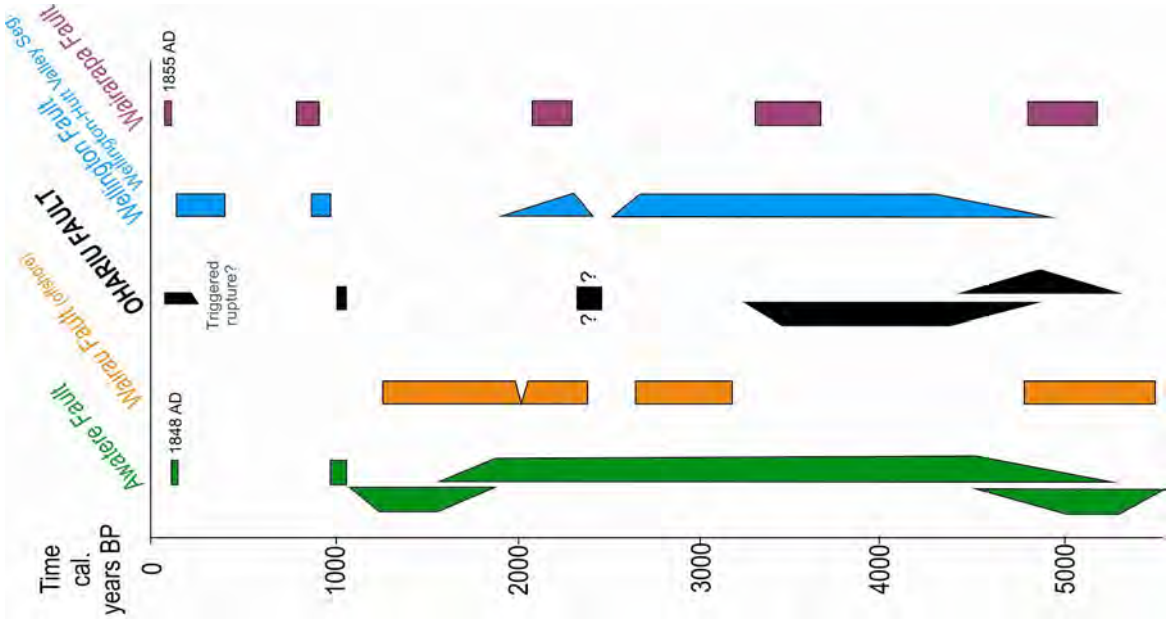

Figure 73 Comparison of the timing of Ohariu Fault surface rupture events with those on other major central New Zealand active faults. From Litchfield et al. (2010b).

5.0 ACKNOWLEDGEMENTS

This guide was prepared by Laura Wallace (Introductory material), Nicola Litchfield (stops 1/1, 1/5, 1/6, 2/6), Agnes Reyes (1/2), Kate Clark (stops 1/3, 1/4, 1/7, 1/8), Andy Nicol (stops 2/1, 2/4, 2/5), and Rob Langridge (stops 2/2, 2/3), with input from Joshu Mountjoy (cover image, stop 1/1). It contains a mixture of published and unpublished material of the authors as well as a significant number of other New Zealand geoscientists, and includes material updated from previous fieldtrip guides (Seismix2003, Friends of the Quaternary 2005, Margins Source-to-Sink workshop, 2009). We thank Stuart Henrys and Kyle Bland for their careful reviews and Kat Hammond for preparation for final publication.

6.0 REFERENCES

Adams, C.E.; Barnett, M.A.F.; Hayes, R.C. 1933: Seismological report of the Hawke's Bay earthquake of 3rd February 1931. New Zealand Journal of Science and Technology 15: 93-107.

Anderton PW 1981. Structure and evolution of the South Wanganui Basin, New Zealand. New Zealand Journal of Geology and Geophysics 24: 39-63.

Barker, D.H.N.; Sutherland, R.; Henrys, S.A.; Bannister, S. 2009. Geometry of the Hikurangi subduction thrust and upper plate, North Island, New Zealand. Geochemistry, Geophysics, Geosystems, 10(2), doi:10.1029/2008GC002153.

Barnes, P.M.; Nicol, A. 2004. Formation of an active thrust triangle zone associated with structural inversion in a subduction setting, eastern New Zealand, Tectonics, 23, TC1015, doi:10.1029/2002TC001449.

Barnes, P.M.; Mercier de Lepinay, B. 1997. Rates and mechanics of rapid frontal accretion along the very obliquely convergent southern Hikurangi margin, New Zealand, Journal of Geophysical Research, 102(B11), 24,931-24,952.

Barnes, P. M.; Nicol, A.; Harrison, T. 2002. Late Cenozoic evolution and earthquake potential of an active listric thrust complex above the Hikurangi subduction zone, New Zealand.: Geological Society of America Bulletin, v. 114, no. 11, p. 1379-1405.

Barnes, P.; Lamarche, G.; Bialas, J.; Henrys, S.; Pecher, I.; Netzeband, G. L.; Greinert, J.; Mountjoy, J.; Pedley, K.; Crutchley, G. 2010. Tectonic and geological framework for gas hydrates and cold seeps on the Hikurangi subduction margin, New Zealand: Marine Geology, v. 272, no. 1-4, p. 26-48.

Beanland, S. 1995. The North Island dextral fault belt, Hikurangi subduction margin, New Zealand, Unpublished Ph.D. thesis, Victoria Univ. of Wellington, Wellington New Zealand.

Beanland, S.; Haines, J. 1998. The kinematics of active deformation in the North Island, New Zealand, determined from geological strain rates, NZ J. of Geol. and Geophys., 41, 311-323.

Beanland, S.; Melhuish, A.; Nicol, A.; Ravens, J. 1998. Structure and deformation history of the inner forearc region, Hikurangi subduction margin, New Zealand, *N.Z. J. Geol. Geophys.*, *41*, 325-342.

Beavan, J.; Haines, J. 2001. Contemporary horizontal velocity and strain-rate fields of the Pacific-Australian plate boundary zone through New Zealand, *J. Geophys. Res. 106*, 741-770.

Bell, R.; Sutherland, R.; Barker, D.H.N.; Henrys, S.; Bannister, S.; Wallace, L.; Beavan, J. 2010. Seismic reflection character of the Hikurangi subduction interface, New Zealand, in the region of repeated Gisborne slow slip events, Geophysical Journal International, 180(1), 34-48).

Berryman, K. 1990. Late Quaternary movement on the Wellington Fault in the Upper Hutt area, New Zealand. New Zealand Journal of Geology and Geophysics 33: 257-270.

Berryman, K. R. 1993a. Age, height, and deformation of Holocene terraces at Mahia Peninsula, Hikurangi subduction margin, New Zealand.: Tectonics, v. 12, no. 6, p. 1347-1364.

Berryman, K. R. 1993b. Distribution, age, and deformation of Late Pleistocene marine terraces at Mahia peninsula, Hikurangi subduction margin, New Zealand.: Tectonics, v. 12, no. 6, p. 1365-1379.

Berryman, K.; Marden, M.; Eden, D.; Mazengarb, C.; Ota, Y.; Moriya, I. 2000. Tectonic and paleoclimatic significance of Quaternary river terraces of the Waipaoa River, east coast, North Island, New Zealand. New Zealand Journal of Geology and Geophysics, 43: 299-245.

Berryman, K.; Marden, M.; Palmer, A.; Litchfield, N. 2009. Holocene rupture of the Repongaere Fault, Gisborne: implications for Raukumara Peninsula deformation and impact on the Waipaoa Sedimentary System. New Zealand Journal of Geology and Geophysics 52: 335-347.

Brown, L.J. 1995. Holocene shoreline depositional processes at Poverty Bay, a tectonically active area, northeastern North Island, New Zealand. Quaternary International, 26: 21-33.

Bullen, K.E. 1938: An analysis of the Hawke's Bay earthquakes during February 1931. New Zealand Journal of Science and Technology 19: 497-519.

Carne, R.C.; Little, T.A.; Rieser, U. 2011. Using displaced river terraces to determine Late Quaternary slip rate for the central Wairarapa Fault at Waiohine River, New Zealand. New Zealand Journal of Geology and Geophysics 54: 217-236.

Carter, L.; Orpin, A.R.; Kuehl, S.A. 2010. From mountain source to ocean sink - the passage of sediment across an active margin, Waipaoa Sedimentary System, New Zealand. Marine Geology 270: 1-10.

Chague´-Goff, C.; Nichol, S.L.; Jenkinson, A.V.; Heijnis, H. 2000. Signatures of natural catastrophic events and anthropogenic impact in an estuarine environment, New Zealand. Marine Geology 167, 285–302.

Clark, K.; Berryman, K.; Litchfield, N.; Cochran, U.; Little, T. 2010. Evaluating the coastal deformation mechanisms of the Raukumara Peninsula, northern Hikurangi subduction margin, New Zealand and insights into forearc uplift processes. New Zealand Journal of Geology and Geophysics 53: 341-358.

Cochran, U.; Berryman, K.; Mildenhall, D.; Hayward, B.; Southall, K.; Hollis, C.; Barker, P.; Wallace, L.; Alloway, B.; Wilson, K. 2006. Paleoecological insights into subduction zone earthquake occurrence, eastern North Island, New Zealand.: Geological Society of America Bulletin, v. 118, no. 9/10, p. 1051-1074.

Collot, J.-Y.; and fifteen co-authors. 1996. From oblique subduction to intra-continental transpression: structures of the southern Kermadec-Hikurangi margin from multibeam bathymetry, side-scan sonar and seismic reflection, Marine Geophysical Researches, 18, 357-381.

Cutten, H.N.C. 1994. Geology of the middle reaches of the Mohaka River. Institute of Geological and Nuclear Sciences Geological Map 6.

Davey, F.J.; Hampton, M.; Childs, J.; Fisher, M.A.; Lewis, K.; Pettinga, J.R. 1986. Structure of a growing accretionary prism, Hikurangi margin, New Zealand, Geology, 14, 663-666.

Davy, B.; Wood, R. 1994. Gravity and magnetic modelling of the Hikurangi Plateau, Marine geology, 118, 139-151.

Davy, B.R.; Hoernle, K.; Werner, R. 2008. The Hikurangi Plateau – crustal structure, rifted formation and Gondwana subduction history. Geochem. Geophys. Geosys. 9, Q07004, doi:10.1029/2007GC001855.

Eden, D.N.; Page, M.J. 1998: Palaeoclimatic implications of a storm erosion record from late Holocene lake sediments, North Island, New Zealand. Palaeogeography, Palaeoclimatology,Palaeoecology, 139: 37-58.

Froggatt, P.C.; Howorth, R. 1980: Uniformity of vertical faulting for the last 7000 years at Lake Poukawa, Hawke's Bay, New Zealand. N.Z. J. Geol. Geophys., 23(4): 493-497.

Gibb, J.G. 1984. Coastal Erosion. In: Speden, I., Crozier, M.J. (Eds.), Natural Hazards in New Zealand. New Zealand national Commission for UNESCO, Wellington, pp 134-158.

Giggenbach, W.F.; Sano, Y.; Wakita, H. 1993. Isotopic composition of helium, and CO2 and CH4 contents in gases produced along the New Zealand part of a convergent plate boundary. Geochimica et Cosmochimica, 57: 3427-3455.

Gomez, B.; Page, M.; Bak, P.; Trustrum, N. 2002. Self-organized criticality in layered, lacustrine sediment formed by landsliding. Geology 30: 519-522.

Gomez, B.; Carter, L.; Orpin, A.R.; Cobb, K.M.; Page, M.J.; Trustrum, N.A.; Palmer, A.S. In press. ENSO/SAM interactions during the middle and late Holocene. The Holocene.

Grapes, R.H. 1991. Aggradation surfaces and implications for displacement rates along the Wairarapa Fault, southern North Island, New Zealand. Catena 18: 453-469.

Guthrie-Smith, H. 1921. Tutira: the story of a New Zealand sheep station. University of Washington Press (paperback edition published in 1999).

Haines, A.J.; Darby, D.J. 1987: Preliminary dislocation models for the 1931 Napier and 1932 Wairoa earthquakes. New Zealand Geological Survey report EDS 114. Lower Hutt, New Zealand Geological Survey. 64 p.

Hancox, G.T.; Perrin, N.D.; Dellow, G.D. 2002. Recent studies of historical earthquake-induced landsliding, ground damage, and MM Intensity in New Zealand. Bulletin of the New Zealand Society for Earthquake Engineering 35, 59-95.

Hayward, B. W.; Grenfell, H. R.; Sabaa, A.; Carter, R.; Cochran, U.; Lipps, J. H.; Shane, P.; Morley, M. S. 2006, Micropaleontological evidence of large earthquakes in the past 7200 years in southern Hawke's Bay, New Zealand.: Quaternary Science Reviews, v. 25, no. 11-12, p. 1186-1207.

Henderson, J. 1933: The geological aspects of the Hawke's Bay earthquakes (New Zealand), February 3, 1931). New Zealand Journal of Science 15: 38-75.

Henrys, S.; Reyners, M.; Pecher, I.; Bannister, S.; Nishimura, Y.; Maslen, G. 2006. Kinking of the subducting slab by escalator normal faulting beneath the North Island of New Zealand: Geology, v. 34, p. 777-780.

Heron, D.; Van Dissen, R.; Sawa, M. 1998. Late Quaternary movement on the Ohariu Fault, Tongue Point to MacKays Crossing, North Island, New Zealand. New Zealand Journal of Geology and Geophysics 41: 519-439.

Hicks, D.M.; Shankar, U. 2003. Sediment from New Zealand rivers. NIWA Chart. Miscellaneous Series No. 79.

Holt, W.E.; Stern, T.A. (1994). Subduction, platform subsidence, and foreland thrust loading: The late Tertiary development of Taranaki Basin, New Zealand. *Tectonics*, 13, 1068-1092.

Hull, A.G. 1986. Pre-A.D. 1931 tectonic subsidence of Ahuriri Lagoon, Napier, Hawkes Bay, New Zealand. *New Zealand Journal of Geology and Geophysics* 29, 75-82.

Hull, A.G. 1990: Tectonics of the 1931 Hawke's Bay earthquake. N.Z. J. Geol. Geophys., 33(2): 309-320.

Kamp, P.J.J.; Vonk, A.J.; Bland, K.J.; Hansen, R.J.; Hendy, A.J.W.; McIntyre, A.P.; Ngatai, M.; Cartwright, S.J.; Hayton, S.; Nelson, C.S. 2004. Neogene stratigraphic architecture and tectonic evolution of Wanganui, King Country, and eastern Taranaki Basins, New Zealand. New Zealand Journal of Geology and Geophysics 47 (4): 625–644.

Kelsey, H.M.; Cashman, S.M.; Beanland, S.; Berryman, K.R. (1995), Structural evolution along the inner forearc of the obliquely convergent Hikurangi margin, New Zealand, *Tectonics* 14, 1-18.

Kennedy, E.M.; Alloway, B.V.; Mildenhall, D.C.; Cochran, U.; Pillans, B. 2008. An integrated terrestrial paleoenvironmental record from the Mid-Pleistocene transition, eastern North Island, New Zealand. Quaternary International 178: 146-166.

Kerr, J.; Nathan, S.; Van Dissen, R.; Webb, P.; Brunsdon, D.; King, A. 2003. Planning for development of land on or close to active faults. A guideline to assist resource management planners in New Zealand. Report prepared for the Ministry for the Environment (http://www.mfe.govt.nz/publications/rma/planning-development-active-faults-dec04/index.html).

Lamarche G.; Proust J.N.; Nodder, S.D. 2005. Long-term slip rates and fault interactions under low contractional strains, Wanganui Basin, New Zealand. Tectonics 24: TC4004, doi:10.1029/2004TC001699.

Langridge, R.M.; Berryman, K.R.; Van Dissen, R.J. (2005), Defining the geometric segmentation and Holocene slip rate of the Wellington Fault, New Zealand: the Pahiatua section. *N.Z. J. Geol. Geophys.,* 48, 591-607.

Lewis, K.; Pettinga, J. 1993. The emerging, imbricate frontal wedge of the Hikurangi margin, in South Pacific Sedimentary Basins. Sedimentary Basins of the World 2, edited by P.B. Ballance, pp 225-250, Elsevier Science Publishers B.V., Amsterdam.

Lewis, K.B.; Collot J.Y.; Lallemande, S.E. 1998. The dammed Hikurangi Trough: a channel-fed trench blocked by subducting seamounts and their wake avalanches (New Zealand-France GeodyNZ Project), Basin Research 10 (4), doi:10.1046/j.1365-2117.1998.00080.x

Litchfield, N. 2003. Maps, stratigraphic logs and age control data for river terraces in the eastern North Island. Institute of Geological and Nuclear Sciences Science Report 2003/31.

Litchfield, N. 2008. Using fluvial terraces to determine Holocene coastal erosion and Late Pleistocene uplift rates: an example from northwestern Hawke Bay, New Zealand. Geomorphology 99: 369-386, doi:10.1016/j.geomorph.2007.12.001.

Litchfield, N.J.; Berryman, K.R. 2005. Correlation of fluvial terraces within the Hikurangi Margin, New Zealand: Implications for climate and baselevel controls. Geomorphology 68: 291-313.

Litchfield, N.J.; Berryman, K.R. 2006. Relations between postglacial fluvial incision rates and uplift rates in the North Island, New Zealand. Journal of Geophysical Research, 111: F02007, doi:10.1029/2005JF000374.

Litchfield, N.; Van Dissen, R.; Langridge, R; Heron, D.; Prentice, C. 2004: Timing of the most recent surface rupture event on the Ohariu Fault near Paraparumu, New Zealand. New Zealand Journal of Geology and Geophysics 47(1): 123-127.

Litchfield, N.; Van Dissen, R.; Heron, D.; Rhoades, D. 2006. Constraints on the timing of the three most recent surface rupture events and recurrence interval for the Ohariu Fault: trenching results from MacKays Crossing, Wellington, New Zealand. New Zealand Journal of Geology and Geophysics 49(1): 57-61.

Litchfield, N.; Ellis, S.; Berryman, K.; Nicol, A. 2007. Insights into subduction-related uplift in the Hikurangi Margin, New Zealand, using numerical modeling. Journal of Geophysical Research, 112: F02021, doi:10.1029/2006JF000535.

Litchfield, N.; Wilson, K.; Berrryman, K.; Wallace, L. 2010a. Coastal uplift mechanisms at Pakarae River mouth: constraints from a combined Holocene fluvial and marine terrace dataset. Marine Geology 270: 72-83, doi:10.1016/j.margeo.2009.10.003.

Litchfield, N.; Van Dissen, R.; Hemphill-Haley, M.; Townsend, D.; Heron, D. 2010b. Post c. 300 year rupture of the Ohariu Fault in Ohariu Valley, New Zealand. New Zealand Journal of Geology and Geophysics 53: 43-56.

Lyon, G.L.; Giggenbach, W.F.; Francis, D. 1992. The stable isotopic composition of some east coast natural gases. Proceedings 1991 New Zealand Oil Exploration Conference, 310-319.

Marshall, P. 1933. Effects of earthquake on coast-line near Napier. New Zealand Journal of Science and Technology 15, 79-92

Mazengarb, C.; Harris, D.H.M. 1994. Cretaceous stratigraphic and structural relations of Raukumara Peninsula, New Zealand : stratigraphic patterns associated with the migration of a thrust system. *Annales Tectonicae 8(2)*: 100-108.

Marden, M.; Mazengarb, C.; Palmer, A.; Berryman, K.; Rowan, D. 2008. Last glacial aggradation and postglacial sediment production from the non-glacial Waipaoa and Waimata catchments, Hikurangi Margin, North Island, New Zealand. Geomorphology, 99: 404-419.

Mazengarb, C.; Speden I.G. (compilers). 2000. Geology of the Raukumara area. Institute of Geological and Nuclear Sciences 1:250 000 geological map 6. 1 sheet + 60 p. Institute of Geological and Nuclear Sciences Limited, Lower Hutt, New Zealand.

McCaffrey, R. 2002. Crustal block rotations and plate coupling, in Plate Boundary Zones, edited by S. Stein and J. Freymueller, AGU Geodynamics Series vol. 30, 100-122.

Mongillo, M.A.; Clelland, L. 1984. Concise listing of information on the thermal areas and thermal springs of New Zealand. Wellington: New Zealand Department of Scientific and Industrial Research. DSIR geothermal report 9. 228 p.

Mortimer, N.; Parkinson, D. 1996. Hikurangi Plateau: A Cretaceous large igneous province in the southwest Pacific Ocean, *J. geophys. Res.*, *101*(B1), 687–696.

Mountjoy, J.J.; Barnes, P.M. 2011. Active upper plate thrust faulting in regions of low plate interface coupling, repeated slow slip events, and coastal uplift: Example from the Hikurangi Margin, New Zealand. Geochemistry, Geophysics, Geosystems 12, Q01005, doi:10.1029/2010GC003326.

Mouslopoulou, V.; Nicol, A.; Little, T.A.; Walsh, J.J. (2007). Termination of large strike-slip faults: an alternative model from New Zealand, in Tectonics of Strike-Slip Restraining and Releasing Bends, Cunningham, W. D., and P. Mann (Editors), Geol. Soc. Lond. Spec. Publ. 290, 387-415.

Mouslopoulou, V.; Nicol, A.; Walsh, J.J.; Beetham, D.; Stagpoole, V. 2008. Quaternary temporal stability of a regional strike-slip and rift fault intersection. J. Struct. Geol. 30, 451-463.

Mouslopoulou, V.; Nicol, A.; Little, T.A.; Begg, J.G. 2009. Palaeoearthquake surface rupture in a transition zone from strike-slip to oblique-normal slip and its implications to seismic hazard, North Island Fault System, New Zealand, in Palaeoseismology: Historical and Prehistorical Records of Earthquake Ground Effects for Seismic Hazard Assessment Reicherter, L., Michetti, A. M., and P. G. Silva (Editors), Geol. Soc. Lond. Spec. Publ. 316, 269-292.

Naish, T.R.; Field, B.D.; Zhu, H.; Melhuish, A.; Carter, R.M.; Abbott, S.T.; Edwards, S.; Alloway, B.V.; Wilson, G.S.; Niessen, F.; Barker, A.; Browne, G.H.; Maslen, G. 2005. Integrated outcrop, drill core, borehole and seismic stratigraphic architecture of a cyclothemic, shallow-marine depositional system, Wanganui Basin, New Zealand. Journal of the Royal Society of New Zealand 35 (1–2): 91–122.

Nicol, A. 2011. Landscape history of the Marlborough Sounds, New Zealand. *New Zealand Journal Geology Geophysics* 54, 2, 195-208.

Nicol, A.; Wallace**,** L.M. 2007. Temporal stability of deformation rates: comparison of geological and geodetic observations, Hikurangi subduction margin, New Zealand, *Earth and Planetary Science Letters*, doi: 10.1016/j.epsl.2007.03.039

Nicol, A.; Beavan, J. 2003. Shortening of an overriding plate and its implications for slip on a subduction thrust, central Hikurangi Margin, New Zealand, *Tectonics, 22*, 1070 doi:10.1029/2003TC001521.

Nicol, A.; Van Dissen, R.; Vella, P.; Alloway, B.; Melhuish, A. 2002. Growth of contractional structures during the last 10Ma, Hikurangi forearc, New Zealand, *N.Z. J. Geol. Geophys., 45*, 365-385.

Nicol, A.; Mazengarb, C.; Chanier, F.; Rait, G.; Uruski, C.; Wallace, L. 2007. Tectonic evolution of the active Hikurangi subduction margin, New Zealand, since the Oligocene. Tectonics 26, TC4002, doi:10.1029/2006TC002090.

Orpin, A.R.; Carter, L.; Page, M.J.; Cochran, U.A.; Trustrum, N.A.; Gomez, B.; Palmer, A.S.; Mildenhall, D.C.; Rogers, K.M.; Brackley, H.L.; Northcote, L. 2010. Holocene sedimentary record from Lake Tutira: A template for upland watershed erosion proximal to the Waipaoa Sedimentary System, northeastern New Zealand, Marine Geology 270:11-29.

Ota, Y., Berryman, K.R., Hull, A.G., Miyauchi, T., Iso, N. 1988. Age and height distribution of Holocene transgressive deposits in eastern North Island, New Zealand. Palaeogeography, Palaeoclimatology, Palaeoecology 68: 135-151.

Ota, Y.; Hull, A.G.; Iso, N.; Ikeda, Y.; Moriya, I.; Yoshikawa, T. 1992. Holocene marine terraces on the northeast coast of North Island, New Zealand, and their tectonic significance. New Zealand Journal of Geology and Geophysics, 35: 273-288.

Page, M.J.; Trustrum, N.A.; De Rose, R.C. 1994a: A high-resolution record of storm-induced erosion from lake sediments, New Zealand. Journal of Paleolimnology, 11: 333-348.

Page, M.J.; Trustrum, N.A.; Dymond, J.R. 1994b. Sediment budget to assess the geomorphic effect of a cyclonic storm, New Zealand. Geomorphology 9: 169-188.

Page, M.J.; Trustrum, N.A. 1997: A late Holocene lake sediment record of the erosion response to land use change in a steepland catchment, New Zealand. Zeitschrift für Geomorphologie N.F., 41 (3): 369-392.

Page, M.J.; Trustrum, N.A.; Orpin, A.R.; Carter, L.; Gomez, B.; Cochran, U.A.; Mildenhall, D.C.; Rogers, K.M.; Brackley, H.L.; Palmer, A.S.; Northcote, L. 2010. Storm frequency and magnitude in response to Holocene climate variability, Lake Tutira, North-Eastern New Zealand, Marine Geology 270: 30-44.

Pettinga, J.R. 1982. Upper Cenozoic structural history, coastal southern Hawkes Bay, New Zealand, *N.Z. J. Geol. Geophys., 25,* 149-191.

Pillans, B. 1991. New Zealand Quaternary stratigraphy: an overview. Quaternary Science Reviews 10, 405-418.

Pondard, N.; Barnes, P.M. 2010. Structure and paleoearthquake records of active submarine faults, Cook Strait, New Zealand: implications for fault interactions, stress loading, and seismic hazard. Journal of Geophysical Research 115, B12320, doi:10.1029/2010JB007781.

Reyes, A.; Christenson, B.; Faure, K. 2010. Sources of solutes and heat in low enthalpy mineral waters and their relation to tectonic setting, New Zealand, Journal of Volcanological and Geothermal Research, 192: 117-141.

Reyners, M. 1980: A microearthquake study of the plate boundary, North Island, New Zealand. *Geophysical journal of the Royal Astronomical Society 63*: 1-22.

Reyners, M.; Cowan, H. (1993), The Transition from Subduction to Continental Collision: Crustal Structure in the North Canterbury Region, New Zealand, Geophys. J. Int., 115, 1124–1136.

Reyners, M.; Eberhart-Phillips, D.; Stuart, G.; Nishimura, Y. 2006. Imaging subduction from the trench to 300 km depth beneath the central North island, New Zealand, with Vp and Vp/Vs, Geophys. J. Int., 165, 565-583.

Robinson, R.; Van Dissen, R.; Litchfield, N. Submitted. Synthetic Seismicity of the Wellington Region. Geophysical Journal International.

Rockel, I.: 1986. Taking the waters, early spas in New Zealand. Government Printing Office, Wellington, 195 p.

Segschneider, B.; Landis, C.A.; White, J.D.L.; Wilson, C.J.N.; Manville, V. 2002a. Resedimentation of the 1.8 ka Taupo ignimbrite in the Mohaka and Ngaruroro River catchments, Hawke's Bay, New Zealand. New Zealand Journal of Geology and Geophysics 45, 85-101.

Segschneider, B.; Landis, C.A.; White, J.D.L.; Wilson, C.J.N.; Manville, V. 2002b. Environmental response to a large, explosive rhyolitic eruption: sedimentology of post-1.8 ka pumice-rich Taupo volcaniclastics in the Hawke's Bay region, New Zealand. Sedimentary Geology 150, 275-299.

Stern, T.A.; Quinlan, G.M.; Holt, W.E. 1992. Basin formation behind an active subduction zone: three dimensional flexural modelling of Wanganui Basin, New Zealand. Basin Research 4: 197–214.

Stern, T.A.; Quinlan, G.M.; Holt, W.E. 1993. Crustal dynamics associated with the formation of Wanganui Basin, New Zealand. In: Ballance PF ed, South Pacific Sedimentary Basins. Sedimentary Basins of the World 2, Elsevier, Amsterdam. Pp. 213-223.

Stirling, M.; McVerry, G.; Gerstenberger, M.; Litchfield, N.; Van Dissen, R.; Berryman, K.; Barnes, P.; Wallace, L.; Bradley, B.; Villamor, P.; Langridge, R.; Lamarche, G.; Nodder, S.; Reyners, M.; Rhoades, D.; Smith, W.; Nicol, A.; Pettinga, J.; Clark, K.; Jacobs, K. Submitted. National Seismic Hazard Model for New Zealand: 2010 Update, Bulletin of the Seismological Society of America.

Thornley, S. 1996. Neogene tectonics of Raukumara Peninsula, northern Hikurangi Margin, New Zealand. Unpublished PhD Thesis, Victoria University of Wellington, Wellington, New Zealand.

Trewick, S.A.; Bland, K. 2011. Fire and slice: palaeogeography for biogeography at New Zealand's North Island/South Island juncture. Journal of the Royal Society of New Zealand, iFirst, 2011, 1-31.

Upton, P.; Kettner, A.; Gomez, B.; Orpin, A.; Litchfield, N.; Page, M. Submitted. Simulating post-LGM riverine fluxes to the coastal zone: The Waipaoa River System, New Zealand. Computers and Geoscience.

Van Dissen, R.J.; Berryman, K.R. 1996. Surface rupture earthquakes over the last ~1000 years in the Wellington region, New Zealand, and implications for ground shaking hazard, Journal of geophysical research. Solid earth, 101(B3): 5999-6019.

Wallace, L. M.; Beavan, J. 2010. Diverse slow slip behavior at the Hikurangi subduction margin, New Zealand, J. Geophys Res., doi:10.1029/2010JB007717.

Wallace, L.; Beavan, J.; McCaffrey, R.; Darby, D. 2004. Subduction zone coupling and tectonic block rotations in the North Island, New Zealand, J. Geophys. Res., 109(B12), doi: 10.1029/2004JB003241.

Wallace, L.; Reyners, M.; Cochran, U.; Bannister, S.; Barnes, P.; Berryman, K.; Downes, G.; Eberhart-Philips, D.; Fagereng, A.; Ellis, S.; Nicol, A.; McCaffrey, R.; Beavan, J.; Henrys, S.; Sutherland, R.; Barker, D.; Power, W.; Litchfield, N.; Townend, J.; Robinson, R.; Bell, R. E.; Wilson, K.; Power, W. L. 2009. Characterizing the seismogenic zone of a major plate boundary subduction thrust: the Hikurangi Margin, New Zealand: Geochemistry Geophysics Geosystems, v. 10, no. 10, p. doi:10.1029/2009GC002610

Wellman, H.W. 1962. Holocene of the North Island: a coastal reconnaissance. Transactions of the Royal Society of New Zealand 1: 29-99.

Wilmshurst, J.M. 1997: The impact of human settlement on vegetation and soil stability in Hawke's Bay, New Zealand. NZ Journal of Botany 35: 97-111.

Wilson, K.; Berryman, R.; Litchfield, N.; Little, T. 2006. A revision of mid-late Holocene marine terrace distribution and chronology at the Pakarae River mouth, North Island, New Zealand. New Zealand Journal of Geology and Geophysics, 49: 477-489.

Wilson, K.; Litchfield, N.; Berryman, K.; Little, T. 2007a. Distribution, age, and uplift patterns of Pleistocene marine terraces of the northern Raukumara Peninsula, North Island, New Zealand. New Zealand Journal of Geology and Geophysics, 50: 181-191.

Wilson, K.; Berryman, R.; Cochran, U.; Little, T. 2007b. A Holocene incised valley infill sequence developed on a tectonically active coast: Pakarae River, New Zealand. Sedimentary Geology, 197: 333-354.

Wilson, K.; Berryman, R.; Cochran, U.; Little, T. 2007c. Early Holocene paleoseismic history at the Pakarae locality, eastern North Island, New Zealand, inferred from transgressive marine sequence architecture. Tectonics, 26: doi:10.1029/2006TC002021.

Wolinsky, M.A.; Swenson, J.B.; Litchfield, N.; McNinch J.E. 2010. Coastal progradation and sediment partitioning in the Holocene Waipaoa Sedimentary System, New Zealand. Marine Geology 270: 94-107, doi:10.1016/j.margeo.2009.10.021.